We must inspire before we expire

Tatiana M. Anderson

A dissertation

submitted in partial fulfillment of the

requirements for the degree of

Doctor of Philosophy

University of Washington

2017

Reading Committee:

Jan-Marino Ramirez, Chair

William J. Moody

John P. Welsh

Program authorized to offer degree:

Neuroscience

University of Washington

Abstract

We must inspire before we expire

Tatiana M. Anderson

Chair of the Supervisory Committee:
Professor Jan-Marino Ramirez
Neurological Surgery and Pediatrics

For mammals, breathing is essential for life and is composed of three phases: inspiration, postinspiration, and active expiration. The networks that generate the three phases are distributed bilaterally and rostrocaudally along the ventral lateral medulla of the brainstem, and are collectively referred to as the ventral respiratory column (VRC). Previous to this work, independent rhythmogenic networks had been identified and characterized for the generation of inspiration, the preBötzinger complex (preBötC), and active expiration, the lateral parafacial nucleus (pF_L), in rodents.

For decades, models and theories have hypothesized that a region called the Bötzinger Complex (BötC), composed primarily of inhibitory, expiratory interneurons, was responsible for the generation of postinspiration. However, this dissertation describes the discovery of a novel, excitatory, rhythmogenic network, termed the postinspiratory

complex, or PiCo, that we have shown to be both necessary and sufficient for the generation of postinspiratory vagal motor output. Techniques including *in vitro* slice electrophysiology (including a new horizontal brain stem preparation), immunohistochemistry, optogenetics, and *in vivo* electrophysiology were utilized to characterize the PiCo network. Data herein demonstrate that PiCo neurons co-express both glutamate and acetylcholine and are located immediately dorsomedial to the rostral nucleus ambiguus and caudal to the facial nucleus. The PiCo rhythm is stimulated by norepinephrine and selectively inhibited by both the inhibitory neuropeptide, somatostatin, and the mu-opioid agonist, DAMGO. While the preBötC and PiCo rhythms are dependent on non-NMDA excitatory mechanisms, they both exert a mutual inhibitory influence on each other. Isolated in a transverse slice, the PiCo functions as an independent rhythm generator.

We hypothesize that PiCo circuitry is involved in mediating postinspiratory behaviors such as vocalization, swallowing and coughing. Higher cortical brain regions likely influence PiCo neurons via pontine nuclei and the periaqueductal gray (PAG). Failure to coordinate breathing with swallowing or coughing can lead to aspiration pneumonia, the leading cause of death in several neurodegenerative disorders including Alzheimer's Disease, Parkinson's Disease, and dementia. PiCo networks could also be involved in the pathology of obstructive sleep apnea. Further work is required to determine PiCo's role in a variety of behaviors and disorders, and to establish whether PiCo neurons could serve as a future therapeutic target.

Dedicated to:

My family for their unconditional love and support during this endeavor,

and

those suffering from disorders involving the dysfunction between breathing and postinspiratory behaviors. I hope this research provides a foundation for the eventual development of a successful therapy.

Table of Contents

Acknowledgements

First, a heartfelt thank you to the entire lab. You took me in as an additional family member right from the beginning. Throughout my graduate work, everyone has always been helpful, kind, and instructive. It has truly been a collaborative and respectful work environment and I consider myself very lucky to have been able to work closely with such a talented group of individuals. Nino, thank you for being a great mentor and role model. You've always been available whenever I needed help or advice, but also stood back enough to let me grow as an independent scientist. I very much respect the fact that you make hypotheses based on the data at hand and aren't afraid to change your hypotheses when new data conflicts with the original interpretation. Also, as a reward for getting my NRSA, you let me attend the Oxford breathing conference in Australia, which was one of the highlights of my graduate experience.

Fred, from day one you took me under your wing and was my go-to for learning everything- slicing, e-phys, patching, mouse husbandry, optogenetics, and data analysis. I had so much fun working side-by-side with you on our neighboring rigs, and you were there for all of the laughter as well as the tears. I'll always fondly remember our patching competitions, slicing races, and after work happy hours. I'm so proud of you for getting a faculty position at the University of Chicago and I wish you every bit of luck for your successful career because I can't think of anyone who deserves it more.

Nathan and Julia, thank you so much for all of your hours of hard work to add invaluable *in vivo* and histological data to the Nature paper. Your contributions elevated the PiCo story to a new level and couldn't have been done without you. Aguan and Shilpa, you two were encyclopedias of knowledge and always had a helpful answer to any of my questions. Sanja and Ibis, you two have been great friends, workout buddies, and never fail to brighten my day. Sanja, thank you for all of your help with the mouse c-sections, we always made a great team. And Ibis, I am so happy that you are carrying on the horizontal slice torch. I know better than anyone how much practice and perseverance it takes to be able to slice consistently and record dual rhythms. Tatiana, it was a fun experience to share my name with someone else in the lab- I doubt I'll ever have that experience again. Chelsea, soon it will be your turn to defend. Keep up the hard work- it was fun having another graduate student in the lab. To all the talented post-bacs we've had through the years- Maggie, Jacob, Katie, Karan, and Hans, I am always impressed by how quickly you learn new techniques. Thank you for always having such a great attitude even when you sometimes have to do fairly mundane tasks. I look forward to seeing what bright futures are in store for you.

I also want to make sure to thank my first neuroscience mentor, Dr. Mark Masino. Without your guidance and instruction, I would not be successfully defending my PhD today. Thank you for introducing me to the world of electrophysiology and the excitement of seeing a project through from design to publication. Additional acknowledgement extends to the other lab members at that time especially Timothy Wiggin, Jack Peck, Jake Montgomery, Aaron Lambert, and John Eian.

A big thank you to the various other talented respiratory neurophysiologists in this field that have given me advice either at conferences or through the peer-review process. Your words have pushed my work to higher levels and forced me to constantly

think critically about my data. There are too many in total to list here, but in particular, I'd like to thank Dr. Mathias Dutschmann and Dr. Paul Gray.

I moved to Seattle to start graduate school, so I didn't know anyone or have any friends out here when I applied. Since then I have met so many wonderful people and I wish I had time to personally thank each and every one of you. I met Curtis during recruitment weekend and he quickly became my first friend. He drove around with my parents and me through the different neighborhoods of Seattle to figure out where I wanted to live. Through him I met another close friend, Lauren, who is one of the nicest and most genuine people I've ever met. I lived with Travis for a little over two years. He is an incredibly hard worker, intelligent, and has the purest heart. I have so many fond memories with you and miss having someone around that laughs at my dumb jokes. Amanda and Erik, you two are great friends. I know that you wanted to be there for my defense, and I think you were in spirit. I miss you guys and look forward to meeting your new dog!

I also have to thank my adorable pup, Jack. He napped by my side through the majority of my dissertation writing, was always there wagging his tail when I came home from work, and has been my closest buddy while Nick has been in China the last several months. He was not able to attend my defense because he's heard me practice presenting this data too many times at home.

I wouldn't be here without the unconditional love and support from my family. Amanda, I'm so happy that we've always been close sisters. I didn't fully appreciate the uniqueness of our bond until I was an adult. A big thank you to my parents for always making it possible to achieve my dreams and supporting me through the highs and lows of my life. It is also special to me that my grandparents were able to make it here today- they drove up from Vancouver, WA. It has been fun getting to see you two more often now that you're only a car ride away!

It is hard to find the right words to fully thank Nick. You've been with me every day through this chapter of my life, even during the time we were physically long distance from each other. I love that you push me to be the best person that I can be, to live life mindfully, and to take time to think about things from every possible angle. We've had so many adventures together, and I look forward to all the adventures yet to come. I love you very much. Thank you for your unwavering love and support.

Chapter 1

Introduction

*This introduction was published with minor reformatting as a peer-reviewed review, titled ‘Respiratory rhythm generation: triple oscillator hypothesis’, to *F1000 Faculty Reviews.* This publication was co-authored by Jan-Marino Ramirez. The full citation is as follows:

Anderson, T.M. and Ramirez, J.M. (February 14th, 2017). Respiratory rhythm generation: triple oscillator hypothesis. *F1000 Faculty Reviews,* 6:139 (doi: 10.12688/f1000research.10193.1).

1.1 Abstract

Breathing is vital for survival but also interesting from the perspective of rhythm generation. This rhythmic behavior is generated within the brainstem and is thought to emerge through the interaction between independent oscillatory neuronal networks. In mammals, breathing is composed of three phases – inspiration, post-inspiration, and active expiration – and this article discusses the concept that each phase is generated by anatomically distinct rhythm-generating networks: the preBötzinger complex (preBötC), the post-inspiratory complex (PiCo), and the lateral parafacial nucleus (pF_L), respectively. The preBötC was first discovered 25 years ago and was shown to be both necessary and sufficient for the generation of inspiration. More recently, networks have been described that are responsible for post-inspiration and active expiration. Here, we attempt to collate the current knowledge and hypotheses regarding how respiratory rhythms are generated, the role that inhibition plays, and the interactions between the medullary networks. Our considerations may have implication for rhythm generation in general.

1.2 Introduction

Rhythms and oscillations function at the core of many brain processes (Ramirez et al., 2016; Watson and Buzsaki, 2015). For example, rhythmic spinal circuits control locomotor gait (Grillner and El Manira, 2015; Kiehn, 2016), thalamic oscillations detect attentional state (Destexhe, 2000; Ketz et al., 2015), cerebellar rhythms are important for motor coordination (Cheron et al., 2016; Llinas, 2013), and circadian rhythms entrain our biological clocks to a 24-hour cycle (Robinson and Reddy, 2014; Rosenwasser and Turek, 2015). Compared to these circuits, respiratory neural networks in the brainstem

offer a uniquely advantageous system in which to study rhythm generation because of (1) the known anatomical location of respiratory rhythm generators (Anderson et al., 2016; Huckstepp et al., 2015; Pagliardini et al., 2011; Ruangkittisakul et al., 2014; Smith et al., 1991) and (2) the ability to reduce the breathing network into various levels in preparations that retain robust and autonomous rhythmic output (Anderson et al., 2016; Barnes et al., 2007; Ramirez et al., 1996; Smith et al., 2007; Smith et al., 1991). As a result, the control of respiration can be studied from the molecular to the systems level. Mammalian respiration consists of three phases: inspiration, post-inspiration, and active expiration (Richter, 1982; Richter et al., 1992). The networks that collectively generate the three respiratory phases are distributed bilaterally in the ventral respiratory column (VRC) of the brainstem (Gourevitch and Mellen, 2014; Muere et al., 2015; Raghuraman et al., 2014).

Within the VRC, the first described respiratory neural network, the preBötzinger complex (preBötC), is both necessary and sufficient for the generation of inspiration (Gray et al., 2010; Johnson et al., 2001; Ramirez et al., 1998b; Smith et al., 1991; Tan et al., 2008). The preBötC can singularly reconfigure to produce the inspiratory phase of eupnea (normal breathing), gasps, and sighs (Lieske et al., 2000). The respiratory rhythm generated within the preBötC is dependent on excitatory mechanisms, and the location of the network within the ventrolateral medulla has been identified in rodents (Ramirez and Richter, 1996; Smith et al., 1991), cats (Ramirez et al., 1998b), and humans (Schwarzacher et al., 2011). Rhythm-generating, glutamatergic, and bilaterally interconnected preBötC interneurons are derived from progenitors that express the homeobox gene *Dbx1* (Bouvier et al., 2010; Gray et al., 2010). The preBötC can be

isolated in an *in vitro* transverse slice that retains fictive inspiratory bursts in phase with inspiratory hypoglossal motor output (Smith et al., 1991). The transverse slice is amenable to rigorous electrophysiological, histochemical, and optogenetic manipulation. Recently, two distinct rhythm generators have been described that are hypothesized to control the other two phases of respiration: the post-inspiratory complex (PiCo) for the control of post-inspiration, and the lateral parafacial nucleus (pF_L), a subpopulation within the retrotrapezoid nucleus parafacial respiratory group (RTN/pFRG), for the control of active expiration (Figure 1). In addition to the previously mentioned transverse *in vitro* slice (Ruangkittisakul et al., 2014; Ruangkittisakul et al., 2011; Ruangkittisakul et al., 2006), en-bloc brainstem-spinal cord (Bouvier et al., 2010; Smith and Feldman, 1987; Thoby-Brisson et al., 2009), *in situ* (Paton, 1996), sagittal slab (Barnes et al., 2007; Mellen and Mishra, 2010), and, most recently, horizontal slice (Anderson et al., 2016) preparations offer further accessibility and tractability to begin to unravel how the three phases of breathing are generated and interconnected.

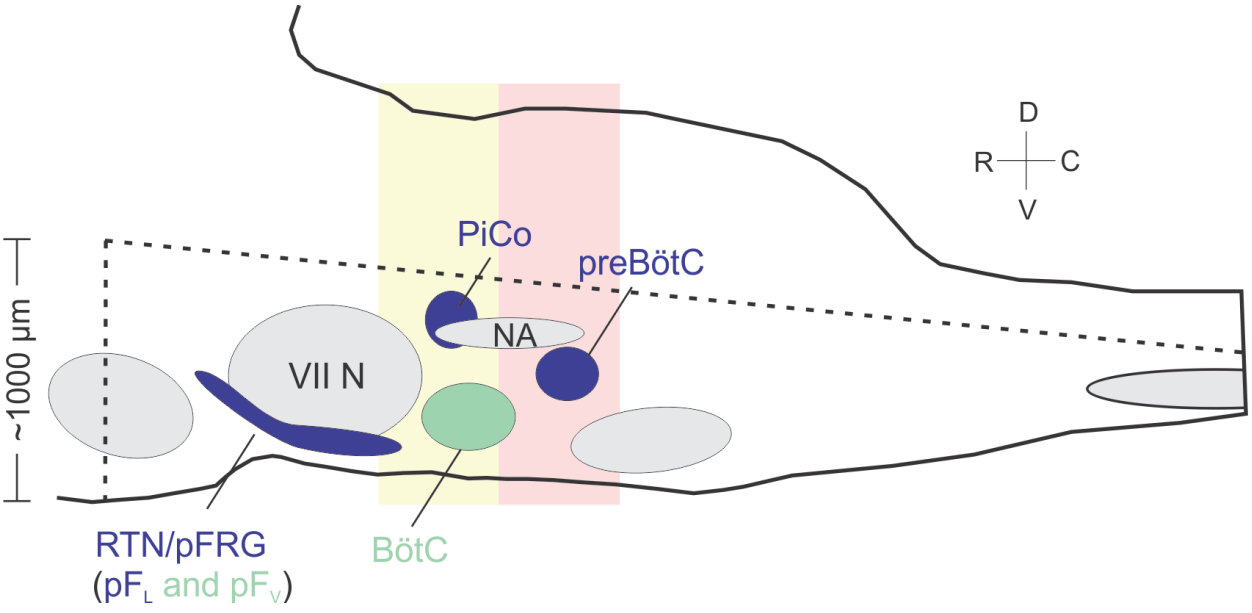

Figure 1. Anatomical map of oscillators in the ventral respiratory column. Schematic of the brainstem from a sagittal view illustrating the approximate anatomical locations of the three respiratory rhythm generators. Shapes in blue represent the three distinct oscillators (preBötC, PiCo, and RTN/pFRG) that are thought to individually control the three phases of respiration. The RTN/pFRG is further segregated into the lateral parafacial nucleus (pF_L), which is more lateral, dorsal, and rhythmogenic, and the ventral parafacial nucleus (pF_V), which is more medial, ventral, and not considered rhythmogenic. Shapes in gray represent motor nuclei, specifically VII N = facial nucleus, and NA = nucleus ambiguus. Green represents neuronal populations that contribute to the respiratory rhythm, but are not thought to be independent rhythm generators. The dotted lines indicate the approximate the boundaries of the horizontal slice, while the pink and yellow boxes illustrate the approximate boundaries of transverse slices isolating preBötC and PiCo, respectively.

1.3 Mammalian respiratory rhythmogenesis

Decades of research have revolved around the endeavor to unmask the underlying processes controlling inspiratory rhythm generation (Lieske et al., 2000; Pena et al., 2004; Smith et al., 1991). Indeed, a long-standing question in the respiratory control field queries how rhythmic, inspiratory activity in the brainstem emerges from the interaction between intrinsic cellular properties and circuit-based synaptic properties. Amid many theories, the answer remains unresolved, but it is likely that multiple rhythmogenic mechanisms exist within the functionally and molecularly heterogeneous preBötC population, and these mechanisms may vary depending on the metabolic, behavioral, and environmental conditions of the organism(Ramirez et al., 2012).

Frequently, models of neural rhythmogenesis include autonomously bursting neurons (pacemakers, or endogenous bursters) as contributors to rhythmogenesis (Garcia et al., 2011b; Koch et al., 2011; Pena, 2008; Ramirez et al., 2011). Endogenous bursting neurons have been described in numerous rhythm-generating networks and the respiratory network is not an exception (Pena, 2008; Ramirez et al., 2004). Approximately

20% of preBötC neurons can be classified as pacemakers, as defined by their tendency to burst in the absence of synaptic input at a period and burst duration similar to the duty cycle of the *in vitro* respiratory rhythm (Del Negro et al., 2005; Feldman et al., 2013; Pena et al., 2004; Thoby-Brisson and Ramirez, 2001). Pacemaker neurons in the preBötC can be either glutamatergic (Pena et al., 2004; Thoby-Brisson and Ramirez, 2001) or glycinergic (Morgado-Valle et al., 2010). The "pacemaker hypothesis", in its strictest interpretation, is the idea that excitatory pacemaker cells play an obligatory role in driving the inspiratory rhythm. It is supported by studies in which antagonists of the persistent sodium current (I_{NaP}; riluzole) and the calcium-activated nonspecific cationic current (I_{CAN}; flufenamic acid [FFA]), the two mechanisms underlying bursting in preBötC neurons, block fictive inspiration *in vitro* (Pena and Ramirez, 2004) and inspiration *in vivo* (Pena and Aguileta, 2007). Moreover, regions such as the preBötC and the RTN/pFRG, that are known to have rhythmogenic functions, are rich in endogenous bursters (Mellen and Mishra, 2010). The exact role of endogenously bursting neurons in respiratory rhythm generation is still a matter of debate (Del Negro et al., 2005; Feldman et al., 2013; Mellen and Thoby-Brisson, 2012; Pena, 2008; Pena et al., 2004; Ramirez and Garcia, 2007; Ramirez et al., 2011; Ramirez et al., 2004). However, it is generally agreed that these bursting neurons do not act as simple "pacemakers" that drive the rhythm. Instead, these neurons are well integrated within the respiratory network, and synaptic and other ionic mechanisms contribute to their timing and discharge properties (Carroll and Ramirez, 2013; Purvis et al., 2007; Ramirez et al., 2012; Ramirez et al., 2011).

Although cellular properties have been identified that differentiate pacemaker from non-pacemaker neurons (Tryba et al., 2003; Tryba and Ramirez, 2004), we shouldn't

think of these in a binary manner. Instead, bursting and non-bursting lie on a continuum of firing characteristics from weak tonic firing to strong bursting (Carroll and Ramirez, 2013), consistent with the hypothesis that preBötC neurons exhibit a continuous distribution of membrane conductances (Del Negro et al., 2002; Koizumi and Smith, 2008; Purvis and Butera, 2005). For example, I_{CAN} and I_{NaP} currents are not exclusive to endogenous burster neurons but are present on many, if not the entire population of, preBötC inspiratory neurons *in vitro* (Del Negro et al., 2002; Del Negro et al., 2005; Rybak et al., 2003; Thoby-Brisson and Ramirez, 2001). The “group pacemaker” theory posits that activity of tonically firing, glutamatergic preBötC neurons can percolate and increase in activity by means of positive feedback (Feldman et al., 2013; Rubin et al., 2009). The pre-inspiratory phase occurs when the positive feedback has surpassed other network constituents and recurrent excitation leads to the initiation of a synchronized inspiratory burst (Feldman and Del Negro, 2006).

This idea was further tested by using *in vitro* physiological data and modeling techniques to hypothesize that each individual population burst is driven by a dynamic, stochastic, and flexible assembly of preBötC neurons within a sparsely connected network (Carroll et al., 2013). Insights into the physiology of the sparsely connected network can be performed by multi-array recordings (Nieto-Posadas et al., 2014). Using this technique, Carroll *et al*. estimated a 1% functional connectivity between preBötC neurons (Carroll et al., 2013), a figure much lower than another study that estimated a 13% probability of one-way excitatory connectivity from dual whole-cell patch recordings of visualized, closely located preBötC neurons (Rekling et al., 2000). Reasons for the

order of magnitude discrepancy in connectivity estimates have yet to be reconciled other than obvious differences in approach and preparation.

Rhythm generation and pattern generation have been suggested to be separable phenomena (Cui et al., 2016; Kam et al., 2013; McCrea and Rybak, 2008). Rhythm generation refers to the generation of timing signals; however, the control of the timing and coordination of muscle activity is referred to as pattern generation (Dick et al., 2015; Kam et al., 2013; Marchenko et al., 2016). Intracellular burst activity and motor outputs can exhibit a variety of shapes such as decrementing, augmenting, or bell-shaped (Ezure, 1990; Ramirez et al., 1996). Under conventional perfusion conditions *in vitro*, preBötC bursts follow a 1:1 ratio with hypoglossal motor output(Ramirez et al., 1996). However, when excitability is lowered with decreased concentrations of extracellular potassium, burst frequency decreases (Johnson et al., 2001; Paton et al., 1994). When a burst is expected, Feldman and colleagues instead observe “burstlets” that are small in amplitude and do not produce a motor output signal. Burstlets appear at multiples of the shortest interburst interval (i.e. are quantized) and can also be observed under specific conditions *in vivo* (Kam et al., 2013). The authors hypothesize that these burstlets represent pre-inspiratory activity that triggers inspiratory bursts when a certain, undefined threshold is reached.

In addition to the preBötC, two other respiratory microcircuits have been identified that function as independent oscillators controlling the other two phases of breathing: post-inspiration and active expiration (Anderson et al., 2016; Huckstepp et al., 2015; Janczewski and Feldman, 2006). Under physiological conditions, expiration is a passive process and mammals largely alternate their breathing between inspiration and post-

inspiration (Morschel and Dutschmann, 2009). Located rostral to the preBötC and dorsomedial to the nucleus ambiguus, the PiCo was recently identified as the putative site for the generation of post-inspiratory activity (Anderson et al., 2016). Similar to the preBötC, PiCo rhythms are also dependent on non-NMDA, excitatory mechanisms (Anderson et al., 2016). Thus, it is likely that the two populations employ similar rhythm-generating mechanisms. Interestingly, one study completed in goats showed that the gradual ablation of the preBötC over the course of two weeks does not result in breathing abnormalities, at least in this species, suggesting that plasticity mechanisms are able to compensate if time is allowed for brainstem networks to reconfigure (Krause et al., 2009). Perhaps PiCo neurons are logical candidates for assuming the preBötC's role?

During periods of higher metabolic activity, for example during exercise, a third phase of breathing is recruited during late expiration, called active expiration, that is required to breathe air out more forcibly than under rest conditions. The active expiratory rhythm reportedly originates in the pF_L (Huckstepp et al., 2015; Pagliardini et al., 2011). This area is defined as a conditional but independent oscillator owing to the observation that it is active only under certain conditions (Janczewski and Feldman, 2006) but can generate rhythmic motor output from facial motor roots in the presence of an opioid agonist, DAMGO (Onimaru and Homma, 2008). Similar to the preBötC and PiCo, the pF_L is dependent on excitatory mechanisms (Onimaru et al., 2008; Thoby-Brisson et al., 2009). Further studies are required to fully elucidate the rhythmogenic mechanisms of these three excitatory oscillatory networks.

1.4 Role of inhibition

While it is generally accepted that the preBötC can burst autonomously *in vitro,* even when inhibition is blocked pharmacologically (Smith et al., 1991), the role of inhibition within the intact respiratory network is still debated. Originally, it was proposed that inspiration and expiration were generated by “half-centered oscillators” in which one population of neurons reciprocally inhibits the other population to generate an alternating two-phase breathing rhythm (Burns, 1963). However, these hypotheses have not been rigorously tested by specifically manipulating identified populations of neurons.

A population termed the Bötzinger complex (BötC) was discovered to contain primarily inhibitory neurons including post-inspiratory and augmenting expiratory neurons (Ezure et al., 2003; Merrill and Fedorko, 1984; Smith et al., 2009). Additionally, approximately 50% of the neurons that make up the preBötC are inhibitory, mostly glycinergic, interneurons (Winter et al., 2009). A contemporary model posits an “inhibitory connectome” or “inhibitory ring” hypothesis in which reciprocal inhibition between the preBötC and other brainstem circuits, such as the BötC, produce the three phases of breathing (Richter et al., 1986a),(Richter and Smith, 2014). The theory states that glycinergic inhibition resets the activity of inspiratory, post-inspiratory, and expiratory neurons in the ventral respiratory network (Richter and Smith, 2014). These interpretations are derived mainly from intracellular recordings *in vivo* or *in situ* paired with computational modeling (for reviews see (Richter and Smith, 2014; Smith et al., 2013a; Smith et al., 2007; Smith et al., 2009)).

However, some aspects of this theory have been considered controversial. The inhibitory ring model would predict that blocking inhibition in the preBötC or the BötC would result in apnea, or cessation of breathing. When Feldman and colleagues tested

this by pharmacologically injecting glycinergic and $GABA_A$ receptor antagonists into the preBötC and BötC in vagotomized rats, they observed little to no effect on the breathing rhythm (Janczewski et al., 2013). They concluded that inhibition is not obligatory for rhythm generation but instead contributes to shaping the pattern of the rhythmic output. Of note, however, the injection of somatostatin, an inhibitory neuropeptide, into the BötC region resulted in the specific elimination of post-inspiratory vagal motor output (Burke et al., 2010).

These experiments were done under the assumption that the BötC was responsible for the generation of post-inspiration. However, as briefly mentioned above, it was recently discovered that the PiCo provides a necessary excitatory drive for the generation of post-inspiratory activity (Anderson et al., 2016). The novel horizontal slice, described by Anderson *et al*., keeps the entire medullary VRC intact, and thus, using this preparation, one can simultaneously record fictive inspiratory bursts (from the preBötC) that are immediately followed by fictive post-inspiratory bursts (from the PiCo) (Anderson et al., 2016) (Figure 1). The PiCo rhythm persists in the absence of inhibition when the network is isolated in a transverse *in vitro* slice immediately rostral to the conventional transverse preBötC slice (Anderson et al., 2016; Ramirez et al., 1998a) (Figure 1). This is similar to the persistence of the preBötC rhythm in the absence of synaptic inhibition *in vitro* (Brockhaus and Ballanyi, 1998; Ren and Greer, 2006; Shao and Feldman, 1997). Similar to the *in vivo* experiment by Burke *et al*. (Burke et al., 2010), the PiCo rhythm was specifically abolished upon the application of somatostatin, with little to no change in the preBötC rhythm. Further experiments are necessary to fully elucidate the role of inhibition between respiratory rhythms *in vivo*.

1.5 Interactions between oscillators

To truly understand how respiration is generated, it is imperative to ascertain the interactions between the different rhythm generators. While this work is far from complete, some progress has been made studying the interactions between the preBötC and the pF_L as well as interactions between the preBötC and the PiCo.

At embryonic day 14.5 (E14.5), before the preBötC is active, the pF_L is rhythmic (Thoby-Brisson et al., 2009). A day later, at E15.5, the preBötC begins to oscillate and rhythmically couples to the pF_L. In postnatal rats, glutamatergic pF_L neurons provide excitatory drive to the preBötC, while the preBötC, in turn, provides inhibitory and excitatory influences on different subsets of pF_L neurons (Onimaru et al., 2007; Takeda et al., 2001). In the *in vivo* adult rat, the preBötC can generate an inspiratory rhythm in the absence of pF_L active expiratory activity (Huckstepp et al., 2015; Huckstepp et al., 2016). However, in the converse situation, in order for the pF_L to be active, a second low level of activity is simultaneously required: either activity from the preBötC or increased chemosensory drive (Huckstepp et al., 2016). Thus, the pF_L drives active expiration, but another source of excitation is required for the network to be rhythmically active.

Neurons in the pF_L are excitatory (Onimaru and Homma, 2008; Thoby-Brisson et al., 2009) and do not express inhibitory biomarkers (Ellenberger, 1999; Tanaka et al., 2003). Therefore, any inhibitory action associated with pF_L activity must be occurring through an intermediate relay of neurons, perhaps from the preBötC (Morgado-Valle et al., 2010). Even excitatory projections from the preBötC to the pF_L appear to be indirect and require an intermediate relay. Neurons in the preBötC send projections rostrally to an area

adjacent to the pF_L, the ventral parafacial nucleus, or pF_V (Tan et al., 2010), which has been shown to provide drive to expiration (Huckstepp et al., 2015; Silva et al., 2016), and could be functioning as the intermediate relay (Huckstepp et al., 2016). While the preBötC and pF_L are anatomically distinct and functionally separate oscillators, the preBötC appears to be dominant, while pF_L activity is conditional and absent at rest.

In contrast, inspiration and post-inspiration are active at rest (Morschel and Dutschmann, 2009), suggesting that this activity may reflect the interaction between anatomically and functionally distinct oscillators, preBötC and PiCo (Anderson et al., 2016). Horizontal slice population recordings of the preBötC and PiCo progressively synchronize when a $GABA_A$ receptor antagonist is applied to the slice. This observation suggests that GABAergic connections between the preBötC and PiCo help to coordinate the timing and phasing of the respiratory rhythms.

Light stimulation of channelrhodopsin-expressing Dbx1 neurons in the preBötC simultaneously evokes inspiratory population activity in the contralateral preBötC and hyperpolarizes a post-inspiratory PiCo neuron (Anderson et al., 2016). However, when this experiment is repeated in the absence of inhibition, light stimulation now both activates an inspiratory population burst and depolarizes the PiCo neuron. Taken together, these results suggest that, under baseline conditions, the preBötC imparts an inhibitory influence on PiCo. However, when inhibition is blocked, it unmasks a concurrent excitatory influence of preBötC onto PiCo.

This work lays the foundation for beginning to understand the dynamic interplay between the three independent rhythm generators. In particular, further studies are needed that probe the interactions between the pF_L and PiCo.

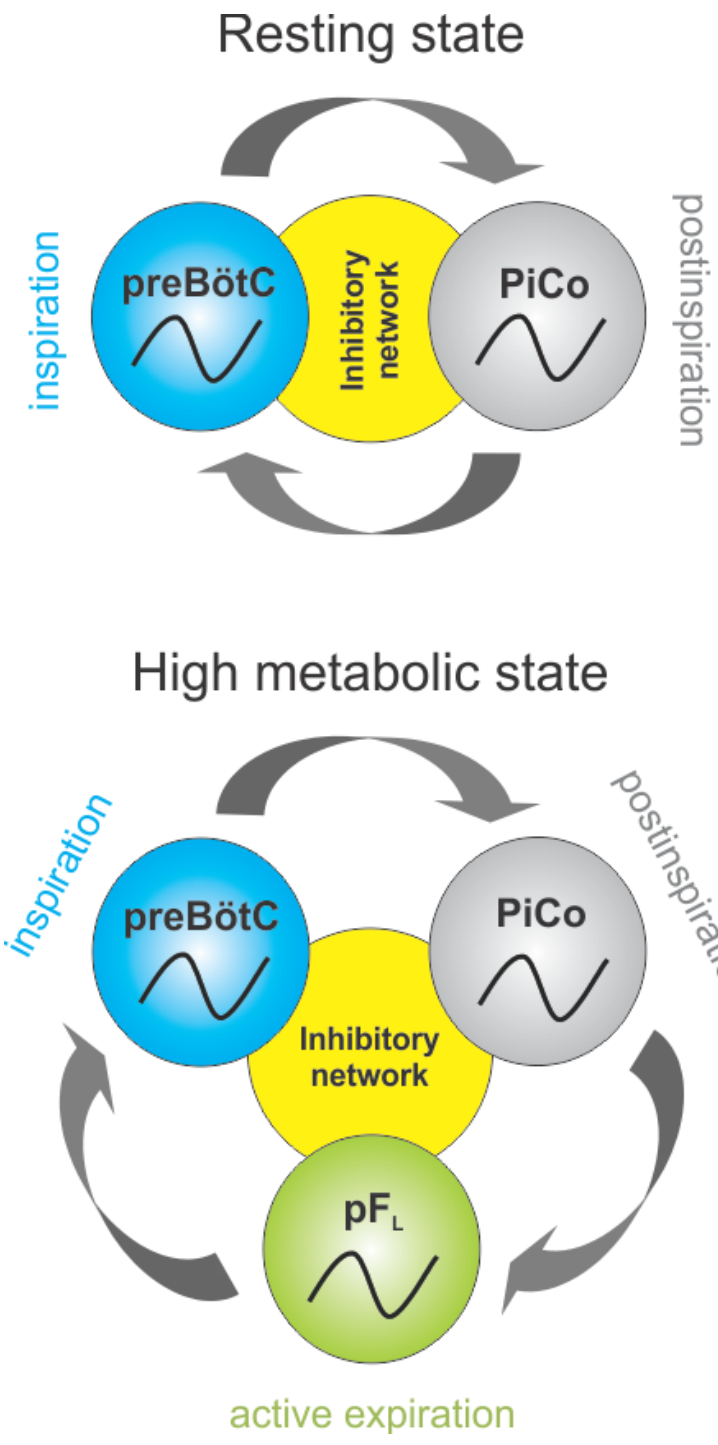
Resting state
inspiration
preBötC
Inhibitory network
PiCo
postinspiration
High metabolic state
inspiration
preBötC
PiCo
postinspiration
Inhibitory network
pF$_L$
active expiration

Figure 2. Illustration of triple-oscillator hypothesis. We propose that at rest, the preBötC and PiCo alternate activity to generate a two-phase rhythm, inspiration and postinspiration. Under periods of high metabolic demand, for instance during exercise, a third oscillator is incorporated to create a three-phase rhythm. We propose that each of the three phases: inspiration, postinspiration, and active expiration are controlled by independent oscillators: the preBötzinger Complex (preBötC), postinspiratory complex (PiCo), and lateral parafacial nucleus (pF_L), respectively. We further postulate that inhibition between these networks coordinates the phasing and timing of the rhythms.

1.6 Conclusion

Reduced preparations that isolate respiratory microcircuits have led to a tremendous understanding of respiratory rhythm generation. Yet, with the availability of ever-more-advanced techniques such as computational modeling, access to transgenic animals, and the possibility of working in intact, alert animals, we will further progress in the unraveling of complex mechanisms.

One of the most established theories for the generation of respiratory rhythms is the dual oscillator hypothesis, which posits that inspiration and expiration are generated by alternating activity between preBötC and RTN/pFRG oscillators and post-inspiration is merely a motor subcomponent of expiration(Feldman and Del Negro, 2006; Janczewski and Feldman, 2006). We propose a triple oscillator hypothesis or that the three phases of breathing in mammals – inspiration, post-inspiration, and active expiration – are generated by anatomically distinct excitatory rhythm generators: the preBötC, PiCo, and the pF_L, respectively (Figure 2). It is interesting to note that three rhythm-generating networks have been hypothesized in the bullfrog(Baghdadwala et al., 2015; Ramirez et al., 2016).

Chapter 2

A novel excitatory network for the control of breathing

*This chapter was published with minor reformatting as a letter with the same title in the peer-reviewed journal, *Nature*. Co-authors of this work included Alfredo J. Garcia 3rd (co-first author), Nathan A. Baertsch, Julia Pollak, Jacob C. Bloom, Aguan D. Wei, Karan G. Rai, and Jan-Marino Ramirez. The full citation is as follows:

Anderson, T.M., Garcia A.J., Baertsch, N.A., Pollak J., Bloom, J.C., Wei, A.D., Rai, K.G., Ramirez, J.M. (August 4th, 2016). A novel excitatory network for the control of breathing. *Nature,* 536: 76-80. doi:10.1038/nature18944

T.A, A.G, and J-M.R. designed all experiments. T.A., A.G., N.B, J.P., J.B., A.W., and K.R. performed the experiments. T.A., A.G., N.B, and J.P. analyzed the data. T.A., A.G., N.B, J.P., and J-M.R. contributed to manuscript preparation. T.A. and J-M.R wrote the manuscript.

2.1 Abstract

Breathing must be tightly coordinated with other behaviors such as vocalization, swallowing, and coughing. These behaviors occur after inspiration, during a respiratory phase termed postinspiration (Richter and Smith, 2014). Failure to coordinate postinspiration with inspiration can result in aspiration pneumonia, the leading cause of death in Alzheimer's disease, Parkinson's disease, dementia, and other neurodegenerative diseases (Troche et al., 2014a). Here we describe an excitatory network that generates the neuronal correlate for postinspiratory activity. Glutamatergic-cholinergic neurons form the basis of this network, while GABAergic inhibition establishes the timing and coordination with inspiration. We refer to this novel network as the postinspiratory complex (PiCo). PiCo has autonomous rhythm generating properties and is necessary and sufficient for postinspiratory activity *in vivo*. PiCo also has distinct responses to neuromodulators when compared with other excitatory brainstem networks. Based on the discovery of PiCo we propose that each of the three phases of breathing is generated by a distinct excitatory network: The preBötzinger complex, which has been linked to inspiration (Huckstepp et al., 2015; Smith et al., 1991), the PiCo as described here for the neuronal control of postinspiration, and the Lateral parafacial region (pF_L) which has been associated with active expiration, a respiratory phase recruited during high metabolic demand (Huckstepp et al., 2015; Pagliardini et al., 2011).

2.2 Main Text

Neurons in phase with postinspiratory activity have previously been identified in the Bötzinger Complex (BötC), a region that is primarily inhibitory (Smith et al., 2009),

(Smith et al., 2007). However, the source of excitation that drives this inhibitory network is not well-defined. Here we identified the location and neurochemical phenotype of an excitatory and rhythmogenic neuronal population that is specifically active during postinspiration.

We developed a horizontal slice preparation in postnatal day (P)5-10 mice that captures the ventral extent of the medulla, including the ventral respiratory column (Alheid and McCrimmon, 2008) (VRC, Fig. 1a, Extended Data Fig. 1), and recorded extracellular, bilaterally-synchronized respiratory rhythmic population activity. Inspiratory population activity was identified within the pre-Bötzinger complex (preBötC) (Fig. 1a) (Ruangkittisakul et al., 2014), a network that is necessary and sufficient for generating inspiration (Smith et al., 1991; Tan et al., 2008). Horizontal slices also generated postinspiratory population activity that: (a) discharged immediately following, but never during, inspiratory activity, and (b) followed sighs generated in the preBötC (Fig. 1a) (Lieske et al., 2000).

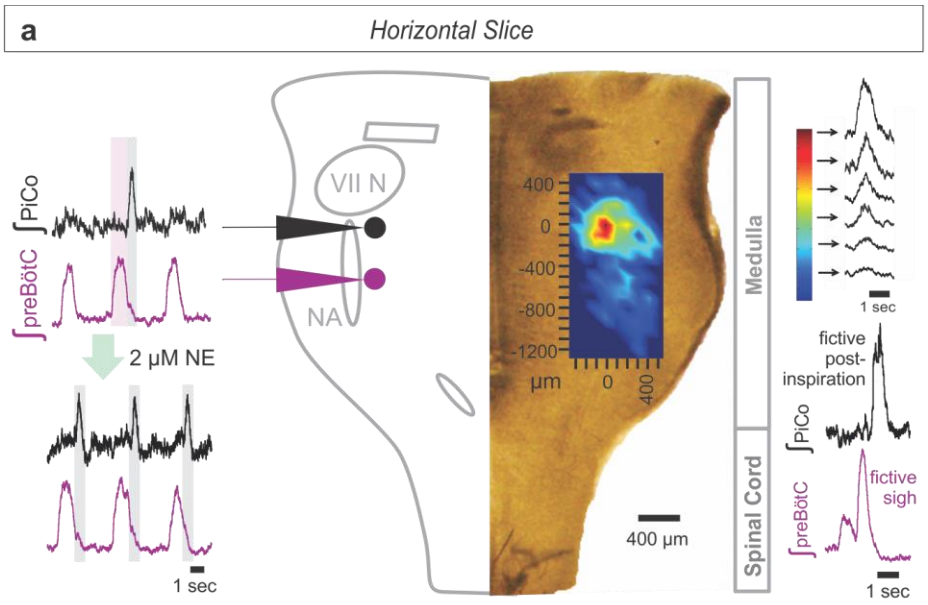
a
Horizontal Slice
∫PiCo
∫preBötC
2 μM NE
1 sec
VII N
NA
400
0
-400
-800
-1200
μm
400 μm
Medulla
Spinal Cord
1 sec
fictive post-inspiration
∫PiCo
fictive sigh
∫preBötC
1 sec

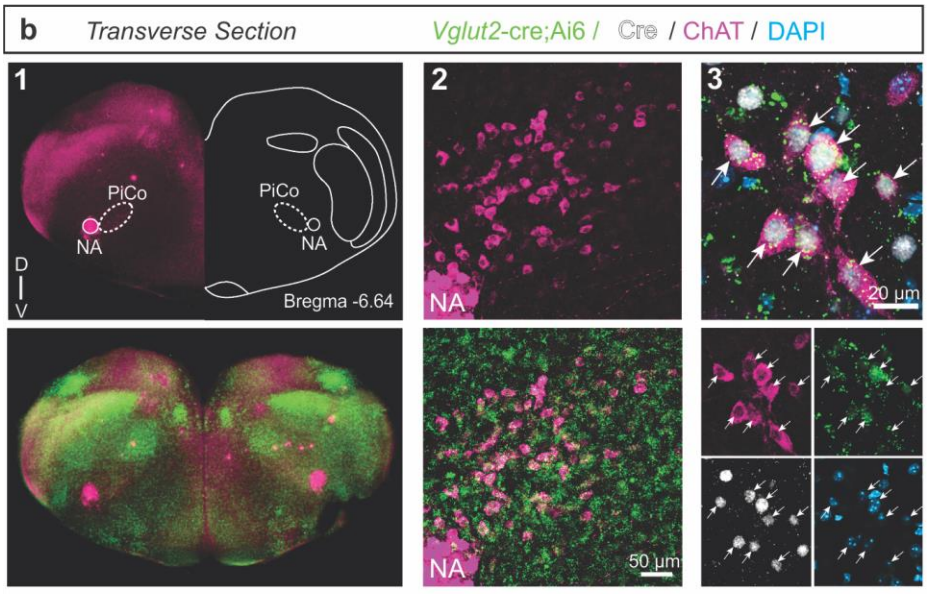
b
Transverse Section
Vglut2-cre;Ai6 / Cre / ChAT / DAPI
1
PiCo
NA
D
V
Bregma -6.64
2
NA
50 μm
3
20 μm

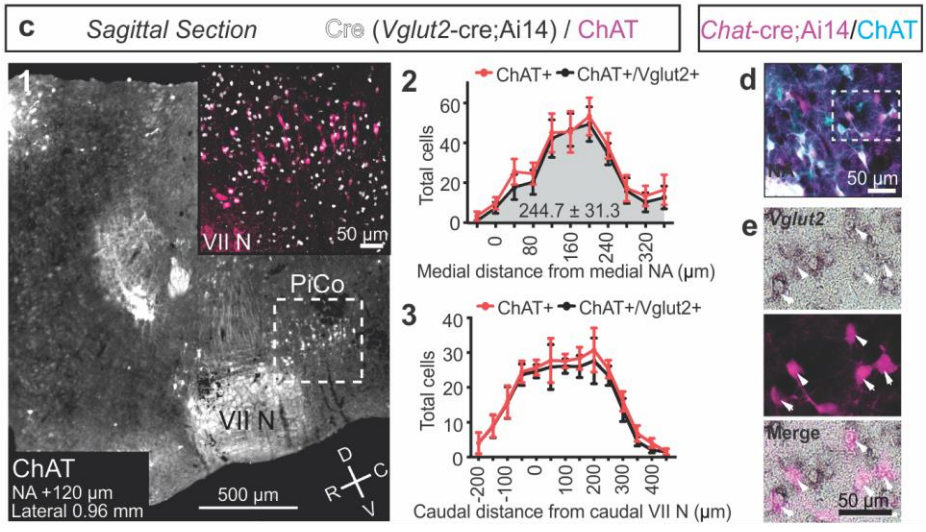
c
Sagittal Section
Cre (Vglut2-cre;Ai14) / ChAT
Chat-cre;Ai14/ChAT
1
VII N
50 μm
PiCo
VII N
ChAT
NA +120 μm
Lateral 0.96 mm
500 μm
D
R
C
V
2
ChAT+ ChAT+/Vglut2+
Total cells
244.7 ± 31.3
Medial distance from medial NA (μm)
3
ChAT+ ChAT+/Vglut2+
Total cells
Caudal distance from caudal VII N (μm)
d
50 μm
e
Vglut2
Merge
50 μm

Figure 1│ **Horizontal slice and anatomy of PiCo. a,** Population bursts PiCo (black), preBötC (purple). 2 µM NE stimulates PiCo bursts (n=23). Left, schematic; right, heat map of PiCo burst amplitude; legend (n=6). PiCo bursts follow fictive sighs. **b1,** Immunohistochemical labeling of PiCo dorsomedial to NA. **b2,** Higher magnification ChAT, *Vglut2*-cre;Ai6 (ZsGreen1) colocalization within PiCo. **b3,** Arrows: higher magnification triple-labeled ChAT+ ZsGreen1+ Cre+ PiCo cells (n=5). **c1,** Sagittal view, ChAT+ PiCo neurons (dashed-box). Inset, magnified dashed-box, colocalization of ChAT+, Cre+ PiCo neurons in *Vglut2*-cre;Ai14 mice. **c2,3,** Quantification of ChAT- and Vglut2-expressing PiCo cells mediolaterally from NA (244.7±31.3 average total # cells; n=5) **c2,** and rostrocaudally from VII N (n=4) **c3,** Bars, mean ± sem. **d,** ChAT+ PiCo neurons, *Chat*-cre;Ai14 mice. **e,** Magnified box (**d)** Arrowheads, *Vglut2* mRNA in *Chat*-derived PiCo neurons.

Postinspiratory bursts spontaneously occurred on average after 1 of 12 preBötC bursts (Fig. 1a, Extended Data Fig. 2). This decreased excitability could be due to the absence of the pons, which provides descending neuromodulatory input, including norepinephrine (NE) (Hilaire et al., 2004). Indeed, postinspiratory activity was exquisitely sensitive to NE. In 2 µM NE postinspiratory population activity occurred with nearly every inspiratory cycle (Fig. 1a, Extended Data Fig. 2). Therefore, we used this NE concentration as a tool to facilitate postinspiratory activity *in vitro*.

Postinspiratory population activity was most pronounced approximately 400 µm rostral to the preBötC, dorsal to the BötC, and caudal to the facial (VII) nucleus. We refer to this area as the Postinspiratory Complex (PiCo, Fig. 1a; Extended Data Fig. 1). To assess the distribution of postinspiratory activity, we positioned one electrode in the PiCo region and a second electrode contralaterally to map the amplitude of postinspiratory population activity across the VRC (Fig. 1a). Postinspiratory activity was concentrated rostral to the preBötC, but extended caudally and partially overlapped with inspiratory activity.

PiCo was anatomically characterized by immunohistological labelling of transverse sections (Fig. 1b1) revealing that ChAT (choline acetyltransferase)-positive cholinergic and Vglut2 (vesicular glutamate transporter 2)-expressing glutamatergic neurons in the *Vglut2*-cre;Ai6 mouse co-localized in PiCo, dorsomedial to Nucleus ambiguus (NA) (Fig. 1b1-b3). In contrast, ChAT-positive neurons in NA lacked substantial Vglut2 expression (Extended Data Fig. 3). In the sagittal plane, ChAT and Vglut2 co-labelled PiCo neurons were located dorsal and caudal to the VII nucleus (Fig. 1c1). Quantifying ChAT and Vglut2 co-expression revealed that PiCo mainly extends from 40 to 280 □m medial to the NA (Fig. 1c2) and 50 to 250 □m caudal to the VII nucleus caudal border (Fig. 1c3). In situ hybridization confirmed expression of *Vglut2* mRNA in *Chat*-derived PiCo neurons from transverse sections of *Chat*-cre;Ai14 mice (Fig. 1d,e).

The Cre-dependent reporter line Ai27, which conditionally expresses channelrhodopsin-2 (ChR2) fused to td-Tomato in the presence of a selective, promoter-driven Cre, allowed for photo-stimulation of specific neuronal sub-populations(Madisen et al., 2012). PiCo neurons were recorded from *Vglut2*-cre;Ai27 and *Chat*-cre;Ai27 horizontal slices. Membrane depolarization of tetrodotoxin (TTX) isolated PiCo neurons during light stimulation demonstrated that functionally identified postinspiratory cells were glutamatergic and cholinergic (Fig. 2a), consistent with the histological results. PiCo neurons generated neither pre-inspiratory bursts nor a biphasic discharge typical of pre-inspiratory neurons in the retrotrapezoidal nucleus parafacial respiratory group (RTN/pFRG) region (Onimaru et al., 1989).

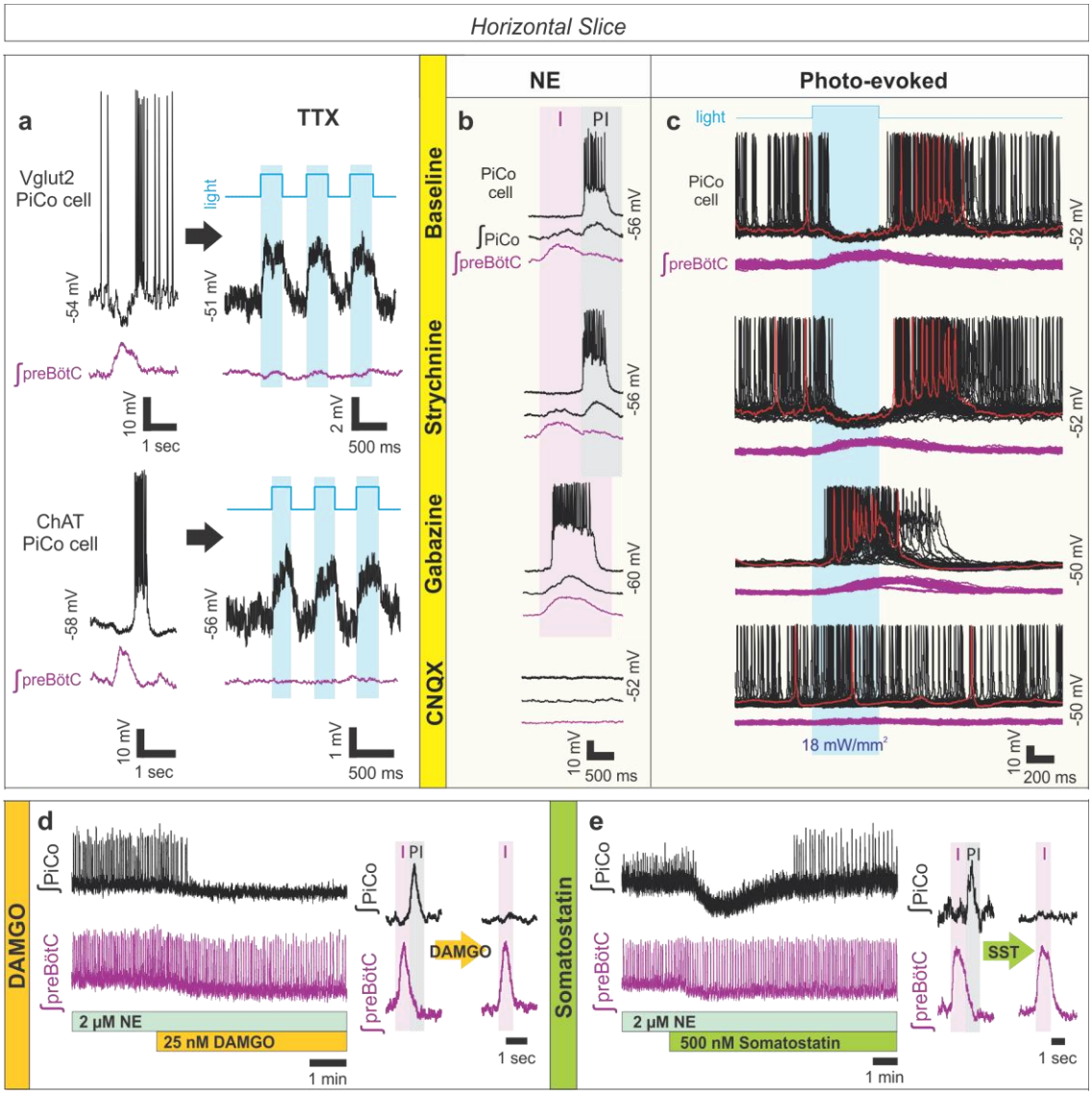

Figure 2 | Glutamatergic, cholinergic PiCo cells and role of synaptic inhibition. a, Intracellular PiCo recordings in *Vglut2*-cre;Ai27 (n=3) and *Chat*-cre;Ai27 (n=5) horizontal slices. Photo-stimulation after TTX depolarizes membrane potential. **b,** PiCo, preBötC in progressive synaptic block (n=5). Rhythms synchronized in gabazine, bursting abolished in CNQX. **c,** PiCo cell in *Dbx1*-cre;Ai27 horizontal slice with progressive synaptic block. PiCo cell inhibited during photo-evoked inspiratory burst in NE/strychnine, bursts with light-stimulation in gabazine, ceases bursting in CNQX (500 ms light, 40 sweeps, n=4). **d,** PiCo bursting eliminated by 25 nM DAMGO; representative bursts (n=5). **e,** PiCo inhibited by 500 nM SST; representative bursts (n=6).

Postinspiratory population activity was unaffected by bath-applied strychnine to block glycinergic inhibition (Fig. 2b, Extended Data Fig. 4). However, PiCo and preBötC

bursts progressively synchronized following blockade of GABAergic inhibition with gabazine, in the presence (Fig. 2b, Extended Data Fig. 5) or absence (data not shown) of strychnine. The burst area of postinspiratory activity was increased during the blockade of synaptic inhibition (Extended Data Fig. 4), indicating that the PiCo rhythm is modulated, but not generated, by inhibitory mechanisms. Inspiratory and postinspiratory bursts persisted following NMDA receptor blockade (CPP, data not shown), while bursting was abolished following non-NMDA glutamatergic blockade (CNQX, Fig. 2b). We conclude that inspiratory and postinspiratory activities are generated by glutamatergic, non-NMDA dependent mechanisms, while the timing of inspiratory and postinspiratory bursts is established by GABAergic mechanisms.

Inspiratory rhythm generating neurons in the preBötC are derived from Dbx1 expressing progenitor cells (Gray et al., 2010). To explore whether these neurons interact with PiCo, we utilized a tamoxifen inducible transgenic line (*Dbx1*-cre-ERT2;Ai27) in which *Dbx1*-positive cells born after embryonic day (E)10.5 express channelrhodopsin-2. Photo-stimulating preBötC neurons in horizontal slices from *Dbx1*-cre-ERT2;Ai27 animals inhibited all recorded PiCo neurons in 2 µM NE and in strychnine (Fig. 2c). In gabazine, this light-evoked inhibition was eliminated. The blockade of GABAergic inhibition revealed that PiCo neurons also received excitatory input from the preBötC, which was blocked by CNQX (Fig. 2c). Thus, inspiratory activity involving *Dbx1*-derived neurons concurrently excites and inhibits PiCo neurons via glutamatergic and GABAergic mechanisms, respectively; however, under normal conditions, GABAergic interactions dominate over the concurrent glutamatergic excitation from the preBötC (Fig. 2c).

Since PiCo neurons co-express acetylcholine and glutamate (Fig. 1), we tested whether the postinspiratory rhythm depends on cholinergic mechanisms. Atropine, a muscarinic receptor antagonist, but not mecamylamine, a nicotinic receptor antagonist, depressed postinspiratory burst frequency. However, postinspiratory bursting persisted in the presence of both blockers and returned to near baseline frequency by raising NE to 4 µM (Extended Data Fig. 6). Thus, PiCo rhythms are modulated by, but not dependent on, cholinergic mechanisms.

PiCo neurons were intrinsically sensitive to the µ-opioid receptor agonist DAMGO (Extended Data Fig. 7). In horizontal slices, PiCo population bursts were nearly eliminated by 25 nM DAMGO, whereas burst frequency in the preBötC was only slightly decreased (Fig. 2d, Extended Data Fig. 8). This exquisite opioid sensitivity unambiguously differentiates PiCo from the previously described RTN/pFRG, a region that is thought to contain the network generating active expiration (Huckstepp et al., 2015) and known to be insensitive to µ-opioid receptor activation (Janczewski and Feldman, 2006). The peptide somatostatin (SST) had little effect on preBötC activity, but inhibited postinspiratory PiCo activity (Fig. 2e, Extended Data Fig. 8). These data are consistent with the inhibition of postinspiration *in vivo* (Burke et al., 2010).

Optogenetic stimulations of ChAT-positive neurons always elicited postinspiratory bursts recorded from PiCo in horizontal slices. These stimulations never evoked an inspiratory burst (Extended Data Fig. 9), nor burst activity in intracellularly recorded NA neurons (data not shown). Because of the specificity for postinspiratory activity, we utilized adult *Chat*-cre;Ai27 animals to stimulate PiCo *in vivo*. Similar to *in vitro* results, optogenetic activation of ChAT-positive neurons at the level of PiCo (Fig. 3a-c) reliably

evoked bursts in the cervical vagal nerve (cVN) (Fig. 3d, Extended Data Fig. 9). Photo-evoked postinspiratory bursts delayed the subsequent inspiration (Fig. 3d,e, Extended Data Fig. 8). This delay was eliminated following bilateral injection of DAMGO into PiCo (Extended Data Fig. 10). Thus, postinspiration has a mutual inhibitory relationship with inspiratory activity.

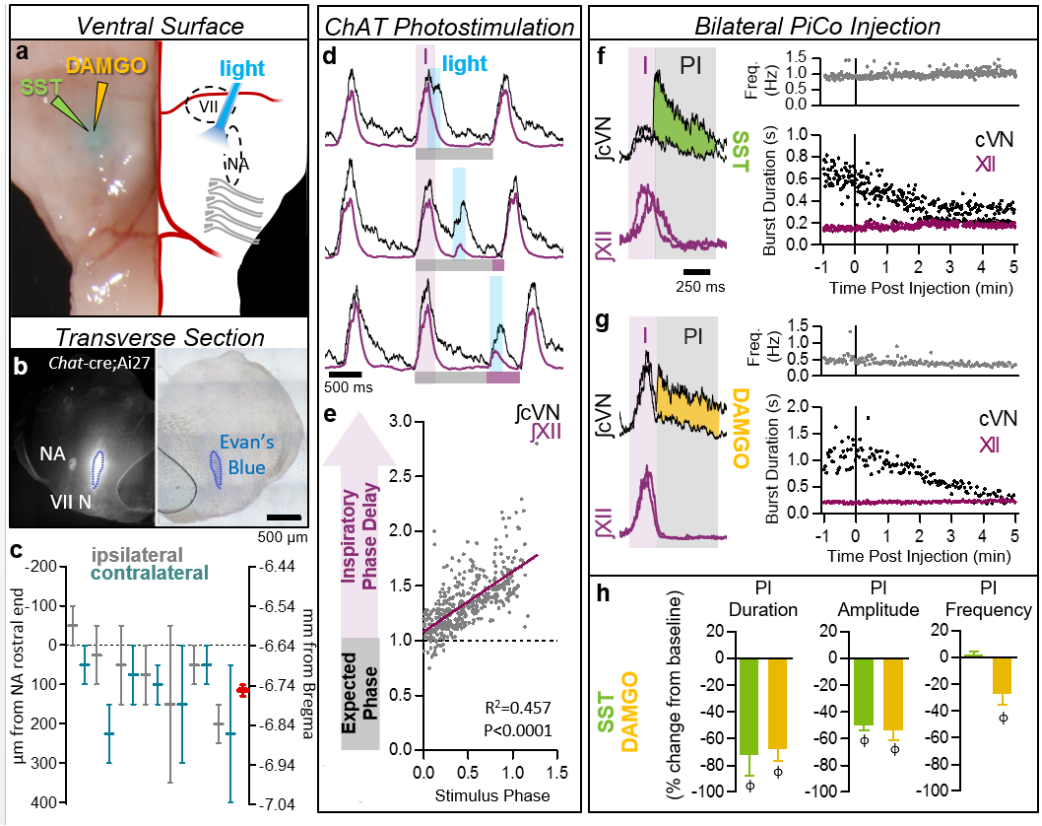

Figure 3 | Stimulation and inhibition of PiCo *in vivo*. a, Left, brightfield image; right, schematic; ventral sites for bilateral photo-stimulation, injection of SST/DAMGO *in vivo*. **b,** Representative dye injection at PiCo level. Left, *Chat*-cre;Ai27; right, brightfield. **c,** Dye-spread (n=7), centered at PiCo (0-200 µm caudal from rostral NA). Ipsilateral (grey), contralateral (teal) injections, bars ±max/min; pooled data in red, mean ± s.e.m. **d**, PiCo photo-stimulation in adult *Chat*-cre;Ai27 mice evokes vagal bursts and delays subsequent inspiration (grey bars = expected inspiratory phase, purple bars = inspiratory phase delay) **e**, Quantification of inspiratory phase delay (n=6); magnitude dependent on stimulus phase (slope: 0.549, linear regression analysis). **f,g,** Injection of

SST or DAMGO progressively decreases cVN, not XII burst duration. **h,** Postinspiratory burst duration, amplitude, and frequency following injection of SST (n=3), DAMGO (n=4). Two-tailed paired t-test, ϕ $P<0.05$ compared to baseline; mean ± s.e.m.

To assess whether PiCo is responsible for generating postinspiratory motor output *in vivo*, we took advantage of PiCo's sensitivity to SST and DAMGO. Injecting SST or DAMGO bilaterally into PiCo *in vivo* (Fig. 3a-c) dramatically reduced spontaneous vagal postinspiratory burst duration and amplitude (Fig. 3f-h). Collectively, these results suggest that PiCo is both necessary and sufficient for generating postinspiratory activity.

Moreover, PiCo seems to possess autonomous rhythmogenic properties. In horizontal slices, NE concentrations above 2 µM generated ectopic PiCo population bursts that outpaced the preBötC rhythm (Fig. 4a, Extended Data Fig. 2). Ectopic bursts occurred in any phase of the inspiratory cycle except during preBötC bursts (Fig. 4b), consistent with photo-evoked PiCo bursts (Extended Data Fig. 9).

To further test the possibility that PiCo is an autonomous rhythm generator, we separated the VRC into two adjacent rostral and caudal transverse slices (Fig. 4c). Together, these slices span a total length of 1-1.1 mm of the rostrocaudal VRC beginning with the caudal portion of the VII nucleus. Recording from the caudal face of each transverse slice revealed a slower rhythm in the rostral transverse slice containing PiCo compared to the caudal slice containing the preBötC (Smith et al., 1991),(Lieske et al., 2000) (Fig. 4c). In 2 µM NE, both transverse slices exhibited regular rhythmic activities with similar burst frequencies (Fig. 4c, Extended Data Fig. 2) that persisted in the presence of strychnine, gabazine, and CPP, but were abolished in CNQX (Extended Data Fig. 4), resembling the findings in horizontal slices. Consistent with our histological characterizations, optogenetic stimulation of either *Vglut2*-cre;Ai27 or *Chat*-cre;Ai27

rostral slices evoked population bursts in PiCo (Fig. 4d). This provides additional evidence that glutamatergic/cholinergic neurons are important for rhythm generation within the PiCo network. Furthermore, PiCo activity was exquisitely sensitive to DAMGO and SST in isolated transverse slices (Extended Data Fig. 8). We conclude that PiCo and preBötC can function as independent oscillators with similar rhythm generating, but distinct modulatory properties.

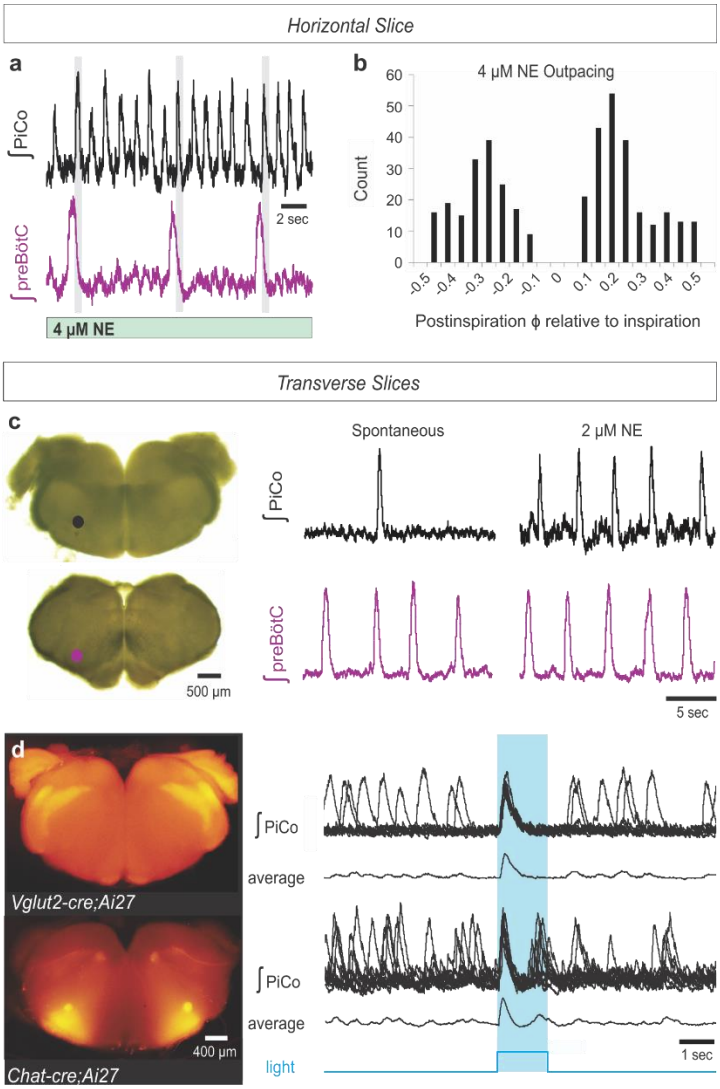

Figure 4 | PiCo is an autonomous, rhythm generating network. **a**, In 3-4 μM NE, PiCo outpaces the preBötC rhythm, but still bursts in the postinspiratory phase (gray bars) in horizontal slices. **b,** PiCo bursts occur in any phase except during inspiration (inspiratory peak=0; count=400 bursts; n=4). **c,** PiCo and preBötC isolated in transverse *in vitro* slices; PiCo bursting stimulated by 2 μM NE (n=33). **d,** Light stimulation evokes a burst in *Vglut2*-cre;Ai27 rostral transverse slices (91.3 ± 5.1% of stimulations, mean ± s.e.m., n=4) and *Chat*-cre;Ai27 slices (91.9 ± 1.8% of stimulations, mean ± s.e.m., n=6). 1.5 second light pulse. Top traces: 10 sweep overlay, bottom traces: sweep average.

As an excitatory rhythmogenic network, PiCo may not only be involved in the context of breathing, but might also contribute to the generation of other postinspiratory behaviors such as swallowing and vocalization. While behavioral assays were not performed in this study, various types of postinspiratory burst waveforms were observed in the vagal nerve (Extended Data Fig. 10) that were similarly affected by the manipulation of PiCo, supporting a potential broad role of this network in postinspiratory activities. In this context it will be interesting to (a) resolve the role of PiCo in specific postinspiratory behaviors and (b) identify how PiCo interacts with other neural networks such as the Kölliker-Fuse Nucleus, a pontine structure that has been hypothesized to gate postinspiratory activity (Dutschmann and Herbert, 2006), and the periaqueductal gray, a structure involved in vocalization and the control of postinspiration (Subramanian and Holstege, 2011).

Based on these results, we propose a triple oscillator model, wherein the three phases of breathing, inspiration, postinspiration, and active expiration, are generated by three spatially distinct excitatory rhythmogenic microcircuits, the preBötC, PiCo, and pF_L, respectively, which are temporally coordinated by inhibitory interactions. The existence of discrete excitatory networks may facilitate the differential and dynamic control of ventilatory and non-ventilatory behaviors. Coupled oscillators (Grillner, 2003) have also

been hypothesized for networks controlling locomotion (Kiehn, 2006), scratching (Stein, 2005), swimming (Wiggin et al., 2012) and the circadian clock (Evans et al., 2010). Thus, this network organization may constitute a general principle of rhythm generation that promotes flexible control of complex biological processes.

2.3 Materials and methods

2.3.1 Animals

All experiments were performed with the approval of the Institute of Animal Care and Use Committee of the Seattle Children's Research Institute. Mice were maintained with rodent diet and water available *ad libitum* in a vivarium with a 12 h light/dark cycle at 22°C. In this study, we utilized both CD1 Swiss mice and Cre reporter mice generated on a C57BL/6 background. Ai27 mice were bred to conditionally express Channelrhodopsin-2 (H134R) fused to tdTomato inserted in the *ROSA26* locus [B6.Cg–*Gt(ROSA)26Sor*$^{tm27.1(CAG-COP4*H134R/tdTomato)Hze}$/J; The Jackson Laboratory]. Ai6 mice were bred to express a green fluorescent protein ZsGreen1 inserted in the *ROSA*26 locus [B6.Gt(ROSA)26Sor$^{tm6(CAG-ZsGreen1)Hze}$; The Jackson Laboratory]. Similarly, Ai14 mice were bred to express a red fluorescent protein tdTomato inserted into the *ROSA*26 locus [Gt(ROSA)26Sor$^{tm14(CAG-tdTomato)Hze}$; The Jackson Laboratory]. Cre-driver mice expressed Cre recombinase under the control of subtype-specific promoters, including *Chat*-cre (B6;129S6–*Chat*$^{tm2(cre)Lowl}$/J; The Jackson Laboratory) and *Vglut2*-cre (B6;Slc17a6$^{tm2(cre)Lowl}$; Bradford Lowell). *Dbx1*-cre-ERT2 (*Dbx1*^{CreERT2}; (Gray et al., 2010),(Hirata et al., 2009)) dams were bred with Ai27 males and pregnancies were timed and monitored. We intraperitoneally injected tamoxifen [25 mg/kg; from 10 mg tamoxifen

(Sigma-Aldrich) dissolved per mL of corn oil] on embryonic day (E)10.5. Mice were typically born after 20 days of gestation. No method of randomization was used to determine how animals were allocated to experimental groups and the investigators were not blinded when analyzing data in this study.

2.3.2 *In Vitro* Slice Preparations:

We dissected the ventral respiratory column (VRC) using three types of brainstem slices: (1) A “caudal” transverse slice that contains the preBötC as previously described (Lieske et al., 2000; Smith et al., 1991), (2) a rostral transverse slice that encompasses the BötC and caudal portions of the VII nucleus, and (3) a horizontal slice that bilaterally isolates the VRC extending from the VII nucleus to the spinal cord. Slices were obtained at postnatal day (P)5-10 from CD1 and transgenic C57BL/6 mice. Animals were anesthetized via rapid hypothermia on ice before quick decapitation at spinal cervical level C4-C5. The three slices types were differentiated by the cutting angle, plane and thickness of the slice.

For transverse slices, the head was pinned in a tissue-culture dish filled with a silicone elastomer (Sylgard). Skin and connective tissues were removed, and fine scissors were used to cut along skull sutures to separate the interparietal region of the skull and expose the cerebellum. A one-sided razor was used to make a single cut between the inferior colliculus and cerebellum. The brainstem was isolated by removing the cerebellum in ice-cold, oxygenated (95% O_2, 5% CO_2) artificial cerebrospinal fluid (aCSF) containing (in mM): 128 NaCl, 3 KCl, 1.5 $CaCl_2$, 1 $MgCl_2$, 24 $NaHCO_3$, 0.5 NaH_2PO_4, and 30 D-glucose (pH 7.4, 305-312 mOSM). A slanted (~15° from vertical)

agar block was secured on a specimen tray, and then the isolated brainstem and spinal cord preparation was glued with cyanoacrylate to the slanted portion of the agar such that the rostral end was facing upward and the dorsal side was glued to the agar. Serial transverse slices proceeded on a vibratome until visual landmarks became clear. Once the 4th ventricle was completely open, a 550 µm slice was taken to obtain the rostral transverse slice containing PiCo. The caudal face of this slice was characterized by containing the rostral-most portion of the NA and the caudal portion of the VII nucleus. The subsequent 550 µm slice isolated the caudal transverse slice. This caudal slice was identical to the well-established transverse slice known to contain the preBötC (Lieske et al., 2000). From an individual animal we routinely obtained both the rostral and the caudal slice preparation and recorded from the caudal side of each of the transverse slices in the same recording chamber.

To obtain the third type of slice preparation, the horizontal slice, the brainstem was mounted as described for the transverse slices. Serial coronal slices were taken from the rostral end of the brainstem until the facial nerves became visible, approximately 800-1000 µm. The agar block was then removed from the specimen tray and reoriented so that the ventral surface of the brainstem faced upward and the blade advanced toward the rostral portion of brainstem. The preparation was angled so that the ventral-most portion of the medulla was approximately level with the ventral-most portion of the spinal cord. The blade was positioned level to the rostroventral edge of the brainstem, stepped 900 µm downward (in the dorsal direction), and a single horizontal slice was cut retaining the ventral portion of the brainstem and spinal cord. The horizontal slice preserves long-range bilateral network interactions throughout the rostral-caudal axis of the VRC.

2.3.3 *In Vitro* Electrophysiology:

All slices were immediately transferred to the recording chamber, where they were superfused with aCSF at a rate of 10 mL/minute, bubbled continuously in carbogen (95% O_2 and 5% CO_2) to oxygenate and adjust pH to 7.4, and allowed to equilibrate to experimental temperature (33 ± 2 degrees Celsius, thermoneutral zone for mice). Population activity was obtained by raising the extracellular potassium concentration from 3 mM to 8 mM in two steps over 30 minutes. This is defined as “spontaneous conditions”.

Population activity was routinely recorded with borosilicate glass microelectrodes (World Precision Instrument) pulled on a Flaming/Brown micropipette puller (model P97, Sutter Instrument Co., <1 MOhm tip resistance) that are placed on the slice surface. Signals were amplified, filtered, and integrated as previously published (Hill et al., 2011). Automated burst analysis software was used to determine population recordings of burst frequency and amplitude (Telgkamp et al., 2002).

The mapping experiment (Fig. 1a) was performed by placing a reference extracellular electrode upon PiCo and a second, mapping extracellular electrode on the contralateral side of a horizontal slice. The mapping electrode was systematically moved in 100 µm stereotaxic steps rostral, caudal, medial, and lateral to PiCo. Postinspiratory burst amplitudes from the mapping electrode were normalized to that from the reference electrode to create a heat map of activity.

In horizontal and rostral transverse slices from transgenic mice expressing ChR2 in a subset of neurons, PiCo (contralateral to the recording electrode) was light stimulated by using fiber optic (DPSSL Driver, blue 473 nm wavelength, 200 µm diameter, <22

mW/mm^2 intensity) for 500 ms or 1.5 s. Collections of 10 or 40 sweeps were recorded in succession (shown overlaid).

Intracellular blind patch recordings were performed on PiCo neurons. Borosilicate glass patch electrodes (with filaments, World Precision Instruments) were pulled (P-97 Flaming/Brown micropipette puller, Sutter Instrument Co.) to a 6-12 MΩ resistance. Electrodes were filled with an intracellular patch solution containing (in mM): 140 K-gluconic acid, 1 CaCl2, 10 EGTA, 2 MgCl2, 4 Na2ATP, 10 HEPES (pH = 7.4). Whole cell patch-clamp recordings were obtained in current clamp configuration using a Multiclamp 700B amplifier (Molecular Devices) sampling at 20 kHz. Extracellularly recorded signal was sampled at 1.67 kHz, amplified 10,000 times, filtered (low pass, 1.5 kHz; high pass, 250 Hz), rectified, and integrated using an electronic filter. Both extracellular and intracellular recordings were obtained with Clampex 10.0 (Molecular Devices). Recordings were stored on a computer for post-hoc analysis.

Receptor antagonists and neuromodulators were bath perfused during *in vitro* extracellular and intracellular recordings. All stock solutions were stored at -20°C in small-volume aliquots to avoid repetitive freezing and thawing. Strychnine (1 µM, glycine receptor antagonist, Sigma Aldrich) and SR 95531 hydrobromide (gabazine, $GABA_A$ receptor antagonist, 10 µM, Tocris) were used to block inhibitory synaptic transmission. To further block all fast synaptic transmission, 3-((±)2-carboxypiperazin-4yl)propyl-1-phosphate (CPP, NMDA receptor antagonist, 10 µM, Tocris) and 6-Cyano-7-nitroquinoxaline-2,3-dione (CNQX, AMPA receptor antagonist, 20 µM, Alimony Labs, diluted in DMSO) was bath applied. To block action potentials, 1 µM tetrodotoxin (TTX, Sigma-Aldrich) was used. To block cholinergic receptors, 10 µM atropine, a muscarinic

receptor antagonist (Sigma-Aldrich) and 1 µM mecamylamine hydrochloride, a nicotinic receptor antagonist (Sigma Aldrich) were bath applied. To stimulate the PiCo rhythm, DL-norepinephrine hydrochloride (NE, 1-4 µM, Sigma-Aldrich) was used; and to inhibit the PiCo rhythm, [D-Ala^2, N-Me-Phe^4, Gly^5-ol]-Enkephalin (DAMGO, 1-300 nM, Sigma-Aldrich) and Somatostatin (SST, 500 nM, Tocris) were applied.

2.3.4 *In Vivo* Electrophysiology

Adult mice were prepared as described previously (Doi and Ramirez, 2010). *Chat*-cre;Ai27 mice (P)140-250 were anesthetized with urethane (1.5 g/kg), placed in a supine position, and the head was stabilized with ear bars. The trachea was exposed via a cervical midline incision and cannulated with a U-shaped tracheal tube. For the remainder of the surgery and experimental protocol, mice were allowed to spontaneously breathe humidified O_2 (FiO_2=100%). The rostral ends of the trachea and esophagus were removed, followed by removal of the muscle and bone covering the ventral brainstem so that the vertebral and basilar arteries were visible. The dura and arachnoid membranes were removed followed by continuous perfusion of the ventral medullary surface with 95% O_2/5% CO_2 equilibrated aCSF solution at 37 ± 0.5°C. The hypoglossal nerve (XII) and cervical vagus nerve (cVN) were isolated, cut, and their activity was measured using a suction electrode containing aCSF. Signals were amplified, bandpass filtered (8 Hz to 3 kHz), and digitized with a Digidata 1400 and pClamp 10 software (Molecular Devices).

After completion of the surgery, mice were allowed to stabilize for 15 min prior to obtaining 15-20 min of baseline respiratory activity. Using the vertebral and basilar arteries as landmarks (Fig. 3a-c), 200 µm diameter optical fibers coupled to a 447 nm

DPSSL Driver lasers at (intensity < 230 mW/mm^2) were placed bilaterally on the ventral surface of the medulla above the region containing PiCo. XII and cVN activity were recorded during 10 second episode files containing a 200 ms light pulse to stimulate *Chat*-cre;Ai27 expressing cells. Inspiratory and postinspiratory (spontaneous or light-evoked) activity was analyzed using Clampfit 10 software (Molecular Devices). The phase of evoked cVN postinspiratory activity was determined as the fraction of the inspiratory cycle (Extended Data Fig. 9) or the fraction of the average duration of the preceding two inspiratory cycles ("expected phase", Fig. 3e). The inspiratory phase duration during cycles containing a light-evoked PiCo burst were then divided by the expected phase to determine the "phase-delay" (Fig. 3e). In some mice, PiCo was photo-stimulated before and after bilateral injection of 5 μM DAMGO to assess the effect of DAMGO on the inspiratory phase-delay (Extended Data Fig. 10).

To test whether PiCo activity is necessary for postinspiration *in vivo*, pulled micropipettes containing somatostatin (SST; 750 μM) or DAMGO (5 μM), and either Evan's Blue or Fast Green to identify the injection site, were inserted (300-400 μm) bilaterally into PiCo. Spontaneous postinspiratory burst amplitude, duration, and frequency were then quantified 3-5 min following a 250 nL injection of either SST or DAMGO and compared (student's t-test) to pre-injection values (GraphPad, Prism 5 software). Postinspiratory burst duration was determined by subtracting the duration of XII nerve inspiratory activity from the duration of the corresponding cVN burst. Postinspiratory amplitude was defined as the amplitude of cVN activity immediately following XII nerve inspiratory activity. Following experimental protocols mice were perfused with 4% paraformaldehyde (PFA), and brainstems were extracted and

cryoprotected (30% sucrose in PBS). Brainstems were then serially sectioned to identify sites of injection.

2.3.5 Immunohistochemistry

200 µm rostral transverse slices from *Vglut2*-cre;Ai14 were fixed with 4% PFA for 1 hour and immunostained as whole-mounts. Slices were washed in PBST (0.1-0.5% Triton X-100), blocked with 10% donkey serum in PBST overnight at 4°C, incubated for 2-3 days in primary antibody in blocking solution at 4°C, washed in PBST, incubated in secondary antibody in blocking solution for 5-8 hr at room temperature, washed in PBST, counterstained with 0.01% DAPI (Life Technologies), and mounted in Fluoromount-G (SouthernBiotech). 40 µm sagittal sections from *Vglut2*-cre;Ai14 mice were also immunolabeled for quantification. Animals were transcardially perfused with 4% PFA, and brainstems were postfixed in 4% PFA overnight. Isolated brainstems were transferred through increasing sucrose gradients (10-30%), embedded in OCT compound (TissueTek), frozen, and cryosectioned. Immunohistochemical labeling followed the same protocol as for whole-mounts with shortened incubation times. Primary antibodies included anti-ChAT (1:100, AB144P, Millipore) and anti-Cre Recombinase (1:200, 908001, BioLegend). Secondary antibodies were Alexa Fluor 568- or 647-conjugated (1:250, Life Technologies). Maximum intensity projections of optical slice z-stacks were acquired using a Zeiss 710 Quasar 34-channel LSCM (Carl Zeiss). Cre-labeled images were despeckled for background noise reduction.

2.3.6 Cell Counting

Maximum intensity projections of 20x optical slice z-stacks were collected -40 to 360 µm medial to the medial end of NA. ChAT+ and Cre+ or tdTomato+ cells were counted within this area, with the exception of ChAT+ cells that clearly belonged to the NA or VII nucleus (distinctive due to location and large cell size). Counts from each hemisphere were averaged for individual animals. Counts in the rostrocaudal direction were taken from sagittal slices 40 to 280 µm medial to the medial end of NA, where PiCo cells are most abundant. ChAT+ and Cre+ or tdTomato+ were counted in 50 µm bins through the rostrocaudal extent and summed across the 240 µm span. For *in vivo* experiments, 50 µm serial transverse brainstem sections were cryopreserved and processed as described above. Sections were imaged through the region encompassing the injection site and noted for the presence of Evan's blue or Fast Green dye. *Chat*-cre;Ai27 expression identified the rostral end of the NA in order to quantify the rostrocaudal location of injection sites relative to NA. Anatomical diagrams and coordinates were based on the adult mouse brain atlas[31].

2.3.7 In situ hybridization

(P)8-11 animals were perfused with 4% PFA (0.1M sodium phosphate, pH 7.0), and brainstems were post-fixed in 4% PFA (0.1M sodium phosphate, pH 7.0) + 4% sucrose, overnight at 4°C. Isolated brainstems were submerged in 30% sucrose, embedded in OCT, frozen at -80°C, and cryosectioned at 20 µm. Prior to hybridization, sections were fixed with 4% PFA/DEPC-PBS, pH 7.0 at 4°C for 5 min, treated with Proteinase K (1 µg/mL) for 10 min at room temperature, fixed with 4% PFA/DEPC-PBS, pH 7.0 at 4°C for 5 min, and acetylation for 10 min at room temperature. DIG labeled *Vglut2*-Dig antisense RNA probe [306 bp fragment of *Vglut2* (1563-1869bp, XM_006540602)] was hybridized onto sections (0.8 µg/mL) at 42°C overnight. Following hybridization, sections were incubated with RNase A (50 µg/mL, Invitrogen) for 30 min at 37°C. DIG Nucleic acid detection kit (Roche) was used for RNA probe detection. The sections were incubated in anti-Digoxigenin-AP conjugate (Roche Applied Science, sheep, 1:1000) for 1 hr at room temperature. Hybridized molecules were visualized after incubation in an enzyme-catalyzed color reaction with a solution of 5-bromo-4-chloro-3-indolyl phosphate (BCIP) and nitroblue tetrazolium salt (NBT) (Roche Applied Science). The sections were developed in the BCIP/NBT solution for 2 hr in the dark at room temperature. The enzyme-catalyzed color reaction was stopped with TE, pH 8.0 and fixed in 4% PFA, pH 7.0 for 20 min at 4°C.

2.3.8 Statistics

All statistics were performed using GraphPad Prism 5. Numerical data are reported as the mean ± s.e.m. Normality was determined by D'Agostino-Pearson normality test.

For normally distributed data, statistical significance was assessed by two-tailed paired Student's *t*-tests and two-way ANOVAs where appropriate. Two-way ANOVAs were followed by Bonferroni *post-hoc* correction. For data that were not normal, we used non-parametric two-tailed Mann Whitney, Kruskal-Wallis, one-way ANOVA, and repeated measures Friedman tests where appropriate. Kruskal-Wallis and Friedman tests were followed by Dunn's multiple comparison *post-hoc* tests. Variance was similar between groups that were statistically compared. Results were considered significant when $P < 0.05$. α was set less than or equal to 0.05 for multiple comparison tests. Sample sizes were chosen on the basis of previous studies.

2.4 Extended Data Figures

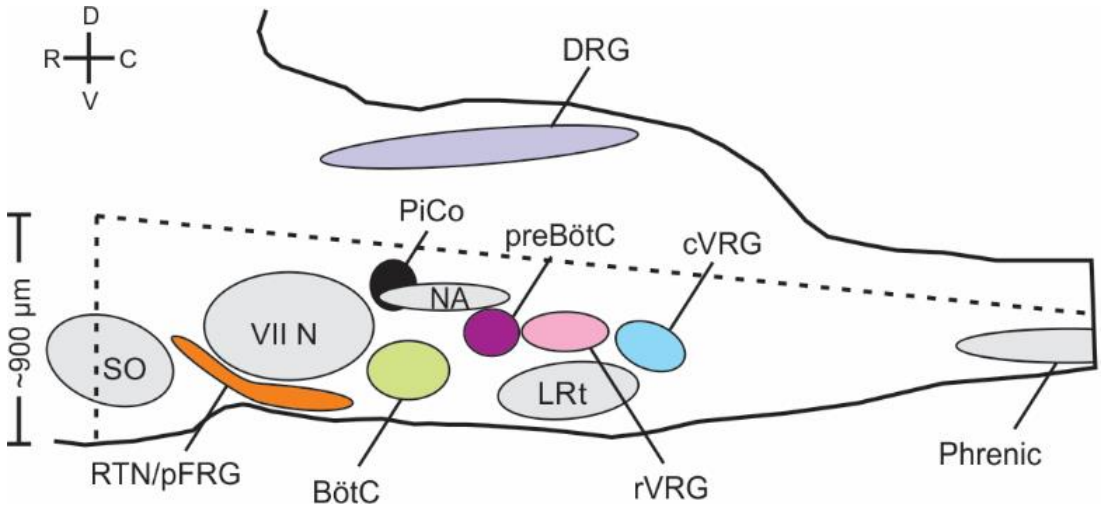

Extended Data Figure 1 | Schematic of the horizontal slice from a sagittal view that retains the medullary ventral respiratory column in the brainstem. Dotted lines represent approximate boundaries of the horizontal slice. Slice retains part of the superior olive (SO), and the entire retrotrapezoidal nucleus/para-facial respiratory group (RTN/pFRG), facial nucleus (VII N), Bötzinger Complex (BötC), Post-inspiratory Complex (PiCo), Nucleus ambiguus (NA), preBötzinger Complex (preBötC), lateral

reticular nucleus (LRT), and the rostral and caudal ventral respiratory groups (rVRG and cVRG, respectively). The slice also retains a portion of the spinal cord and includes part of the phrenic motor nucleus (approximately cervical segment 3 and 4). The slice does not contain the dorsal portion of the medulla including the dorsal respiratory group (DRG). Legend: dorsal (D), ventral (V), rostral (R), caudal (C).

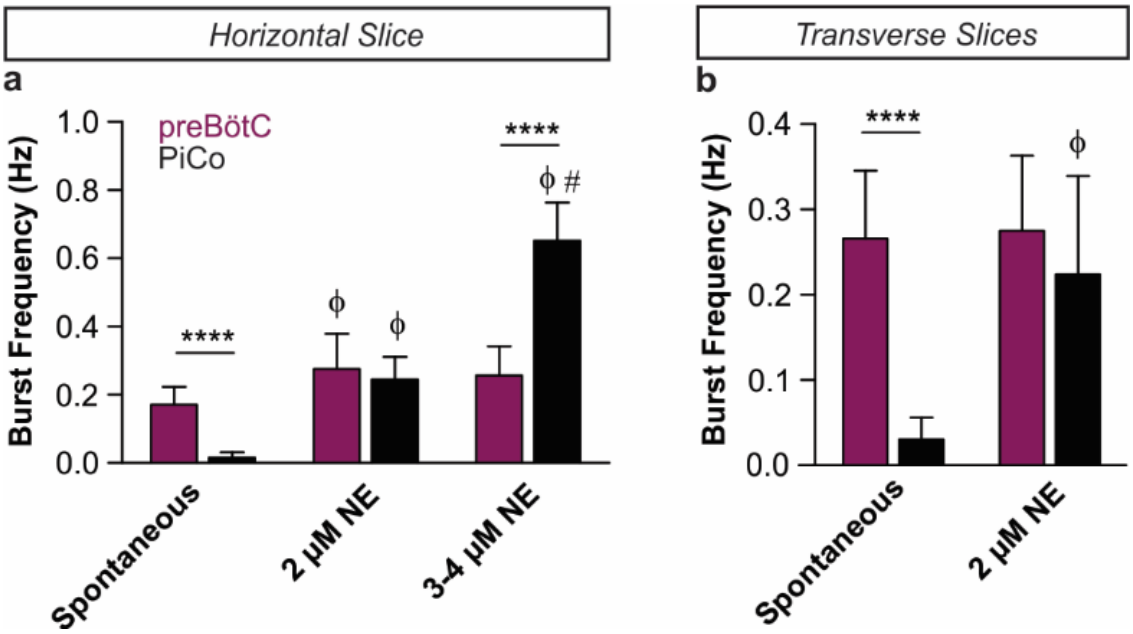

Extended Data Figure 2 | NE dose response of preBötC and PiCo rhythms in horizontal and transverse slices. The frequency of the PiCo rhythm (black) is highly sensitive to the application of low concentrations of NE while the preBötC rhythm (purple) stays relatively constant in both types of slice preparations. **a,** In horizontal slices the PiCo rhythm is slow under spontaneous conditions (n=10), the two rhythms have similar burst frequencies in 2 µM NE (n=6), and the PiCo rhythm significantly outpaces the preBötC rhythm under higher concentrations (n=4, 3-4 µM NE). **b,** Similarly, when isolated in transverse slices, the PiCo rhythm has a slow frequency under spontaneous conditions (n=10), and the preBötC and PiCo have similar frequencies at 2 µM NE (n=7). (mean ± s.e.m.) Two-way ANOVA followed by a Bonferroni *post hoc* test. ****P < 0.0001 comparing PiCo to preBötC, ϕ P<0.05 compared to baseline (Spon.), # P<0.05 compared to 2 µM NE.

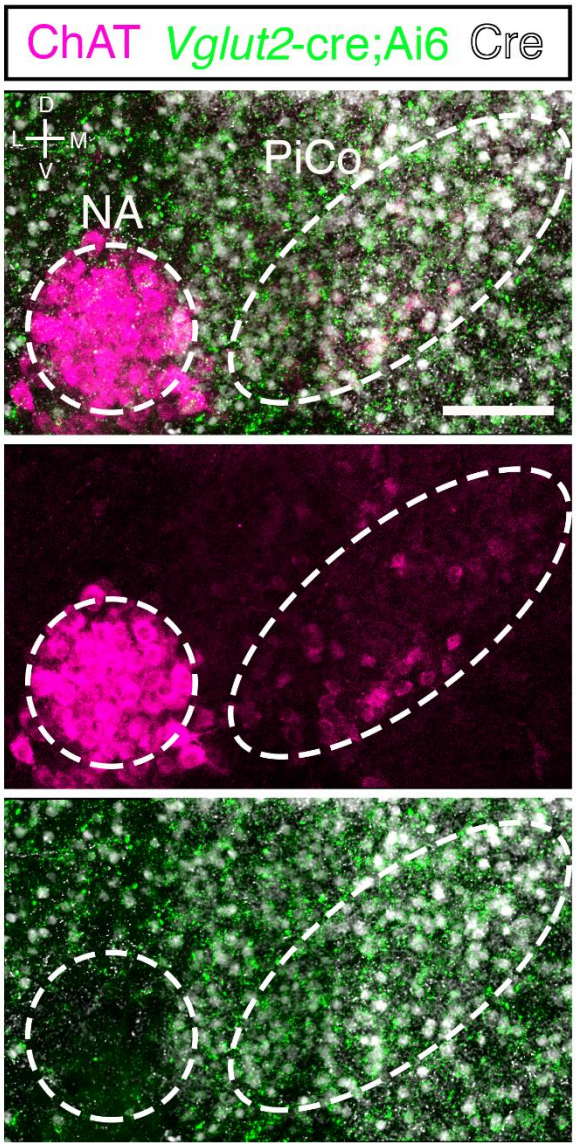

Extended Data Figure 3 | NA neurons lack *Vglut2*-cre expression. High magnification view at the level of PiCo from a *Vglut2*-cre;Ai6 (ZsGreen1; green) mouse immunolabeled with ChAT antibody (magenta) and Cre antibody (white). Note lack of green *Vglut2*-cre expression in the NA. Scale bar 100 µm.

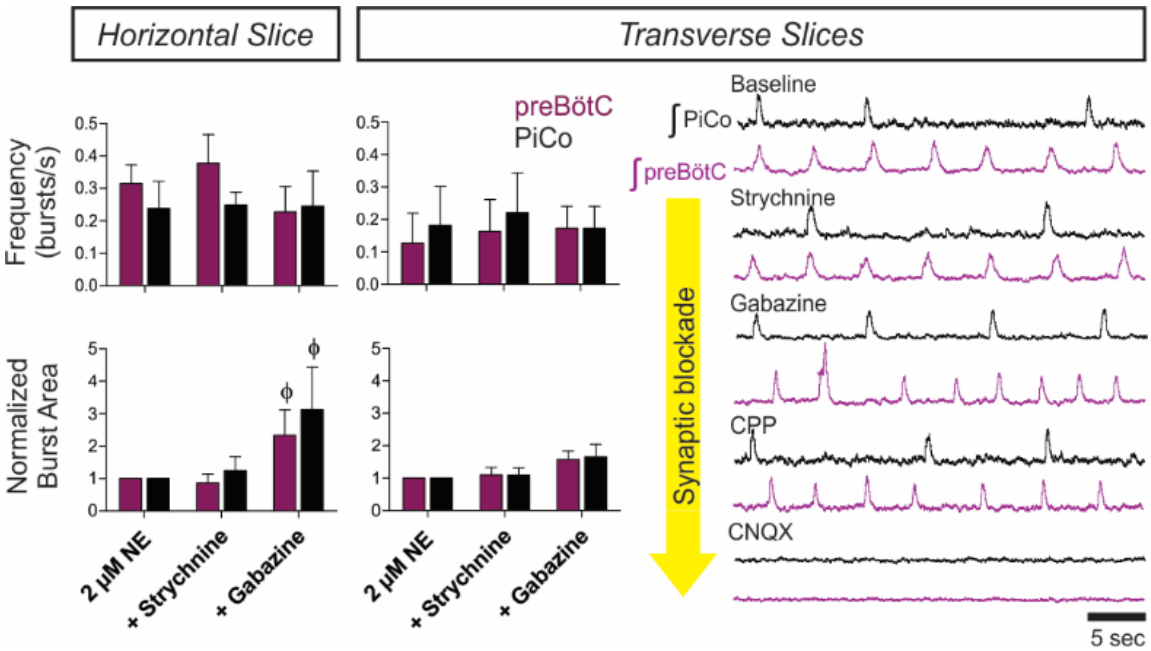

Extended Data Figure 4 | Progressive synaptic blockade in horizontal and transverse slices. (Left) Graphs comparing frequency and normalized burst area between horizontal (n=5) and paired transverse slices (n=5) after the application of strychnine and gabazine. In both horizontal and paired transverse slices, PiCo and preBötC rhythms have nearly identical burst frequencies in the presence of gabazine (top graphs). The burst area of both rhythms also significantly increases with the application of gabazine in both slice preparations (bottom graphs). Two-way ANOVA followed by a Bonferroni *post hoc* test. ϕ $P<0.05$ compared to baseline (2 µM NE). (Right) Synaptic blockers were progressively perfused over paired transverse slices at 10 minute intervals. Both PiCo and preBötC rhythms persist in the presence of 1 µM strychnine, 10 µM gabazine, and 10 µM CPP. Population rhythms ceased in the presence of 20 µM CNQX, indicating that both rhythms are excitatory (n=5). The asterisk denotes a characteristic sigh in the preBötC trace.

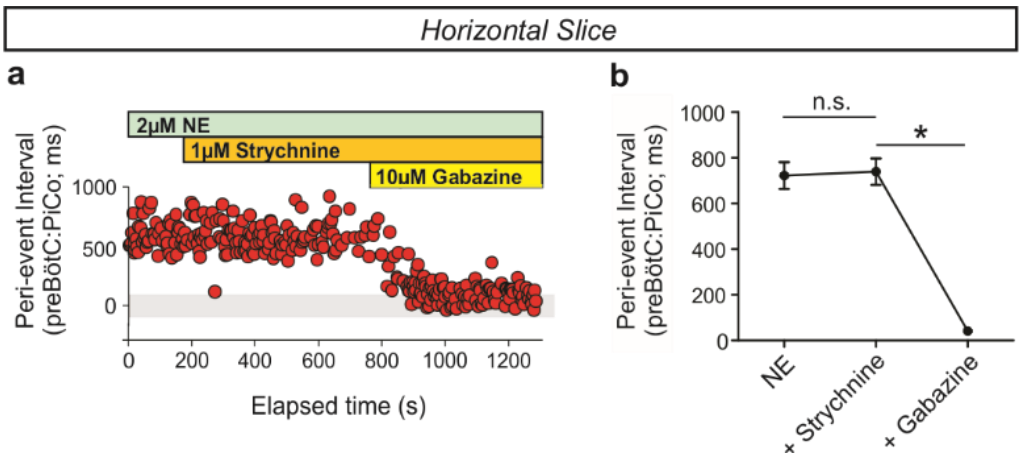

Extended Data Figure 5 | Perievent interval between preBötC and PiCo bursts during inhibitory block in the horizontal slice. a, Peri-event interval, time between peak of preBötC and PiCo bursts, is constant in strychnine; however, gabazine initiates progressive synchronization between rhythms shown here in a representative experiment. **b,** Average peri-event intervals at baseline and after sequential application of strychnine and gabazine (n=6, mean ± s.e.m.). Repeated measures Friedman test followed by Dunn's multiple comparisons *post-hoc* test. *$P < 0.05$.

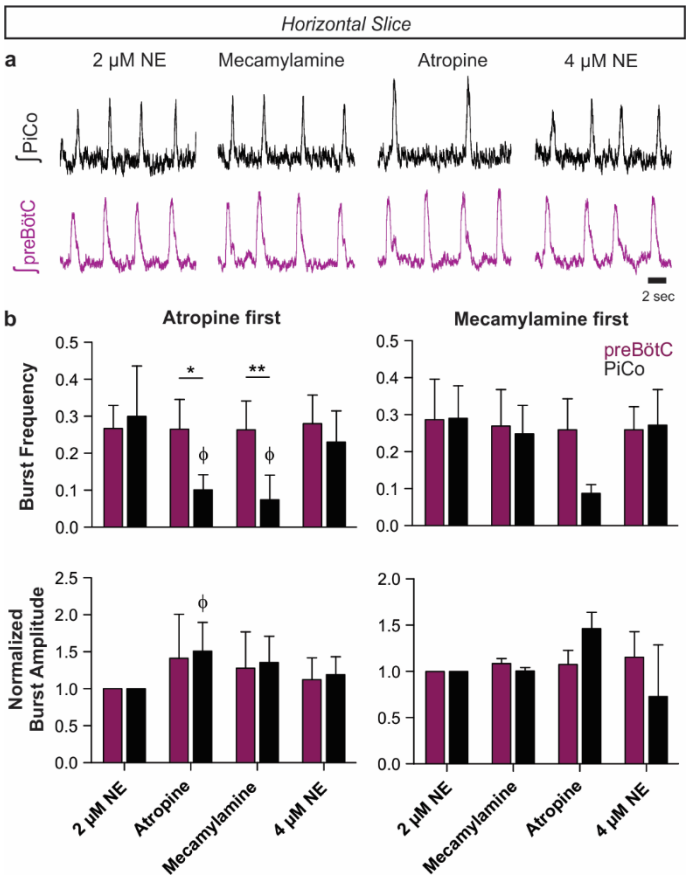

Extended Data Figure 6 | Blocking muscarinic and nicotinic acetylcholine receptors does not abolish the PiCo rhythm. a, Raw population bursts from PiCo and contralateral preBötC with the progressive addition of 1 µM mecamylamine (nicotinic receptor antagonist), 10 µM atropine (muscarinic receptor antagonist), and 4 µM norepinephrine. **b,** The left two graphs show n=5 experiments in which atropine was applied first, and the right graphs illustrate n=3 experiments in which mecamylamine was applied first. Blockade of muscarinic receptors results in a larger decrease in PiCo burst frequency than blocking nicotinic receptors, while preBötC frequency does not change significantly (top graphs). Interestingly, blockade of muscarinic receptors increases the amplitude of PiCo bursts (bottom graphs). The PiCo rhythm persists after concurrent blockade of both types of acetylcholine receptors, and PiCo burst frequency rebounds to near baseline levels when an additional 2 µM NE is applied (total 4 µM NE; top graphs). (mean ± s.e.m.). Two-way ANOVA followed by a Bonferroni *post hoc* test. $^{**}P < 0.01$, $^{*}P < 0.05$ comparing preBötC to PiCo, ϕ $P<0.05$ compared to baseline (2 µM NE).

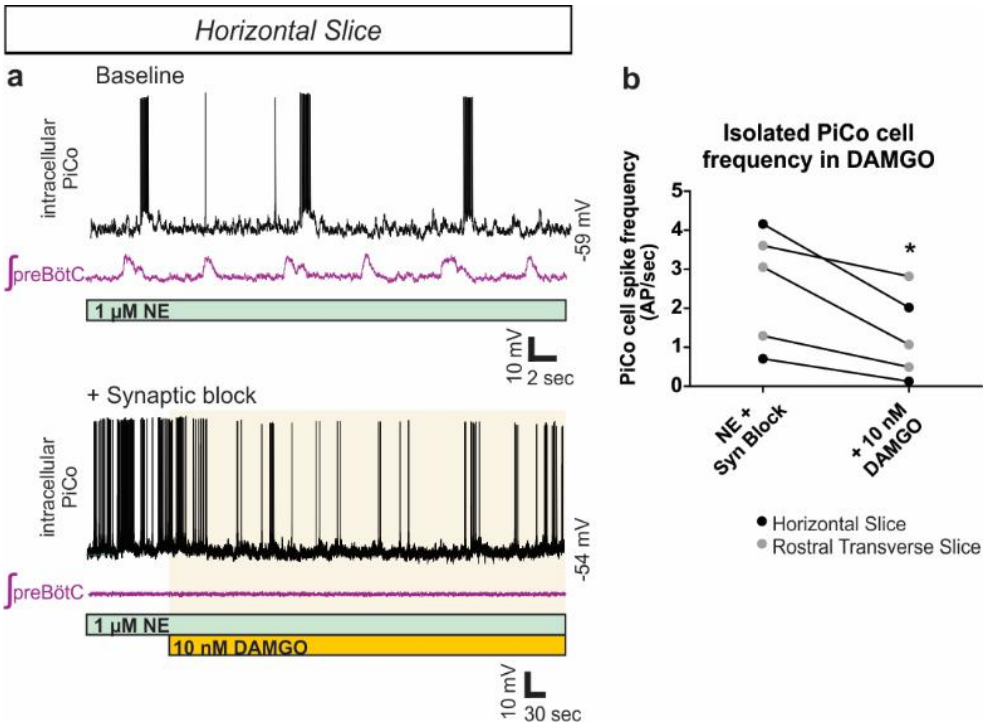

Extended Data Figure 7 | Synaptically isolated PiCo neurons decrease firing frequency in the presence of DAMGO. **a**, Top traces show intracellular recordings from PiCo cells with concurrent extracellular preBötC population activity from a horizontal slice under 1 µM NE baseline conditions. Bottom traces show the same recordings after blocking fast synaptic transmission (1 µM strychnine, 10 µM gabazine, 10 µM CPP, 20 µM CNQX) to synaptically isolate the PiCo neuron. Application of 10 nM DAMGO decreases the cell's intrinsic firing frequency. **b**, Quantified data show that DAMGO significantly decreases action potential (AP) firing frequency of synaptically isolated PiCo neurons both in horizontal slices (black dots) and transverse PiCo slices (gray dots) (two-tailed paired *t*-test, $*P < 0.05$; n=5).

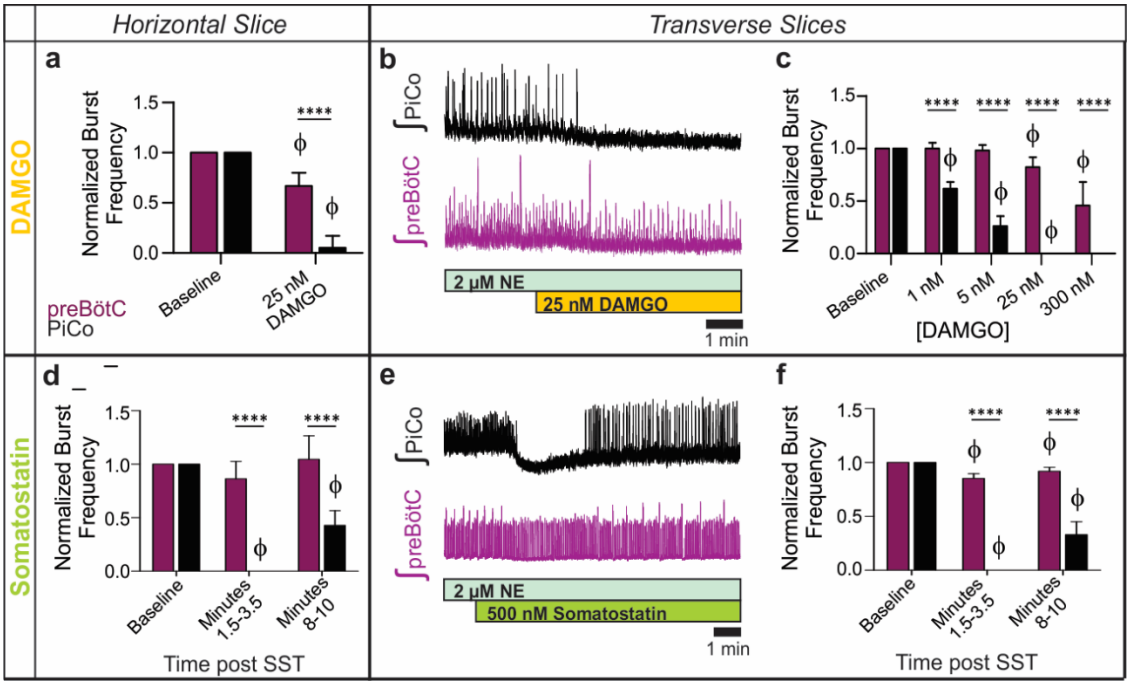

Extended Data Figure 8 | Differential PiCo and preBötC population responses to DAMGO and SST in horizontal and transverse slices. **a,** After the application of 25 nM DAMGO, preBötC burst frequency only slightly decreases (n=5), whereas PiCo bursting is nearly eliminated. **b,** Similar to results observed in horizontal slices, the PiCo rhythm is eliminated by 25 nM DAMGO in transverse slices that isolate PiCo and preBötC in the presence of 2 µM NE (n=5). Periodic large amplitude bursts in the bottom preBötC trace are fictive sighs. **c,** DAMGO dose response of normalized preBötC and PiCo burst frequency in transverse slices, illustrating the differential sensitivity of the PiCo and preBötC rhythms to DAMGO; burst frequency values are normalized to baseline frequency in 2 µM NE. (mean ± s.e.m., n=8 with minimum replicates of 4 for each location and concentration). **d,** The PiCo rhythm is selectively and transiently inhibited by the application of 500 nM SST whereas the preBötC rhythm persists in horizontal slices. Graph shows normalized average burst frequencies of both rhythms at baseline, 1.5-3.5 minutes after SST application, and 8-10 minutes after SST application (n=6). **e,** Similar to the horizontal slice, SST application results in a robust inhibition of PiCo bursting in paired transverse slices. **f,** Similar to **d**, complied normalized burst frequencies for n=6 transverse slices before and after SST application. (mean ± s.e.m.) Two-way ANOVA followed by a Bonferroni *post hoc* test. ****$P < 0.0001$ comparing PiCo to preBötC, ϕ $P<0.05$ compared to baseline.

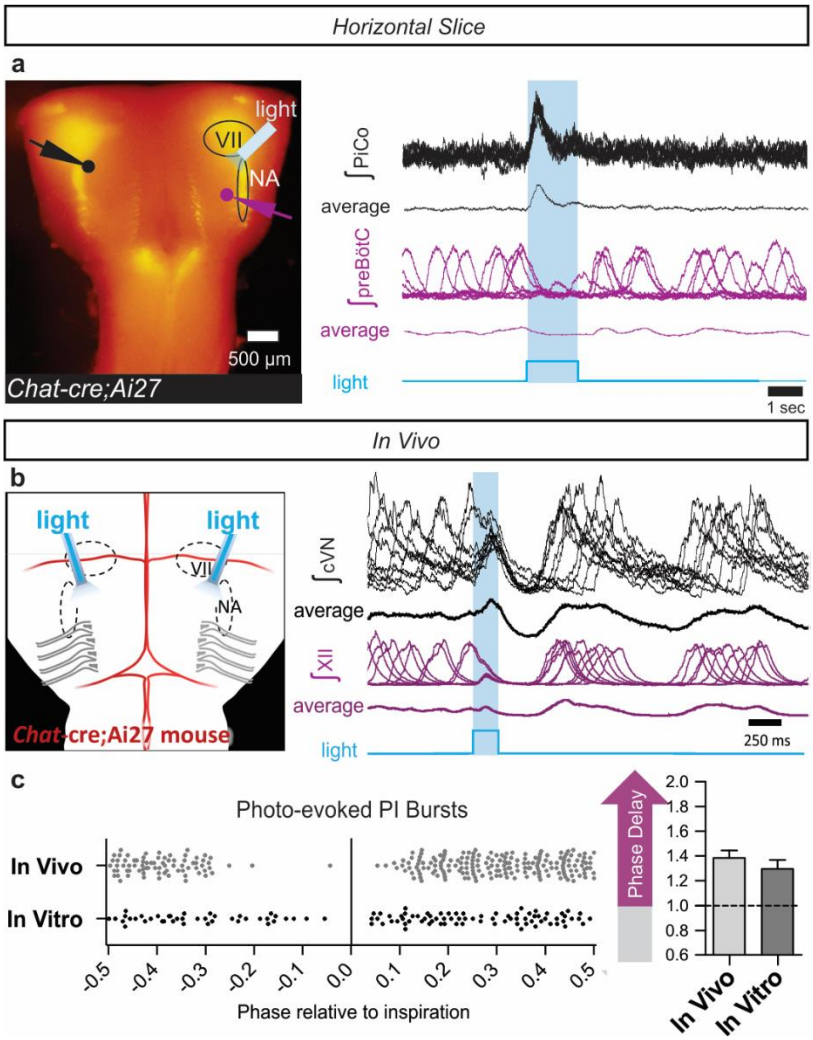

Extended Data Figure 9 | Light stimulation of cholinergic cells evokes postinspiratory activity in horizontal slices and *in vivo*. a, Two population electrodes were placed at the level of PiCo (black dot and trace) and contralateral preBötC (purple dot and trace) in a *Chat*-cre;Ai27 horizontal slice. Under spontaneous conditions (no NE), cholinergic neurons expressing channelrhodopsin-2 were light activated with a fiber optic (labeled 'light') placed over PiCo ipsilateral to the preBötC electrode. PiCo population bursts were triggered upon the onset of a 1.5 second light pulse while no bursts were light evoked in the preBötC (n=6). Figure shows 10 traces overlaid for each electrode with averaged traces below from a representative experiment. **b,** Photo-stimulating PiCo in adult anesthetized *Chat*-cre;Ai27 mice reliably triggers cVN bursts. Figure shows 10 traces overlaid with averages below of cVN and XII activity during a 200 ms light stimulation of PiCo. **c**, Postinspiratory bursts can be photo-evoked both *in vivo* (n=6) and *in vitro* (n=6) at any phase except for during inspiration and just prior to inspiration (bottom left) due to the inspiratory phase delay that occurs when PiCo is stimulated (mean ± s.e.m., bottom right). NA= Nucleus ambiguus, VII= facial nucleus.

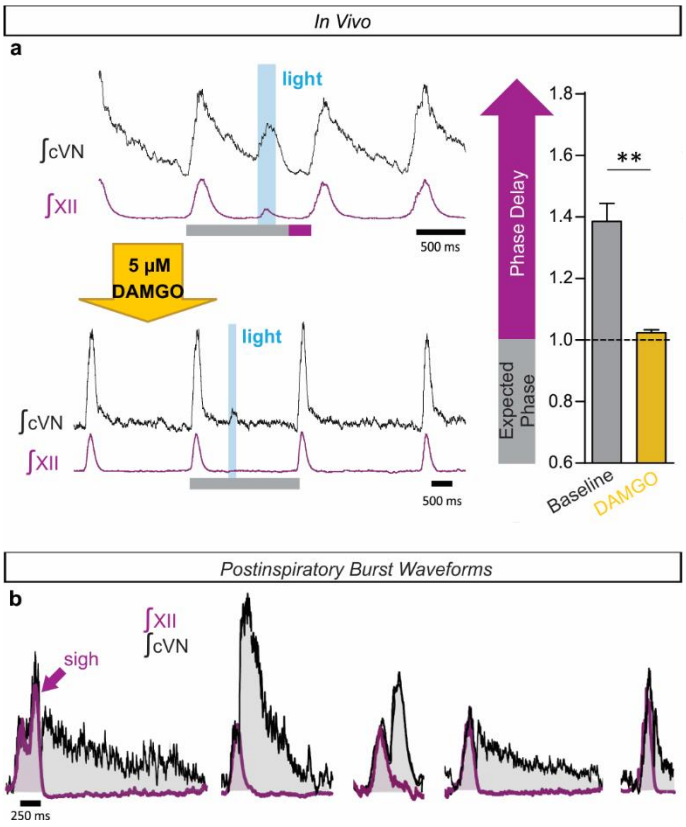

Extended Data Figure 10 | Elimination of phase delay by DAMGO and a diversity of postinspiratory waveforms *in vivo*. a, Injection of 5 µM DAMGO into PiCo eliminates the phase delay elicited by photo-stimulation of PiCo in *Chat*-cre;Ai27 mice. A representative experiment showing cVN and XII recordings during a 200 ms light pulse before and after injection of PiCo with DAMGO (left; gray bars = expected phase, purple bars = inspiratory phase delay) and the average inspiratory phase delay (right) (mean ± s.e.m., two-tailed paired t-test, **P<0.01; n=6). **b,** A diversity of postinspiratory vagal waveforms were recorded *in vivo*. Five examples of cVN (black) and XII (purple) recordings (overlaid) show that postinspiratory activity can vary from large decrementing patterns to small short bursts, potentially representing the neural basis for a variety of postinspiratory behaviors.

Chapter 3

Central and peripheral factors contributing to obstructive sleep apneas.

*This chapter was published with minor reformatting as an article with the same title in *Respiratory Physiology & Neurobiology*. Co-authors of this work included: Jan-Marino Ramirez, Alfredo J. Garcia III, Jenna E. Koschnitzky, Ying-Jie Peng, Ganesh Kumar, Nanduri Prabhakar. The full citation is as follows:

Ramirez J.M., Garcia A.J., Anderson T.M., Koschnitzky J.E., Peng Y.J., Kumar G., & Prabhakar N. (2013). Central and peripheral factors contributing to obstructive sleep apneas. *Respiratory Physiology & Neurobiology, 189*(2), 344-353.

3.1 Abstract

Apnea, the cessation of breathing, is a common physiological and pathophysiological phenomenon with many basic scientific and clinical implications. Among the different forms of apnea, obstructive sleep apnea (OSA) is clinically the most prominent manifestation. The first modern description of OSA was by Burwell and colleagues (Bickelmann et al., 1956) but was documented much earlier (Bray, 1994; Lavie, 1984). OSA is characterized by repetitive airway occlusions that are typically associated with peripheral airway obstructions. However, it would be a gross oversimplification to conclude that OSA is caused by peripheral obstructions. OSA is the result of a dynamic interplay between chemo- and mechano-sensory reflexes, neuromodulation, behavioral state and the differential activation of the central respiratory network and its motor outputs. This interplay has numerous neuronal and cardiovascular consequences that are initially adaptive but in the long-term become major contributors to the morbidity and mortality associated with OSA. However, not only OSA, but all forms of apnea have multiple, and partly overlapping mechanisms. In all cases the underlying mechanisms are neither “exclusively peripheral” nor “exclusively central” in origin. While the emphasis has long been on the role of peripheral reflex pathways in the case of OSA, and central mechanisms in the case of central apneas, we are learning more about the integration of these mechanisms. This review discusses the complex interplay of peripheral and central nervous components that characterizes the cessation of breathing.

3.2 Introduction

Obstructive Sleep Apnea (OSA) is a major health issue worldwide affecting 3-7% of adult men and 2-5% of adult women (Young et al., 2002) with the incidence increasing because of the dramatic rise in obesity (Bhattacharjee et al., 2012). Weight change predicts the incidence of OSA, and a 10% increase in weight is associated with a 32% increase in the apnea/hypopnea index (Peppard et al., 2000a). Furthermore, OSA is an important contributor to the morbidity and mortality associated with obesity (Gozal and Kheirandish-Gozal, 2009; Tuomilehto et al., 2012). OSA is defined as the cessation of breathing caused by the repetitive, episodic collapse of the pharyngeal airway due to an obstruction or increased airway resistance. OSA is distinguished from central apnea (CA), which is primarily caused by the cessation of the central respiratory network. CA is highly prevalent in congestive heart failure but is also present in normal subjects (Eckert et al., 2009a).

The distinction between each form of apnea, however, is not straightforward. OSA (Figure 1) as well as CA is the result of complex interactions between the peripheral and central nervous system (Eckert et al., 2009a). These interactions lead to short-term and long-term changes that contribute to the evolution of OSA and CA. Consequences of these disorders include excessive daytime somnolence, neurocognitive impairment, and increased risk for accidents related to sleep deprivation (Gozal et al., 2012; Gozal and Kheirandish-Gozal, 2012; Jordan and White, 2008; Kim et al., 1997; Young et al., 1997). In addition to these neurological consequences, the number of apneas that patients experience is positively correlated with an increased risk of hypertension (Peppard et al., 2000b). Other serious cardiovascular morbidities include increased risk for stroke, coronary artery disease, and heart failure (Phillips, 2005).

Mechanistically, increased sympathetic activity, endothelial dysfunction, and systemic inflammation as well as oxidative stress are all contributors to myocardial damage and hypertension (Baguet et al., 2012). Thus, the airway obstruction in OSA as well as CA is the beginning of a complex series of events that affect numerous central and peripheral neuronal and cardiovascular mechanisms (Eckert et al., 2009a; Gozal et al., 2013; Jordan and White, 2008; Leung and Bradley, 2001; Meier and Andreas, 2012; Susarla et al., 2010). Some of the long-term consequences of OSA, such as hypertension, often persist even after obstructions are eliminated or prevented through surgery or continuous positive airway pressure (CPAP) (Alchanatis et al., 2001; Vanderveken et al., 2011). Moreover, after surgical removal of the anatomical obstructions, or after treatment with CPAP, patients often remain refractory and shift towards the generation of central apneas (Boyd, 2009; Eckert et al., 2009b; Susarla et al., 2010). In this review we will discuss some of the factors that contribute to the pathogenesis of apneas.

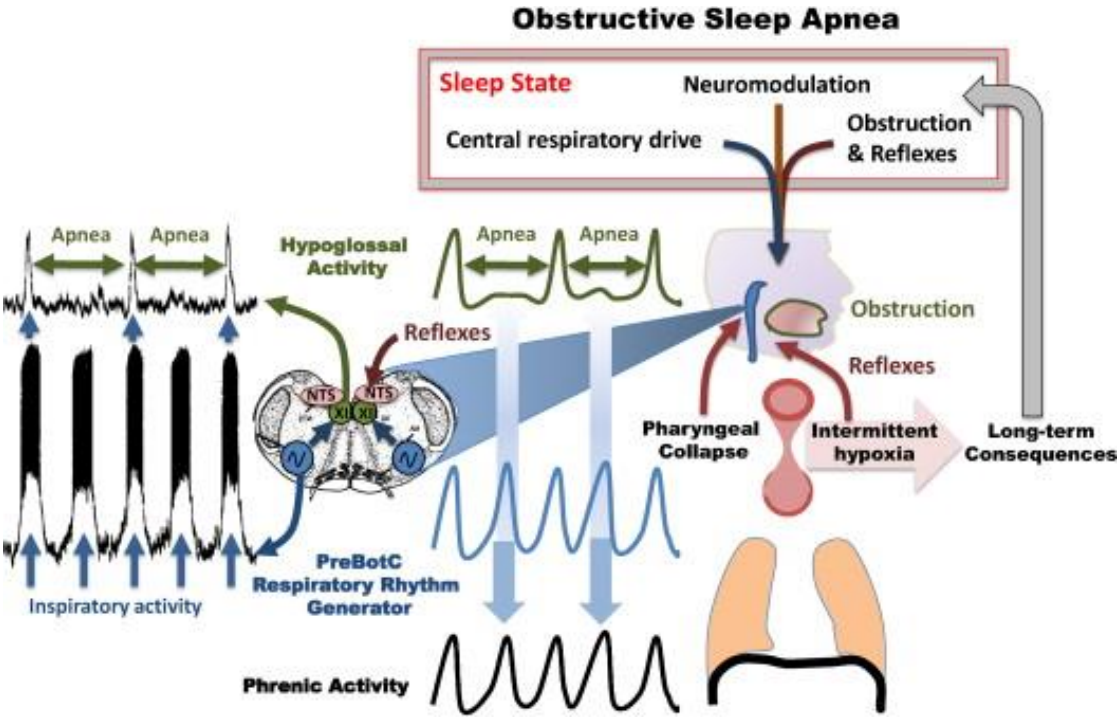

Figure 1. Mechanisms of obstructive apneas. Left panel: Upper trace: integrated extracellularly recorded hypoglossus activity obtained simultaneously with an intracellular recording from an inspiratory neuron located within the pre-Bötzinger complex (lower trace). The recordings were obtained in an isolated transverse slice preparation shown in the schematic. The preparation contains the functionally active pre-Bötzinger complex (blue), the nucleus tractus solitaries (NTS, pink), which in the intact animal would receive reflex inputs. Contained within the slice is also the hypoglossal nucleus (XII, green), which in the intact animal would innervate the genioglossus muscle. Note the XII activity is not always phase-locked with the pre-Bötzinger complex resulting in XII apneas that are uncoupled from the respiratory rhythm generator located within the pre-Bötzinger complex. (Figure modified from Ramirez et al., 1996). The actual data shown on the left panel inspired the middle panel, which schematically illustrates how the rhythmically active pre-Bötzinger complex (blue trace) could continue to activate the phrenic activity (black trace) resulting in diaphragmatic activity, while activity in the XII becomes uncoupled resulting in a cessation of XII activity (green trace, apnea). The right panel illustrates the anatomical components contributing to an airway occlusion: A decreased activity in the genioglossus (tongue in the schematic) and continued activity in the diaphragm (schematically drawn beneath the lung) will lead to the negative pressure that results in a pharyngeal collapse. The bilaterally organized pre-Bötzinger complex isolated in the transverse slice preparation, which was obtained from the lower brainstem (medulla – schematically shown in blue). The airway occlusion is the result of sleep state, neuromodulation, central respiratory drive, reflexes and the airway obstruction. These contributors are altered by long-term consequences of the intermittent hypoxia that is caused by repetitive pharyngeal collapses. For more details see text.

3.3 Airway obstruction and the importance of hypoglossal activity

Various anatomical abnormalities can contribute to the airway obstructions associated with OSA. Thus surgical procedures to remove these obstructions need to be adapted to the individual pattern and type of airway obstruction (Bhattacharjee et al., 2010; Sher et al., 1996). Obstructions can include macroglossia, adenotonsillar hypertrophy, increased nasal resistance, pharyngeal edema, and craniofacial abnormalities such as micrognathia and retrognathia (Bhattacharjee et al., 2010; Enoz, 2007; Lam et al., 2010; Prabhat et al., 2012; Shott and Cunningham, 1992; Verbraecken and De Backer, 2009; White, 2005; Won et al., 2008). Craniofacial factors are particularly important for pediatric OSA (Gozal, 2000). However, alone none of these anatomical determinants is sufficient to cause an airway occlusion.

Under normal conditions airflow is facilitated by a central respiratory drive to the upper airways (Figure 1). Of critical importance are the hypoglossal (XII) motorneurons that innervate the genioglossus muscle via the medial branch of the hypoglossal nerve. The genioglossus muscle is the largest extrinsic muscle of the human tongue (Abd-El-Malek, 1938; Saboisky et al., 2007; Takemoto, 2001). Innervation of the genioglossus is very complex and many types of phasic and tonic motor units originating in the hypoglossal motor nucleus contribute to the genioglossus contraction (Haxhiu et al., 1992; Hwang et al., 1983; Saboisky et al., 2007). The XII motorneurons phasically activate the genioglossus muscle during each inspiration (Figure 1), and some activity is maintained during expiration (Akahoshi et al., 2001; Fogel et al., 2001; Otsuka et al., 2000; Saboisky et al., 2010; Sauerland and Harper, 1976).

Overall, however, respiratory drive increases genioglossus muscle tone preferentially during inhalation, resulting in a contraction that pulls the tongue forward (Brouillette and Thach, 1979) and enlarges the upper airways (Bailey and Fregosi, 2004; Fuller et al., 1999; Mann et al., 2002; Oliven et al., 2001; Sokoloff, 2000). This mechanism largely prevents airway collapse during wakefulness. Indeed during wakefulness, electromyography (EMG) activity of the genioglossus is enhanced in OSA patients when compared to controls (Fogel et al., 2001; Mezzanotte et al., 1992), an adaptation that seems to compensate for the increased upper airway resistance and compliance that characterizes OSA patients (Malhotra and White, 2002; Randerath, 2007; Saboisky et al., 2007). However, during sleep or while anesthetized, the central respiratory drive to the genioglossus muscle weakens, and, as a consequence, anatomical obstructions can occlude the airway during inhalation (Eastwood et al., 2002; Remmers et al., 1978; Sauerland and Harper, 1976). Because a decreased central drive during sleep is necessary for the occlusion to occur during inhalation, OSA must be considered as a neuronal issue.

Indeed, airway obstructions are promoted by multiple central and peripheral nervous systems factors. These factors include sleep state-dependent pathologies and respiratory instabilities that are caused by loop gain changes as has been discussed in great detail (Thomas et al., 2004; White, 2005). Yet, whether and how an obstruction causes the cessation of breathing, i.e. the actual apnea, are not trivial questions. It is safe to conclude that the mechanisms and events leading to apneas are not fully understood. In the following section we will discuss some of the potential mechanisms.

3.4 Biomechanical and modulatory contributions to airway occlusion in OSA.

3.4.1 The pharyngeal collapse

Cessation of airflow with continued respiratory effort is the hallmark of OSA (Praud et al., 1988; Remmers et al., 1978; Zucconi et al., 1996). Figure 2 illustrates two example traces from OSA patients (A from (Praud et al., 1988); B from (Remmers et al., 1978)). In both examples oro-nasal flow is blocked, while respiratory efforts continue in the abdomen. From a biomechanical perspective, continued respiratory effort in the thorax/abdomen increases thoracic volume and decreases pressure at the level of the pharynx, which would normally enable air to flow into the lungs. But, due to the increased oro-nasal resistance, the decreased pharyngeal pressure results in negative intraluminal pressure within the upper airways and leads to pharyngeal collapse (Figure 1). Considering the mismatch between negative intraluminal pressure and the decreased airflow arriving through the upper airways, OSA may not only result from an upper airway obstruction, but it could also be caused by an imbalance in lung volume compared to upper airway size. Thus, various anatomical causes together with decreased XII activation are important contributors to the pharyngeal collapse and thus to the airway occlusion in OSA (Figs. 1, 2).

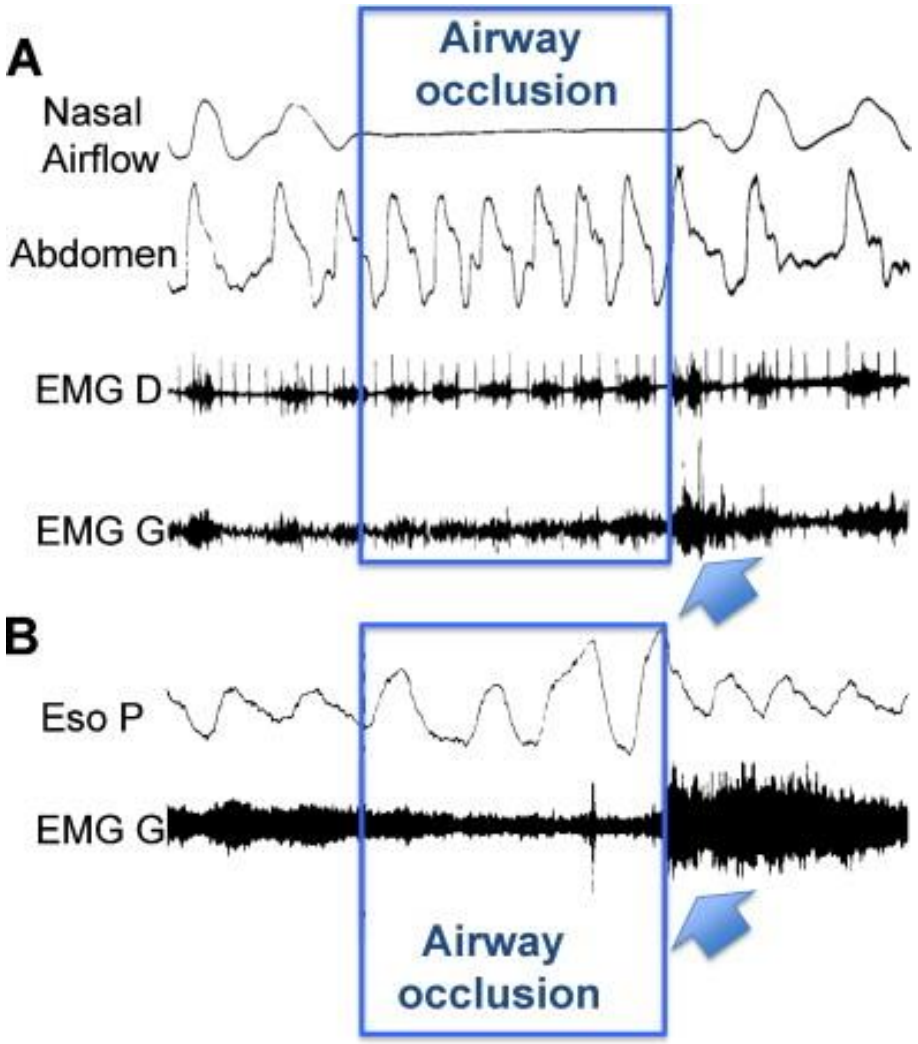

Figure 2. Airway occlusion and genioglossus activity. Obstructive sleep apnea is characterized by airway occlusions that block nasal airflow (A, upper trace), while abdominal respiratory movements continue as illustrated by the abdominal movements (A, second trace) and esophageal pressure changes (B, upper trace). Continuous respiratory activity is also characterized by respiratory rhythmic diaphragmatic EMG (A, third trace, EMG D). While respiratory rhythmic activity continues in the abdomen, genioglossus activity either decreases during the airway occlusion (B, lower trace, EMG G), or the phasic genioglossus EMG becomes increasingly tonic (A, lower trace, EMG G). The termination of the airway occlusion is characterized by a burst of genioglossus activity (A, B). Figure modified from: A: Praud et al. (1988), B: Remmers et al. (1978).

3.4.2 Neuromodulators and transmitters

Multiple neuronal mechanisms contribute to a sleep-related decrease in XII activation as both neurotransmitter and neuromodulatory systems undergo drastic state dependent changes. As demonstrated in intracellular recordings, glutamatergic and GABAergic mechanisms (Chase et al., 1989; Funk et al., 1997; Soja et al., 1991; Soja et al., 1987) as well as a powerful glycinergic premotor inhibitory system likely contribute to the REM specific decrease in XII motorneuron activity (Yamuy et al., 1999). However, the degree of inhibition may only be detectable in intracellular recordings, while active inhibition is difficult to demonstrate in EMG recordings (Funk et al., 2011). This difficulty may partly explain why the relative importance of fast neurotransmission remains a matter of discussion (Chan et al., 2006; Morrison et al., 2003a; Morrison et al., 2003b).

In addition to increased active inhibition by fast synaptic transmitters, there is also a pronounced sleep related decrease in the activity of noradrenergic (Aston-Jones and Bloom, 1981) and serotonergic neurons (Jacobs and Fornal, 1991; Leung and Mason, 1999) suggesting that the loss of noradrenergic and serotonergic neuromodulatory inputs play critical roles (Fenik et al., 2005a; Funk et al., 2011; Horner, 2008, 2009; Kubin et al., 1998; Ladewig et al., 2004). This hypothesis is consistent across various manipulations in unrestrained animals (Chan et al., 2006; Morrison et al., 2003a; Sood et al., 2007; Sood et al., 2005), slice preparations (Funk et al., 1994; Viemari and Ramirez, 2006), and with research in the so-called carbachol model for rapid eye movement (REM) sleep (Fenik et al., 2004; Fenik et al., 2005a, b; Fenik et al., 2005c; Fenik et al., 2008). The noradrenergic neurons from the A5 and A7 regions converge at the level of the XII motorneurons (Aldes et al., 1992) and seem to have their effect through α1 adrenergic receptor activation (Parkis et al., 1995; Selvaratnam et al., 1998; Volgin et al., 2001). Interestingly, the pre-

Bötzinger complex (preBötC), an area critical for breathing also receives noradrenergic and serotonergic inputs and is activated by a variety of serotonergic and adrenergic receptors including the α1 adrenergic receptors (Doi and Ramirez, 2008, 2010; Lalley et al., 1995; Pena and Ramirez, 2002; Ptak et al., 2009; Tryba et al., 2006; Viemari et al., 2011; Viemari and Ramirez, 2006). Thus, noradrenergic and serotonergic excitatory modulation may play a role in linking the central respiratory network with the XII motor output.

Other neuromodulators will also play important roles. Acetylcholine could be a key modulator involved in modulating respiratory activity (Shao and Feldman, 2009; Tryba et al., 2008) and suppressing genioglossus activity during REM sleep (Bellingham and Berger, 1996; Bellingham and Funk, 2000; Grace et al., 2013; Liu et al., 2005; Robinson et al., 2002). The recent study by Grace et al. 2013 demonstrated that REM specific suppression can be overcome by injecting muscarinic antagonists into the XII motorneuron pool (Fig. 3; Grace et al. 2013). At the cellular level, this inhibitory effect appears to involve the activation of G protein-coupled inward rectifying potassium (GIRK) channels. These modulatory mechanisms appear to suppress XII motor activity by acting on the motorneurons themselves (Grace et al., 2013). This cholinergic drive could come from XII premotor neurons, a subpopulation of which is cholinergic (Volgin et al., 2008).

It is important to note, that the neuromodulatory mechanisms contributing to OSA and CA are likely very different. The number of apneas significantly increases during REM sleep in OSA patients, and some patients show apneas exclusively during REM sleep (Eckert et al., 2009b; Findley et al., 1985; Kass et al., 1996). By contrast, the number of central apneas is lowest during REM sleep (Eckert et al., 2007a). Thus, further research

will need to explain how the modulatory and activity characteristics associated with the different sleep states relate to the different forms of apnea.

With regards to OSA the modulatory mechanisms during REM sleep could indeed explain the decrease in airway tone (Remmers et al., 1978; Sauerland and Harper, 1976), but can only partly explain how decreased XII motorneuronal activation predisposes the upper airways to a pharyngeal collapse. Thus, it remains uncertain how the apneas themselves are generated.

Indeed, the possibility that modulators are causing the decreased tone but not the apnea itself is consistent with the well-known inefficiency of aminergic therapies that have largely failed to alleviate OSA (Dempsey et al., 2010; Funk et al., 2011). Moreover, noradrenergic and serotonergic innervation is strengthened following exposure to chronic intermittent hypoxia which may oppose the decreased muscle tone during sleep (Rukhadze et al., 2010), and OSA patients show a variety of neurogenic changes in the upper airways that could potentially compensate for decreased muscle tone. These adaptations include increased activation, earlier firing, and increased sprouting of the XII motorneurons (Saboisky et al., 2007; Saboisky et al., 2012). As illustrated in Figure 2 there is not a general suppression of the upper airways as seen in Figure 3, but instead the airflow is “suddenly” disturbed for a few cycles and then the oral-nasal flow reappears and re-synchronizes with the respiratory abdominal muscles. Thus, while a persistently decreased drive to the XII motorneurons may predispose the pharynx to sudden collapse, the sudden failure in XII motor activity cannot be entirely explained by altered modulatory tone generating persistent atonia during a specific sleep state.

As illustrated in Figure 2, genioglossus EMG activity is specifically weakened and less phasic during the airway occlusion but not before or after the occlusion. Thus, in addition to a neuromodulator- and transmitter-driven decrease in muscle tone, one needs to consider additional central nervous and reflex mechanisms that contribute to the disconnect between the ongoing phasic respiratory activity that drives the diaphragmatic activity and the decrease in phasic respiratory drive to the XII motorneurons which is specifically associated with the airway occlusion.

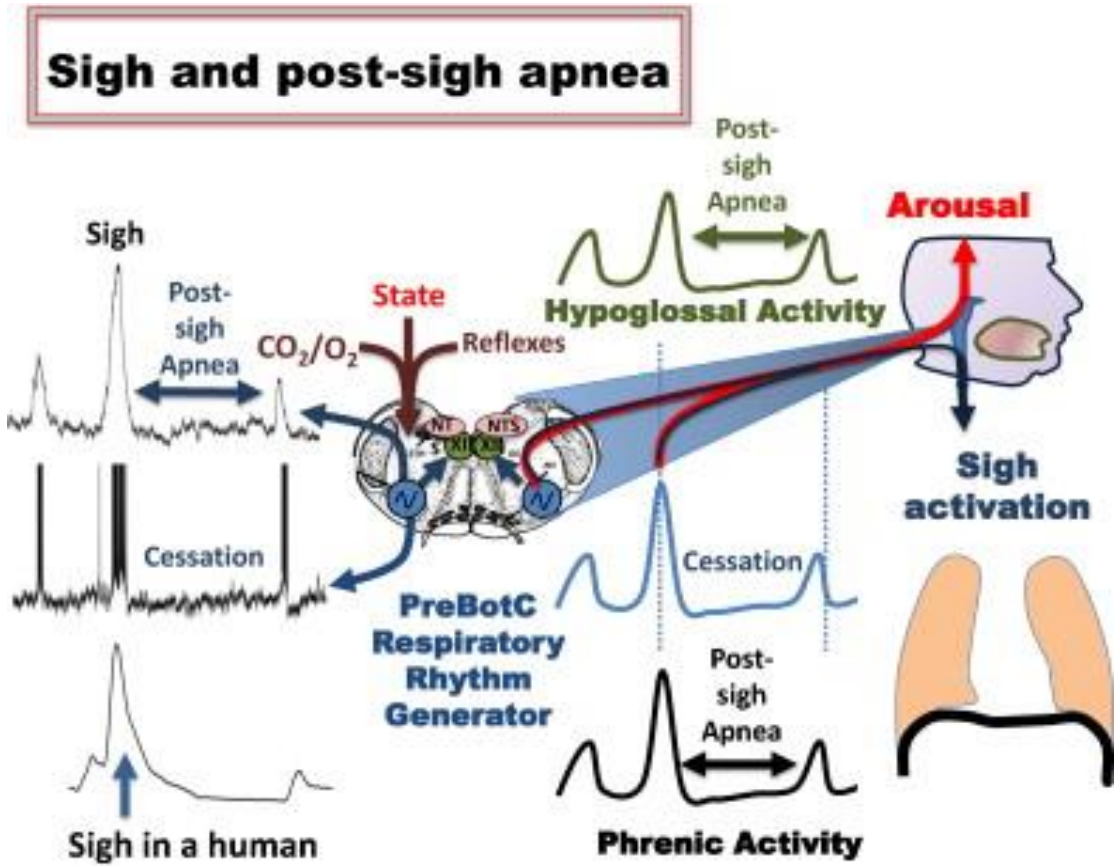

Figure 3. Mechanisms of sigh and post-sigh apnea. Left panel: Upper trace: integrated extracellularly recorded pre-Bötzinger complex population activity obtained simultaneously with an intracellular recordings from an inspiratory neuron located within the pre-Bötzinger complex (middle trace). The lower trace represents a recording from a

human subject. While the lower trace was obtained using induction plethysmographic recording (for more details see Weese-Mayer et al., 2006), the upper and middle traces were obtained in an isolated transverse slice preparation shown in the schematic. The preparation contains the functionally active pre-Bötzinger complex (blue), the nucleus tractus solitaries (NTS, pink), which in the intact animal would receive reflex inputs. Contained within the slice is also the hypoglossal nucleus (XII, green), which in the intact animal would innervate the genioglossus muscle. The actual data shown on the left panel inspired the middle panel, which schematically illustrates how the rhythmically active pre-Bötzinger complex (blue trace) could activate a sigh and apnea in the phrenic nucleus (black trace) resulting in diaphragmatic activity, and sigh activity and apnea in the XII (green trace, apnea). The right panel illustrates the anatomical components contributing to the central apnea associated with the sigh, as well as the illustration of arousal that is associated with the generation of the sigh. The bilaterally organized pre-Bötzinger complex isolated in the transverse slice preparation was obtained from the lower brainstem (medulla – schematically shown in blue). The sigh is activated by changes in the state, oxygenation and CO_2 levels. For more details see text.

3.5 Reflex regulation

In OSA, airway occlusion also involves reflex mechanisms (Fig.1) that are characterized by pathological gain changes in the mechano- and chemosensory reflex loops regulating ventilation. These reflex pathways become specifically dysregulated during sleep and could therefore destabilize the respiratory response to an airway obstruction resulting in pharyngeal collapse during sleep and not wakefulness (Douglas et al., 1982; White, 2005).

3.5.1 Mechano-sensory reflexes

To prevent pharyngeal collapse, mechanoreceptors located within the pharyngeal walls specifically regulate the XII motorneurons (Fig.1). These receptors are activated by negative intraluminal pressure generated during inspiration. They transmit this afferent information via the superior branch of the internal laryngeal nerve, and genioglossus pre-motorneurons located near the obex mediate the reflex (Chamberlin et al., 2007). This is

an important reflex, as activation of the hypoglossal muscles caused by a pressure drop should counteract a pharyngeal collapse (Eckert et al., 2007b; Horner et al., 1991; Malhotra et al., 2000). Under physiological conditions this mechano-sensory pathway, as well as central nervous system components that are not involved in the reflex, contribute to the phasic genioglossus contraction during inspiration (Chamberlin et al., 2007; Fogel et al., 2001; Horner, 2000; Susarla et al., 2010; van Lunteren, 1993). Importantly, the reflex activation of the genioglossus during these pressure drops is dramatically reduced or even suppressed during sleep, a finding that is of great significance in understanding OSA (Wheatley et al., 1993).

3.5.2 Arterial chemosensory mechanisms

Hypoxia and hypercapnia initiated chemoreflexes are known to contribute to the regulation of ventilation (Fig.1), and a high gain in any of these chemosensory loops could contribute to breathing instabilities (White, 2005). The following lines of evidence suggest that the arterial chemoreflex is augmented in OSA subjects: a) brief hyperoxic exposure, which inhibits chemoreceptor activity, reduces blood pressure in OSA patients but not in control subjects (Narkiewicz et al., 1998), b) the hypoxic ventilatory response, a hallmark response of the chemoreflex, is augmented in OSA subjects compared to controls (Hedner et al., 1992), and c) activation of muscle sympathetic nerve activity by apneas is more pronounced in OSA subjects compared to controls (Smith et al., 1996). Development of altered chemosensory reflexes in OSA is further supported by studies using intermittent hypoxia (IH), the hallmark manifestation of recurrent apnea. Rodents exposed to chronic IH showed: a) enhanced carotid body sensitivity to hypoxia, and b) a

progressive increase in baseline carotid body sensory activity, a phenomenon termed sensory long-term facilitation (sLTF) (Pawar et al., 2008; Peng et al., 2009; Peng et al., 2003; Peng and Prabhakar, 2004; Peng et al., 2006; Rey et al., 2004). The subnuclei of the nucleus tractus solitarius (NTS, Fig. 1), especially the commissural part of the NTS (cNTS), receive inputs from the carotid body (Chitravanshi and Sapru, 1995; Zhang and Mifflin, 1993). Neuronal activity in cNTS is regulated by various neurotransmitters, including glutamate, an excitatory amino acid transmitter, and dopamine, an inhibitory biogenic amine. Chronic IH up regulates GluR2/3 glutamate receptor subunit expression in cNTS (Costa-Silva et al., 2012) and down regulates tyrosine hydroxylase (TH) expression, the rate-limiting enzyme in dopamine (DA) synthesis (Gozal et al., 2005; Kline et al., 2002). It is likely that chronic IH, by down regulating the synthesis of DA, enhances glutamatergic excitatory transmission in NTS (Chen et al., 1999) resulting in the enhanced hypoxic ventilatory response (HVR). Collectively, these studies indicate that the augmented chemoreflex by chronic IH involves reconfiguration of neurotransmitter profiles in the central nervous system.

Does an augmented chemoreflex contribute to pathogenesis of apnea? It was proposed that the increased carotid body sensitivity to hypoxia can lead to a greater magnitude of hyperventilation during each episode of apnea, thus driving the respiratory controller below the apneic threshold for CO_2, leading to greater number of apneas (Prabhakar, 2001). In other words, the heightened hypoxic sensitivity of the carotid body might act as a “positive feedback,” thereby exacerbating the occurrence of apneas. Supporting such a possibility is the finding that chronic IH exposed rats with intact carotid bodies exhibit greater incidence of spontaneous apneas. This effect was absent in carotid

body sectioned rats exposed to chronic IH (Prabhakar, 2013). Since peripheral chemoreceptors regulate hypoglossal motorneuron activity (Bruce et al., 1982), it remains to be established whether the chemoreflex directly or indirectly contributes to the hypoglossal motorneuron dysfunction leading to OSA.

3.6 Airway occlusion and the central respiratory network.

Chemo- and mechanosensory afferents and modulatory inputs converge via the NTS on the XII motorneurons where they closely interact with the central respiratory drive acting on the XII motorneurons. As shown in Fig.1, an apnea generated at the level of the XII motorneurons could involve a temporary drop-out of central XII activity while respiratory rhythmic activity continues to be generated within the central respiratory network. Neuronal mechanisms that could lead to such a drop out could occur locally within the medulla. Located within the same transverse plane as the XII nucleus is the pre-Bötzinger complex (preBötC; Fig.1). The preBötC is a well-defined neuronal network that is essential for breathing. Selective lesion of the preBötC in intact animals abolishes breathing (Gray et al., 2010; Ramirez et al., 1998b; Tan et al., 2008). Moreover, isolated in medullary slice preparations that encompass the preBötC (Figure 1, preBötC, blue), this neuronal network continues to spontaneously generate inspiratory rhythmic activity (Fig.1, left panel). Inspiratory activity generated within the preBötC is transmitted to the XII nucleus and leads to the phasic activation of an inspiratory population burst within the hypoglossal nucleus (Fig.1, left panel). Located within this slice preparation are premotor neurons that transmit the respiratory signal from the preBötC to the XII motorneurons (Chamberlin et al., 2007; Dobbins and Feldman, 1995; Luo et al., 2006; Peever et al.,

2002; Sebe and Berger, 2008). These premotor neurons are not simple followers, but they seem to play a major role in generating synchronous oscillations within the XII motor nucleus (Sebe and Berger, 2008). Interestingly, not every burst in the preBötC is transmitted to the XII and in some slice preparations the XII can fail to burst in phase with the respiratory cycle generated within the preBötC (Fig.1; (Ramirez et al., 1996)). It is conceivable that such an activation failure could provide a mechanistic explanation for XII inactivity during continued inspiratory respiratory rhythm generation from the preBötC. The inspiratory rhythm generated in the preBötC would then continue to be transmitted to the phrenic nucleus (Fig.1). Continued activation of the diaphragm is an important aspect of OSA, as it is the activated diaphragm that produces the expansion of the thorax which together with a lack of genioglossus activation creates negative pressure and pharyngeal collapse. At this point, we do not know how the respiratory drive from the preBötC is transmitted under conditions that mimic sleep states or conditions that mimic sleep apnea. During hypoxia, however, transmission failure from the preBötC to the XII motorneurons is increased (Pena et al., 2008). Thus, an important avenue for future research will be to understand how chronic intermittent hypoxia or certain neuromodulatory conditions associated with sleep can cause such transmission failures between the respiratory rhythm generator and the XII motor output. Investigating this issue could provide important and much needed clues into the pathology of OSA.

3.7 The recovery from airway occlusion.

In addition to the onset and maintenance of airway occlusion, recovery from an airway obstruction has been the subject of intense discussions (Fig.2). One notion is that

reflex recruitment of pharyngeal dilator muscles is insufficient to open the airway once it is occluded and that arousal is required for the termination. This is an important consideration, since breathing instabilities that promote OSA likely involve pathological changes in arousal threshold (Younes, 2004). Arousal is stimulated by increased negative pharyngeal pressure and increasingly hypoxic and hypercapnic conditions that in turn increase respiratory drive (Berry and Gleeson, 1997; Gleeson et al., 1990; Kimoff et al., 1994). The stimulation of arousal then activates dilator activity and opens the airways (Remmers et al., 1978). Yet, arousal is not required for apnea termination (Younes et al., 2012). Figure 2 illustrates the recovery from an airway occlusion which is typically abrupt and associated with a sudden burst of genioglossus EMG (Berry and Gleeson, 1997; Rees et al., 1995; Remmers et al., 1978; Wulbrand et al., 1998, 2008). The abrupt increase in genioglossus muscle activity seems to be due to the recruitment of phasic inspiratory motor units (Wilkinson et al., 2010). Wulbrand and coworkers proposed that this burst is synchronized with the generation of sigh or sigh-like neuronal mechanisms (Wulbrand et al., 1998). The induction of sighs by airway occlusion has also been reported by Alvarez et al. (1993). Sighs are large amplitude inspiratory efforts that are mechanistically different from normal “eupneic” breaths (Fig.4) (Lieske and Ramirez, 2006a, b; Lieske et al., 2000). Although, it was initially believed that sighs are exclusively dependent on lung stretch receptor stimulation (Bartlett, 1971; Reynolds, 1962; Wulbrand et al., 2008); there is ample evidence to the contrary – i.e. sighs are generated within the central nervous system and do not require afferent input (Orem and Trotter, 1993). For example sighs can be generated following deafferentation *in vivo* (Cherniack et al., 1981), and humans continue to generate sighs following lung transplantation (Shea et al., 1988).

Moreover, sighs are even generated in the in situ working heart preparation, a fully deafferented brainstem preparation, (Ramirez and Viemari, 2005), as well as transverse slice preparations that contain the preBötC (Fig.4) (Hill et al., 2011; Lieske et al., 2000; Pena et al., 2004), and “preBötC islands” isolated from the transverse slice (Garcia et al., 2011a; Johnson et al., 2001; Viemari et al., 2011). Important for the discussion of OSA, this centrally generated mechanism is specifically facilitated under hypoxic conditions (Bartlett, 1971; Bell et al., 2009; Bell and Haouzi, 2010; Cherniack et al., 1981; Hill et al., 2011; Lieske et al., 2000; Schwenke and Cragg, 2000). Although peripheral chemoreceptors certainly play a facilitatory role (Cherniack et al., 1981; Glogowska et al., 1972; Matsumoto et al., 1997), even in the absence of peripheral chemoreceptors, hypoxic conditions within the preBötC are sufficient to centrally activate the generation of sighs (Hill et al., 2011; Koch et al., 2013; Pena et al., 2004; Telgkamp et al., 2002). Thus, the hypoxic conditions associated with OSA will likely play a role in activating sighs. As characterized in infants, sighs triggered by an airway occlusion are coordinated with a sleep startle, that marks the beginning of arousal (Figs.4,5), and accompanying changes in electroencephalogram (EEG) and EMG activity (Wulbrand et al., 2008). Although cortical arousal is not always observed, sighs consistently coincide with a sudden rise in limb EMG activity and a distinct neck extension, an adaptive response that can contribute to the termination of an airway occlusion (Wulbrand et al., 2008). Not only in infants, but also in adults, sighs are linked to EMG activation and EEG changes (Perez-Padilla et al., 1983).

Sighs are also associated with a heart rate increase followed by a heart rate decrease (Haupt et al., 2012; McNamara et al., 1998; Porges et al., 2000; Weese-Mayer

et al., 2008; Wulbrand et al., 2008). The heart rate changes associated with the sigh are often altered in human diseases such as familial dysautonomia, sickle cell anemia, and SIDS (Franco et al., 2003; Sangkatumvong et al., 2011; Weese-Mayer et al., 2008). From the organismic perspective, the hypoxic sensitivity of the sigh becomes a very important central nervous system mechanism that allows the organism to detect and respond to hypoxic conditions. Hypoxia-induced sighs activate important muscles and can lead to subcortical and cortical arousal (Fig.4). Once aroused, an organism can avoid the hypoxic condition by for example changing its sleeping position. The sigh may therefore link the hypoxic condition caused by OSA to arousal, which eventually results in sleep deprivation, one of the detrimental consequences of OSA. Interestingly sighs may also play an important role in the generation of periodic breathing as postulated by (Guntheroth, 2011).

This centrally generated mechanism is very sensitive to state changes (Orem and Trotter, 1993). The transition from sleep to wakefulness is often characterized by the activation of a sigh and arousal (Figure 4) (Eckert et al., 2007a). Note, in Figure 4, the sigh seems to contribute to a decrease in CO_2 level. This decrease in CO_2 may be involved in the generation of the apnea that typically follows the sigh. Indeed, during an "augmented" breath simulated by a ventilator, a decreased CO_2 drive can generate a brief apnea as elegantly demonstrated by Remmers et al. 1978. However, these simulated augmented breaths evoked brief apneas only under certain conditions such as hypoxia. Moreover, we know that the post-sigh apnea can be generated centrally within the preBötC under conditions in which oxygen and CO_2 are not altered (Fig.4). Thus, the post-sigh apnea is indeed a "central apnea" generated within the ventrolateral medulla.

Interestingly, a “post-sigh-like apnea” can be simulated centrally, by maximally stimulating isolated medullary respiratory pacemaker neurons. This purely central electrical stimulation is followed by a prolonged pause in the rhythmic bursting of these respiratory neurons (Tryba et al., 2008).

The post-sigh apnea is an important manifestation of a central apnea (Eckert et al., 2007a; Radulovacki et al., 2001; Saponjic et al., 2007). Post-sigh apneas are very common in children (Haupt et al., 2012; O'Driscoll et al., 2009) but are also present in adults (Vlemincx et al., 2010). Post-sigh apneas can be exaggerated in neurological disorders such as Leigh Syndrome (Quintana et al., 2012; Saito, 2009; Yasaki et al., 2001), Familial Dysautonomia (Weese-Mayer et al., 2008), and Rett Syndrome (Voituron et al., 2010). Although it is clearly generated centrally, it must be emphasized that in the intact organism, additional chemosensory mechanisms will contribute and potentially exaggerate the post-sigh apnea.

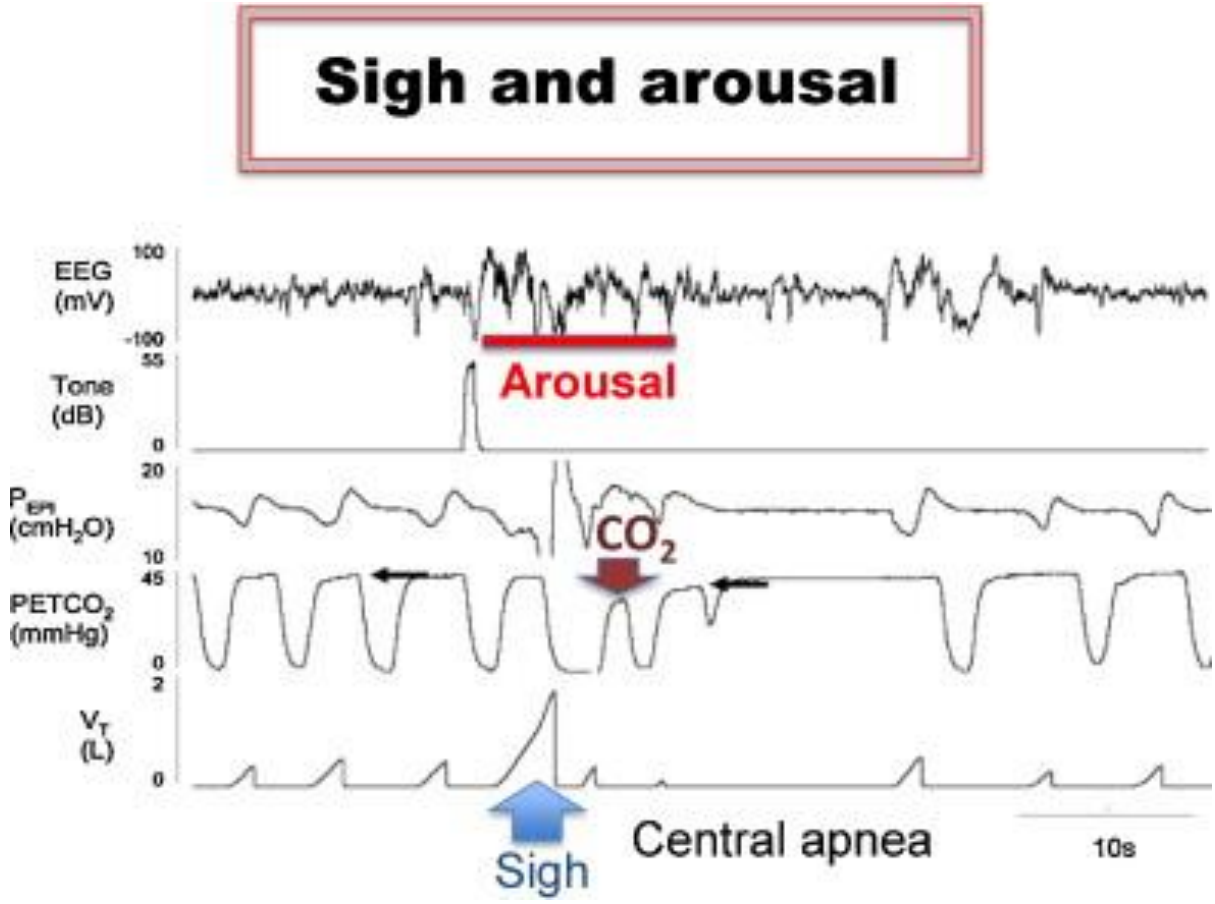

Figure 4. The generation of the sigh is associated with arousal. The example was obtained during the transition from sleep to wakefulness. Note, the sigh (lower trace) is associated with a prolonged central apnea that follows a decrease in the level of CO_2, which was caused by the sigh, suggesting that the hypocapnia may contribute to the generation of the apnea that followed the sigh.
Figure modified from Eckert et al., 2007a and Eckert et al., 2007b.

3.8 Conclusion

Apneas emerge through a complex interplay between peripheral and central nervous system factors that affect all levels of integration: from the molecular to the cellular and organismic level. This interplay affects many aspects of respiratory control making it difficult to clearly separate central versus peripheral contributions to the generation of the apnea. Moreover, OSA as well as central apneas have numerous long-

term consequences that include changes in the neuromodulatory milieu, mechano- and chemosensory reflex loops, cardiorespiratory integration and neurotransmitter systems. These changes may be partly adaptive during wakefulness but they often fail to adequately adapt the organism during the night. Indeed, many of the consequences become critical contributors to the morbidity of the apneas. While traditionally, much emphasis has been placed on understanding the contributions of chemo- and mechanosensory reflexes, the changes in blood gases, and the biomechanics of the apneas, we have only recently begun to understand how these contributors interact with the central respiratory network, an integration that still raises many unanswered questions. Future research will elucidate many of these questions and may inspire novel avenues for therapies that could target the most detrimental and persisting consequences of sleep apnea, a health issue that affects an increasing proportion of the pediatric and adult populations.

Chapter 4

Defining modulatory inputs into CNS neuronal subclasses by functional pharmacological profiling

*This chapter was published with minor reformatting as an article with the same title in *Proceedings of the National Academy of Sciences of the United States of America* (PNAS). Co-authors of this work included: Shrinivasan Raghuraman, Alfredo J. Garcia, Vernon D. Twede, Kigen J. Curtice, Kevin Chase, Jan-Marino Ramirez, Badldomero M. Olivera, and Russell W. Teichert. The full citation is as follows:

Raghuraman, S., Garcia, A.J., Anderson, T.M., Twede, V.D., Curtice, K.J., Chase, K. Ramirez, J.M., Olivera, B.M., Teichert, R.W. (2014). Defining modulatory inputs into CNS neuronal subclasses by functional pharmacological profiling. *Proceedings of the National Academy of Sciences of the United States of America, 111*(17), 6449-54.

4.1 Significance

We functionally profiled cells from a locus of the mouse brainstem that contains the neuronal network responsible for generating breathing patterns. By uncovering cell-specific constellations (i.e., distinctive combinations of receptors and ion channels that define each cell type), we identified specific neuronal classes and subclasses within the network. We discovered neuromodulators affecting the activity of specific neuronal subclasses within the functional network. This study provides proof-of-principle that a pharmacological strategy for altering the activity of a specific type of neuron can be developed which has potential as a parallel or complementary approach to genetic strategies for functionally perturbing a specific neuronal cell type *in vivo*. Additionally, unlike genetic approaches, this pharmacological approach is directly applicable to non-model organisms.

4.2 Abstract

Previously we defined neuronal subclasses within the mouse peripheral nervous system using an experimental strategy called “constellation pharmacology.” Here we demonstrate the broad applicability of constellation pharmacology by extending it to the CNS and specifically to the ventral respiratory column (VRC) of mouse brainstem, a region containing the neuronal network controlling respiratory rhythm. Analysis of dissociated cells from this locus revealed three major cell classes, each encompassing multiple subclasses. We broadly analyzed the combinations (constellations) of receptors and ion channels expressed within VRC cell classes and subclasses. These were strikingly different from the constellations of receptors and ion channels found in

subclasses of peripheral neurons from mouse dorsal root ganglia. Within the VRC cell population, a subset of dissociated neurons responded to substance P, putatively corresponding to inspiratory pre-Bötzinger complex (preBötC) neurons. Using constellation pharmacology, we found that these substance P-responsive neurons also responded to histamine, and about half responded to bradykinin. Electrophysiological studies conducted in brainstem slices confirmed that preBötC neurons responsive to substance P exhibited similar responsiveness to bradykinin and histamine. The results demonstrate the predictive utility of constellation pharmacology for defining modulatory inputs into specific neuronal subclasses within central neuronal networks.

4.3 Introduction

Progress in understanding the mammalian brain has been impeded by the extraordinary complexity of cell types comprising the circuitry and the difficulty in bridging different levels of biological organization from the molecular to the cellular and systems level (Bernard et al., 2009; Franco and Muller, 2013; Nelson et al., 2006; Sugino et al., 2006). Systems neuroscientists study the circuitry and high-level functions of the brain, whereas molecular neuroscientists study the molecular components. The large divide between these two branches of neuroscience clearly needs to be bridged to understand fully neuronal and behavioral functions in health and disease. To this end, we recently demonstrated an experimental approach we call “constellation pharmacology” to identify different neuronal subclasses by the combinations (constellations) of receptors and ion channels functionally expressed in each subclass (Smith et al., 2013b; Teichert et al., 2014; Teichert et al., 2012a; Teichert et al., 2012b). This experimental approach initially

was applied to somatosensory neurons of the peripheral nervous system (PNS). In the present study, we use constellation pharmacology to identify neuronal subclasses of the CNS and to characterize these subclasses at the network level. Specifically, we have used constellation pharmacology to define the diverse cell types found in the mouse ventral respiratory column (VRC) and surrounding brainstem tissue.

The VRC contains a variety of neurons that are active during either inspiratory or expiratory phases of breathing. One key network within the VRC is the pre-Bötzinger complex (preBötC), which contains the circuitry essential for generating the respiratory rhythm (Gray et al., 2010; Ramirez et al., 1998b; Smith et al., 1991; Tan et al., 2008). This network of inspiratory neurons is heterogeneous, encompassing neurons with unique pharmacological profiles (Gray et al., 1996; Lieske et al., 2000; Pena et al., 2004; Pena and Ramirez, 2004; Ramirez et al., 2012). Moreover, the tissue immediately surrounding the preBötC also contains neuronal networks important to cardiovascular control, such as cardiac parasympathetic vagal neurons of the nucleus ambiguus and noradrenergic neurons of the A2/C2 region (Dergacheva et al., 2010; Zanella et al., 2006). This anatomical convergence of networks responsible for respiratory and cardiovascular control creates an avenue through which different control elements may coordinate and couple (Garcia et al., 2013) but also produces a cellular population that is heterogeneous in the responsiveness to neuromodulation.

Here we used constellation pharmacology to identify three major cell classes from the VRC and surrounding tissue. Each of these major cell classes encompasses additional subclasses that exhibit unique pharmacological profiles. We focused on one specific neuronal subclass that is responsive to substance P because substance P is an

established modulator of inspiratory preBötC neurons (Pena and Ramirez, 2004). Constellation pharmacology suggested that substance P-responsive inspiratory neurons also would be responsive to histamine and bradykinin. This hypothesis was confirmed in the acute brainstem slice. Thus, this study demonstrates the utility of constellation pharmacology for investigating cell-specific constellations of receptors and ion channels expressed within neuronal and glial subclasses of the mouse brainstem and the broader potential for bridging molecular and systems neuroscience at the cellular level.

4.4 Results

4.4.1 Dissociated VRC cell cultures

We prepared cultures of dissociated VRC cells as described in SI Materials and Methods (see section 3.7). Briefly, for each culture, we prepared a brainstem slice ~200 microns thick, at the level of the preBötC, from a mouse at postnatal day 7 or 8 (P7-8). We followed the same experimental approach and same protocols that we developed for producing rhythmically active brainstem slice preparations (Lieske et al., 2000; Pena et al., 2004; Ramirez et al., 1996). The region containing the preBötC and surrounding VRC was microdissected from the brainstem slice; then the cells were dissociated by enzymatic (trypsin) and mechanical methods. Cells were cultured overnight before calcium-imaging experiments were performed.

Fig. S1shows images of dissociated VRC cell cultures of inadequate, optimal, and excessive density. In our hands, the optimal plating density was ~800 cells/mm^2 (not all cells survive). This plating density allowed us to perform calcium-imaging experiments in which we could monitor the individual responses of more than 100 cells simultaneously

while avoiding an excessive number of cells that overlapped or made contact with neighboring cells. This optimal density enabled us to report the intrinsic responses of individual cells confidently in this study.

4.4.2 Calcium imaging

Fig. S1 exemplifies a VRC cell culture that was used for a calcium-imaging experiment. The images in Fig. S1 D-G show the same field of view. Fig. S1D is bright-field image. A fluorescence image of the same cells loaded with Fura-2-AM dye (380-nm excitation and 510-nm emission) is shown in Fig. S1E. Fig. S1F is a pseudocolored ratiometric image of cells loaded with Fura-2-AM dye at rest. The ratio of fluorescence intensities at 510-nm emission, when excited alternately with 340-nm and 380-nm light, provides a relative measure of cytosolic calcium concentration, $[Ca^{2+}]_i$. Fig. S1G is a ratiometric image taken immediately after a stimulus to which a subset of the cells in the culture responded with an increase in $[Ca^{2+}]_i$.

The essence of the constellation pharmacology strategy is to probe a heterogeneous population of dissociated cells with a panel of selective pharmacological agents, among other physicochemical perturbations, and to monitor simultaneously the individual responses of more than 100 cells by calcium imaging. By monitoring the different response phenotypes, we can parse cell populations into major cell classes and minor subclasses.

4.4.3 Pharmacological profiling of VRC cells

Fig. 1 exemplifies calcium-imaging traces from selected VRC cells in response to a set of receptor agonists and to depolarization by a high concentration (e.g., 100 mM) of extracellular potassium (high $[K^+]_o$). Abbreviations and concentrations for each of the pharmacological agents and other cellular perturbations used in this study are summarized in Table 1. Three major classes of cells within these cultures could be differentiated by their distinct response profiles.

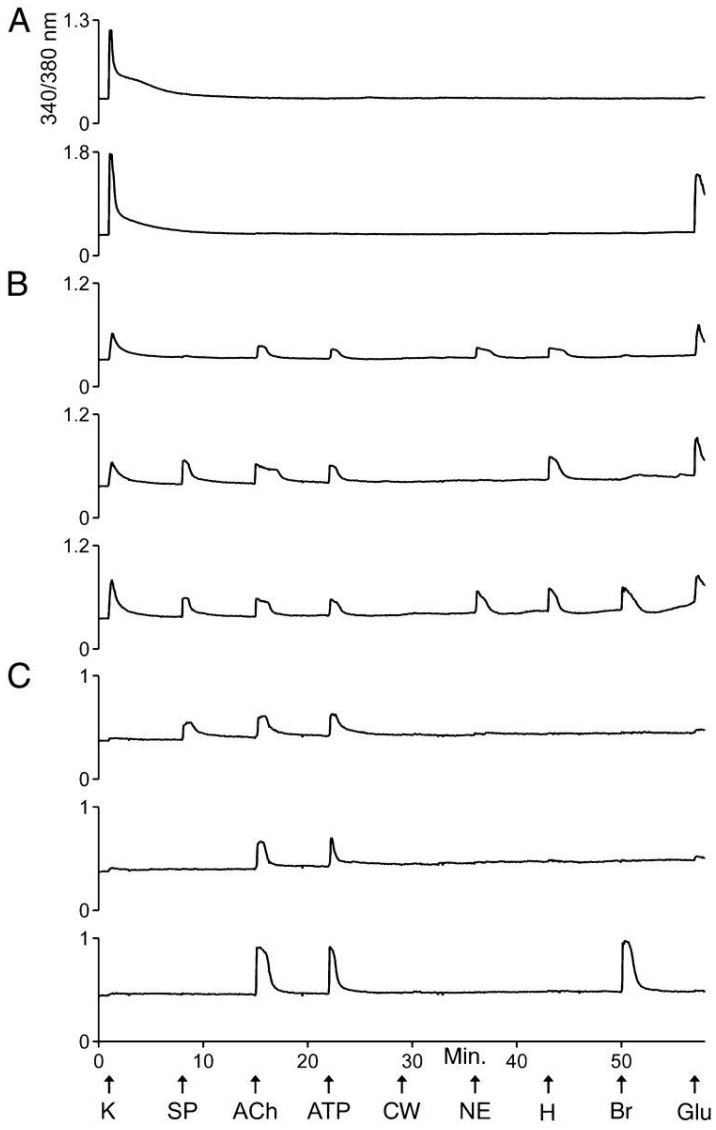

Figure 1. Examples of calcium-imaging traces from dissociated VRC cells in culture. Each trace is the response of a single cell to the experimental protocol depicted at the bottom of the figure. In each experimental trial, the individual responses of >100 cells were monitored simultaneously. The *x*-axis and experimental protocol at the bottom of the figure apply to all traces in the figure. The units of the *x*-axis are time in minutes. The arrows identify time points when various types of stimuli were applied to the cells for 15 s. The abbreviations for these stimuli are defined in Table 1. "CW" represents a control wash, i.e., the replacement of bath solution (artificial CSF, aCSF) with identical bath solution. The *y*-axis for each trace is the ratio of fluorescence intensities obtained at 510-nm emission from the alternating excitation by 340-nm or 380-nm light. It is a measure of relative changes in $[Ca^{2+}]_i$. (*A*) Examples of traces from class A cells. Both cells responded strongly to depolarization by high $[K^+]_o$, but only one responded to glutamate with an increase in $[Ca^{2+}]_i$. (*B*) Examples of traces from class B cells. Notably, these cells responded less strongly than class A cells to high $[K^+]_o$. They typically responded to several receptor agonists, as shown. (*C*) Examples of traces from class C cells. These cells either did not respond to depolarization by high $[K^+]_o$ or responded very weakly.

Abbreviation	Compound	Working concentration
ACh	Acetylcholine	1 mM
ArIB	α-Conotoxin ArIB[V11L;V16D]	200 nM
ATP	Adenosine 5′ triphosphate	20 μM
Br	Bradykinin	10 μM
CW	Control Wash	NA
Glu	Glutamate	300 μM
H	Histamine	50 μM
K	$[K^+]_o$	100 mM
NE	Norepinephrine	20 μM
NMDA	*N*-methyl-D-aspartate and	100 μM
D-ser	D-serine	10 μM
PNU	PNU-120596	5 μM
SP	Substance P	1 μM

Table 1. Abbreviations of compounds cited in figures and tables

The first major cell class, class A, was defined by responsiveness to high $[K^+]_o$ and by the lack of responses to a panel of receptor agonists (Fig. 1A and Table 2). The second major cell class, class B, was defined by responsiveness to high $[K^+]_o$ and one or more receptor agonists tested (Fig. 1B and Table 2). Notably, responsiveness to glutamate was excluded as a criterion for classifying cells, because ~75% of both class A and class B

cells responded to glutamate. However, only class B cells responded to the other receptor agonists (Table 2). In fact, the majority of class B cells responded to each of the receptor agonists, with the exceptions of the neuropeptides substance P and bradykinin, to which a minority of the class B cells responded (Table 2).

Criteria for classification			Total cells	% of total cells	% responsive cells in each cell class						
Cell class	Average response to 100 mM $[K^+]_o$ ± SD	Responsiveness to pharmacological compounds			SP	ACh	ATP	NE	H	Br	Glu
Ventral respiratory column (p7-8 mouse)											
Class A	0.8 ± 0.4	Responsive to glutamate only and response to 100 mM $[K^+]_o$ ≥ 0.1	220	13	0	0	0	0	0	0	78
Class B	0.3 ± 0.2	Responsive to other receptor agonists and response to 100 mM $[K^+]_o$ ≥ 0.1	574	33	8	91	68	65	74	35	76
Class C	0.0 ± 0.0	Response to 100 mM $[K^+]_o$ < 0.1	965	55	1	6	8	4	5	6	6
Dorsal root ganglia (p8 mouse)											
Class A/B	Responsive	Response to 100 mM $[K^+]_o$ ≥ 0.1	787	32	0	7	76	1	6	27	3
Class C	0	Response to 100 mM $[K^+]_o$ < 0.1	1,673	68	0	7	86	0	0	5	0

Table 2. The average response to 100 mM $[K^+]_o$ ± SD is a relative measure of the change in $[Ca^{2+}]_i$ elicited by 100 mM $[K^+]_o$ (i.e., change in the 340/380-nm ratio shown in figures and described in Supplementary Materials and Methods). Larger numbers indicate a greater response or greater relative change in $[Ca^{2+}]_i$ elicited by high $[K^+]_o$. The VRC dataset was compiled from five independent experimental trials using cells prepared separately from four different mice. The DRG dataset was compiled from six independent experimental trials using cells prepared separately from two different mice. ACh,

acetylcholine; Br, bradykinin; Glu, glutamate; H, histamine; NE, norepinephrine; SP, substance P.

On average, class A cells responded to depolarization by high $[K^+]_o$ with large, transient increases in $[Ca^{2+}]_i$ (Fig. 1A and Table 2), indicating that they express high levels of voltage-gated calcium channels as is characteristic of neurons. On average, class B cells responded less strongly than class A cells to depolarization by high $[K^+]_o$ Fig. 1B and Table 2). This difference was statistically significant (*P* value = 0.001, Student *t* test). At present it is unclear whether class B cells are all neurons or are a mixed population of neurons and glia.

The third major cell class, class C, comprises putative nonneuronal cells (glial cells and potentially other nonneuronal cells) that did not respond to depolarization by high $[K^+]_o$ or responded very weakly (i.e., a change in 340/380-nm ratio <0.1) (Fig. 1C and Table 2), suggesting that, unlike neurons, they do not express voltage-gated calcium channels or express these channels at very low levels. A small minority of class C cells responded to each of the receptor agonists tested (Table 2). However, when we reduced the resting $[K^+]_o$ from 3 mM to 0.2 mM, 30% of the class C cells responded with an increase in $[Ca^{2+}]_i$ (Fig. S2). Such responses (putatively mediated by $K_{ir}4.1$) have been shown to be specific to astrocytes in the VRC (Hartel et al., 2009; Hartel et al., 2007). This evidence supports the hypothesis that many class C cells are glial (astrocytes and other glial cells). Furthermore, none of the class A cells responded to 0.2 mM $[K^+]_o$, thus supporting the hypothesis that class A cells are all neurons. However, 6% of the class B cells responded to 0.2 mM $[K^+]_o$, suggesting that some of the class B cells are astrocytes.

4.4.4 Cluster analysis of VRC cells

With the eight stimuli shown in Fig. 1, it theoretically is possible to identify 256 unique cell-response profiles, but 103 unique response profiles actually were observed. We first grouped these 103 response profiles into three broad cell classes, A, B, and C, as described above and as shown in Table 2. We then performed cluster analysis to determine whether these broad cell classes were supported by an unbiased data analysis. The cluster analysis included 1,586 cells, representing the 103 unique response profiles, which clustered robustly into three broad cell classes in all 500 bootstrap trials. These broad cell classes were consistent with our original designations of cell classes A, B, and C.

As a lower bound on the number of unique cell profiles robustly identified, we estimated the number of clusters required to explain most of the variation in cell responses. The cluster analysis summarized in Table S1 grouped cells into 36 clusters that explain 99% of the cell responses. We then sorted those 36 clusters from Table S1 into broader groups that essentially correspond to our original assignments of class A cells (the top two clusters), class B cells (the middle 24 clusters), and class C cells (the bottom 10 clusters). Notably, for each cluster shown in Table S1, the predominant response profiles (the prototype response profile) and the mean responses to depolarization by high $[K^+]_o$ (the mean K^+response) agree with these broader cell class designations.

4.4.5 Comparison of VRC and DRG cells

For direct comparison with VRC cells, we conducted the profiling protocol shown in Fig. 1 with cultures of dorsal-root ganglion (DRG) cells from mice of the same age (P7-8). Table 2 shows the direct comparison between VRC and DRG cells in response to the same panel of pharmacological agents. We divided DRG cells into a combined class A/B group and a separate class C group. The distinction between class A and B cells that was obvious in the VRC was not evident in the DRG. Furthermore, in the DRG, the cell bodies of the neurons are morphologically distinct from the other cell bodies in the culture: The neuronal cell bodies are larger in diameter than the nonneuronal cell bodies and are rounder than the cell bodies of the satellite glial cells, which are relatively flat and elongated (Chen et al., 2012). Therefore, we can conclude that in DRG cultures the class A/B cells are neurons and the class C cells are various nonneuronal cells.

There are several notable points of comparison and contrast between VRC and DRG cultures from P7-8 mice (Table 2): A very high percentage of the class C cells in DRG cultures responded to ATP, in contrast to the low percentage of ATP-responsive class C cells in VRC cultures. In VRC cultures, the majority of the class B cells and a small subset of class C cells responded to norepinephrine with an increase in $[Ca^{2+}]_i$, but almost none of the DRG cells responded to norepinephrine in this way. In VRC cultures, the majority of class A and B cells responded to glutamate, in contrast to the low percentage of glutamate-responsive class A/B cells in DRG cultures. A qualitative assessment of the glutamate responses indicated that the glutamate responses in VRC cells were relatively large compared with the very small responses observed in DRG cells. Other interesting points of comparison and contrast are shown in Table 2.

4.4.6 Acetylcholine-receptor expression in VRC cell classes

In addition to the experimental protocols shown in Fig. 1 and Fig. S2, we investigated the expression of acetylcholine (ACh) receptors (AChRs) in VRC cells (Fig. S3). We observed that responses to ACh were blocked by atropine, suggesting that these responses were mediated primarily by muscarinic acetylcholine receptors (mAChRs) and not nicotinic acetylcholine receptors (nAChRs) (Fig. S3). When the cells were preincubated with a positive allosteric modulator of α7 nAChRs, PNU-120596 (PNU), then a different subset of cells responded to ACh. Notably, α7 nAChRs desensitize very rapidly upon application of ACh (Hone et al., 2012). Such rapid desensitization may prevent a measurable increase in $[Ca^{2+}]_i$ in the absence of PNU. To confirm that the ACh responses in the presence of PNU were mediated by α7 nAChRs, we blocked the responses with the highly subtype-selective blocker of α7 nAChRs, α-conotoxin ArIB[V11L;V16D] (Fig. S3) (Whiteaker et al., 2007).

As shown in Fig. S3, we divided VRC cells into classes A, B, and C, on the basis of their responses to high $[K^+]_o$, ACh (before PNU application), substance P (as shown in Fig. S3), and norepinephrine. Cells were classified as class A if they responded only to high $[K^+]_o$ and as class B if they responded to high $[K^+]_o$and to ACh (before PNU application) or substance P or norepinephrine. Class C cells were determined by the same criterion used in Table 2, a change in the 340/380-nm ratio <0.1 in response to high $[K^+]_o$. On average, the class A cells exhibited greater responses to high $[K^+]_o$ than class B cells, as expected and as demonstrated in Fig. S3D. None of the class A cells responded to ACh before the application of PNU. However, after preincubation with PNU, the majority of class A cells (66%) began to respond to ACh, indicating that they express

functional α7 nAChRs Fig. S3 A and D). In contrast to class A cells, the majority of class B cells (73%) responded to ACh before PNU application. Those responses were blocked by atropine, indicating that the majority of class B cells express functional mAChRs (Fig. S3 B and D).

4.4.7 Glutamate-receptor expression in VRC cell classes

For the following experiments exploring glutamate-receptor expression, cells were parsed into classes A, B, and C by the following criteria: Cells were considered class A if they responded only to high $[K^+]_o$ and as class B if they responded to high $[K^+]_o$and either ACh (in the absence of PNU) or ATP (Fig. 2). Class C cells were determined by the criterion used in Table 2, a change in 340/380-nm ratio <0.1 in response to high $[K^+]_o$. On average, the class A cells exhibited greater responses to high $[K^+]_o$ than class B cells, as expected and as demonstrated in Fig. 2C*C*. Notably, approximately half of class A cells were found to express functionally NMDA receptors [see response to NMDA/D-serine (D-ser) at minute 57 in Fig. 2 A and C] and metabotropic glutamate receptors [for the portion of glutamate-elicited response not blocked by 6-cyano-7-nitroquinoxaline-2,3-dione (CNQX) in Fig. 2*A*], with or without detectable expression of non-NMDA (AMPA or kainate) receptors (for the portion of glutamate-elicited response blocked by CNQX in Fig. 2 A and C). The majority of class B cells functionally expressed AMPA and/or kainite receptors, but only a small minority expressed NMDA receptors (Fig. 2 B and C). Class C cells did not express NMDA receptors Fig. 2C.

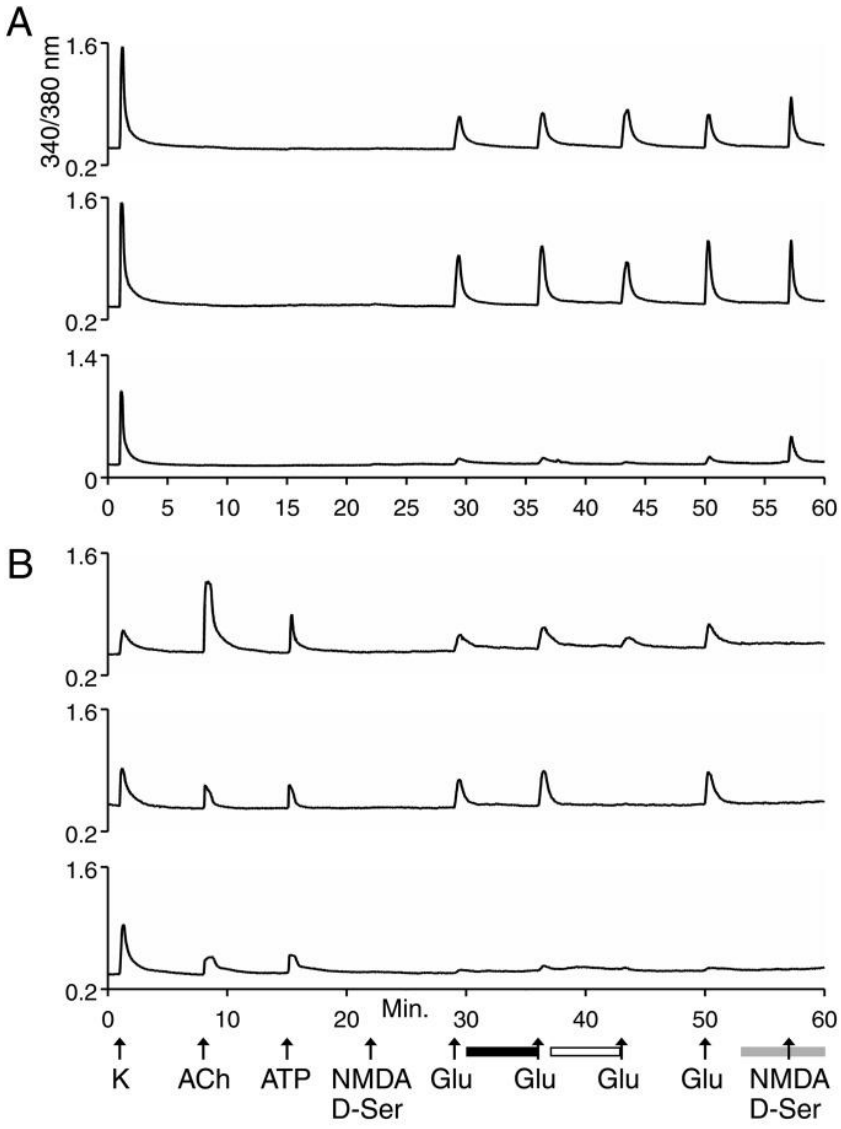

C

			% of responsive cells in each cell class			
Cell Class	**Avg Resp. to 100 mM $[K^+]_o$**	**% of Total Cells**	**NMDA-R**	**Non-NMDA-R**	**Glu Resp. Blocked by CNQX (>5% block)**	**Avg %block by CNQX(S.D.)**
A	1.2	7%	49%	51%	84%	60% (31%)
B	0.3	30%	6%	84%	99%	81% (24%)
C	0.0	63%	0%	1%	99%	89% (16%)

Figure 2. Examples of calcium-imaging traces from experiments investigating glutamate receptors in dissociated VRC cells presented as in Fig. 1. (*A*) Examples of traces from class A cells. (*B*) Examples of traces from class B cells. In *A* and *B* there was no response to NMDA/D-ser in the presence of Mg^{2+} at minute 22 (because Mg^{2+} blocks NMDA receptors without a depolarizing stimulus; compare with NMDA/D-ser application at minute 57 in the absence of Mg^{2+}), indicating that the subsequent responses to 300 μM glutamate were mediated by AMPA/kainite receptors and/or metabotropic glutamate receptors. The black horizontal bar below the *x*-axis indicates the presence of 100 μM AP5 (an NMDA receptor inhibitor) in the bath. The presence of 100 μM AP5 did not block the response to the second application of 300 μM glutamate, confirming that these responses were not mediated by NMDA receptors. The open horizontal bar below the *x*-axis indicates the presence of 10 μM CNQX (an AMPA/kainite receptor inhibitor) in the bath. In general, CNQX partially blocked glutamate-elicited responses, indicating expression of a mix of AMPA/kainite receptors and metabotropic glutamate receptors. The gray horizontal bar below the *x*-axis indicates the time point when the bath solution (aCSF) was changed to Mg^{2+}-free aCSF. The application of NMDA/D-ser in the absence of Mg^{2+} demonstrated that about half of class A cells but only a small minority of class B cells expressed NMDA receptors. (*C*) Compilation of data for class A and B cells. This dataset was compiled for 2,483 cells from eight independent experimental trials, using cells prepared separately from five different mice. Notably, there are some minor discrepancies between the data compiled in *C* from the experimental protocol depicted in *A* and *B* and the data compiled in Table 2 from the experimental protocol depicted in Fig. 1; these discrepancies demonstrate a range of experimental variability.

4.4.8 From dissociated cells to functional networks

Histological studies within the VRC demonstrate that neurokinin-1 receptors within this brainstem region are concentrated most densely at the level of the preBötC (Gray et al., 1999; Guyenet et al., 2002; Pagliardini et al., 2003) and that the application of substance P to the preBötC stimulates both rhythmic network activity and excitability of synaptically isolated preBötC neurons in the brainstem slice preparation (Gray et al., 1999; Pena and Ramirez, 2004). Thus, we focused on class B cells within our dissociated cell preparations that responded to substance P. Fig. 1B and Table S1 demonstrate that there were two main clusters (or subclasses) of substance P-responsive (class B) cells. Although both cellular subclasses were responsive to histamine, only one was responsive

to bradykinin (Table S1). Thus, we hypothesized that histamine and bradykinin may directly modulate the activity of inspiratory preBötC neurons. Patch-clamp recordings were made from inspiratory preBötC neurons in rhythmically active brainstem slice preparations. When these neurons were identified in the functional network, they were isolated from fast synaptic transmission. Fig. 3 shows that histamine and bradykinin exhibited neuromodulatory effects in inspiratory neurons that also were responsive to substance P. Histamine or bradykinin changed firing patterns and increased the firing rate of many inspiratory neurons (Fig. 3). Moreover, as is consistent with the dissociated-cell experiments, substance P-responsive inspiratory neurons within the brainstem slice exhibited a variable sensitivity to bradykinin, as illustrated in the bradykinin response alone (Fig. 3 B and C) and when comparing the individual bradykinin response with that of the respective substance P response (Fig. 3D).

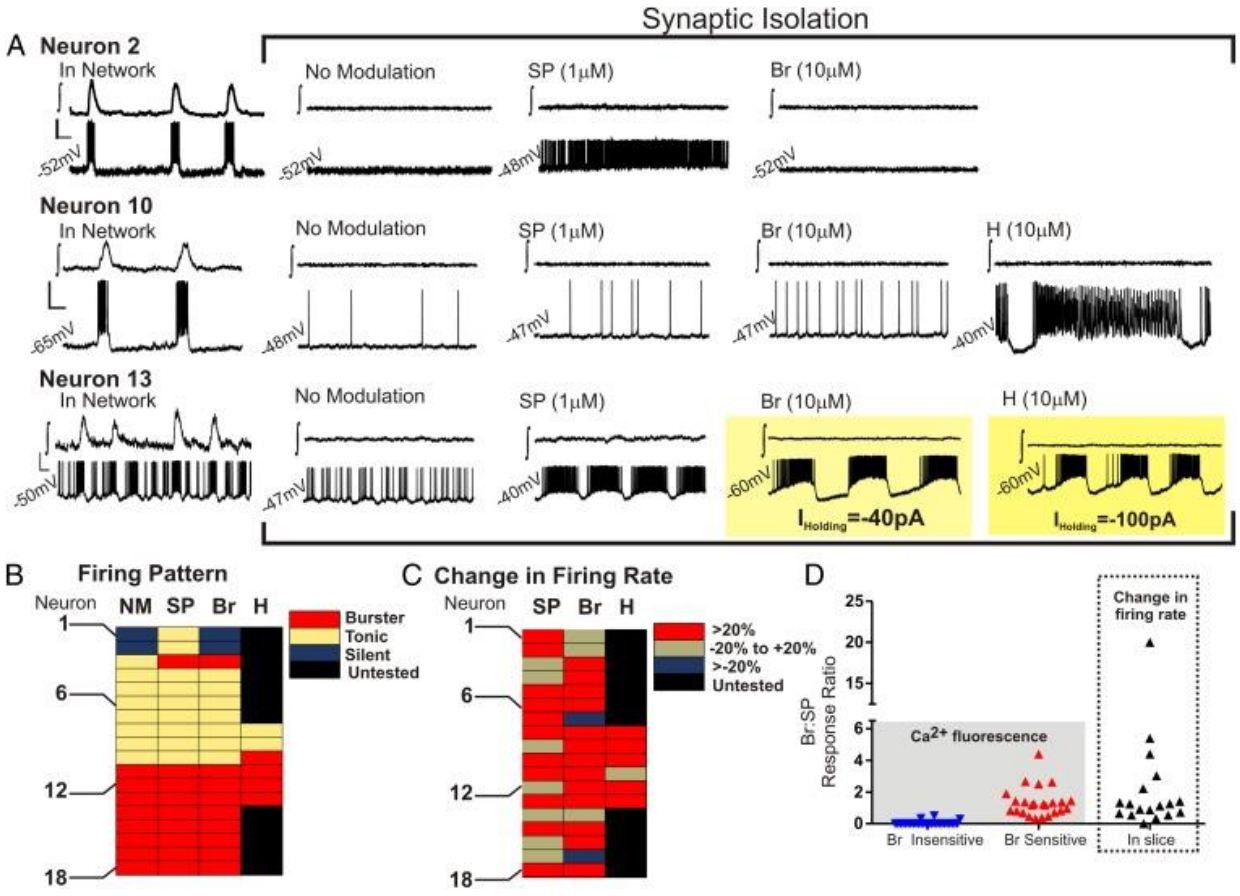

Figure 3. The effects of substance P, bradykinin, and histamine on inspiratory neurons of the preBötC within a brainstem slice preparation. (*A*) Electrophysiology traces are shown in pairs from the preBötC population (∫, upper trace in each case) and a single inspiratory neuron of the preBötC (lower trace in each case) during synaptic isolation, without modulation, and in response to substance P (SP; 1 μM), bradykinin (Br; 10 μM), and histamine (H; 10 μM). (*Top*) Neuron 2 is silent in the absence of exogenous neuromodulation, is stimulated in the presence of substance P to exhibit a tonic firing pattern, is silent in the presence of bradykinin, and was not tested in the presence of histamine. (*Middle*) Neuron 10 is tonic in the absence of exogenous neuromodulation. Although both substance P and bradykinin stimulate a tonic firing rate, histamine changes the tonic firing pattern to a burster phenotype. (*Bottom*) Neuron 13 exhibits a burster phenotype in the absence of exogenous neuromodulation. Substance P stimulates the burster phenotype, whereas both bradykinin and histamine caused Neuron 13 to depolarize (>1.5 mV), requiring the injection of a hyperpolarizing current to prevent depolarization block. [Scale bars: 1 s (*x*-axis) and 20 mV (*y*-axis).] (*B–D*) Summaries of isolated inspiratory neurons (n = 18). These summaries demonstrate the diverse effects of substance P, bradykinin, and histamine on synaptically isolated inspiratory neurons. Examples of silent, tonic, and burster firing patterns are shown in *A*. (*B*) Firing pattern. (*C*) Change in firing rate. (*D*) Comparison of bradykinin responses as a ratio of substance

P responses from individual substance P-sensitive dissociated cells (*Left*) and inspiratory preBötC neurons within the brainstem slice preparation (*Right*).

4.5 Discussion

The results shown in Fig. 3 have two broad implications. (*i*) Constellation pharmacology can identify neuronal subclasses in dissociated cultures that maintain specific properties of neuronal subclasses within an organized network. (*ii*) Constellation pharmacology can be used to generate hypotheses that are testable, and in this case confirmed, within more intact systems. In conjunction with our prior studies of the PNS (5–8), this study suggests that constellation pharmacology may be applied productively to any locus of the CNS. Thus, our ultimate goal is to use constellation pharmacology broadly across different organisms, in different anatomical loci, and at different stages of development to characterize single cells by elucidating their cell-specific constellations of signaling proteins.

Previously, we reported a similar characterization of cells from mouse DRG (Smith et al., 2013b; Teichert et al., 2012a; Teichert et al., 2012b), which we recently have extended to both trigeminal ganglia (TG) and DRG at different developmental stages (Teichert et al., 2014). . In the latter study, neurons from a genetic model organism (mouse) were compared with homologous neurons from a nonmodel organism (rat). In this report, we have extended constellation pharmacology to the comparison of cellular subclasses in the CNS and PNS. In contrast to the DRG and TG neurons that transduce many different sensory modalities from the periphery to the brain, the VRC comprises neuronal networks with integrated physiological functions, i.e., cardiorespiratory control.

Not surprisingly, the constellations of DRG cells are strikingly different from the constellations of VRC cells (Table 2).

In this study, we initiated the classification of different VRC cell types within the mouse brainstem at the level of the preBötC. We have identified three major cell classes: A, B, and C. Class A cells, on average, were strong responders to a depolarizing stimulus. The majority also responded to glutamate but not to any of the other receptor agonists tested in Fig. 1 (see Table 2). However, after pre-incubation with PNU, the majority of class A cells began to respond to ACh, indicating that they express α7 nAChRs (Fig. S3). In contrast to class A cells, class B cells, on average, were relatively weaker responders to a depolarizing stimulus, and the majority of class B cells responded to several different receptor agonists (Fig. 1, Table 2, and Table S1). Class C cells either did not respond to a depolarizing stimulus or responded very weakly, suggesting that they include glial cells and potentially other nonneuronal cells (Fig. 1 and Table 2). A subset of class C cells (30%) responded to 0.2 mM $[K^+]_o$, suggesting that many of these cells are astrocytes (Fig. S2).

Within class B, the substance P-responsive neuronal subclasses are of particular interest because of their putative roles in generating the breathing pattern within the preBötC. Although the neurokinin-1 receptor does not discretely define the boundaries of the preBötC, histological studies demonstrate that neurokinin-1 receptors are highly concentrated at the level of the preBötC (Gray et al., 1999; Guyenet et al., 2002; Pagliardini et al., 2003). Furthermore, the application of substance P to the preBötC stimulates rhythmic network activity and excitability of synaptically isolated preBötC neurons (Gray et al., 1999; Pena and Ramirez, 2004). The two major subclasses of

substance P-responsive neurons identified in dissociated cell culture (Table S1) appeared to be preBötC neurons because they responded to neuromodulators (substance P, ATP, and norepinephrine) previously shown to modulate the activity of inspiratory preBötC neurons (Doi and Ramirez, 2010; Pena and Ramirez, 2004; Viemari et al., 2011; Viemari and Ramirez, 2006). Additionally, both subclasses responded to histamine, and one subclass responded to bradykinin (Table S1). Constellation pharmacology correctly predicted that preBötC neurons would include both bradykinin-insensitive and -sensitive cells (Figs. 1 and 3 and Table S1). Although previous work demonstrated a role for histamine H1 receptors in stimulating breathing (Qian et al., 2010), our study demonstrates that histamine directly stimulates inspiratory preBötC neurons. The impact of bradykinin on the excitability of preBötC neurons was unknown previously. Thus, we show that constellation pharmacology, coupled with investigations in more organized network structures, can provide insight into biologically relevant cell classifications and cell-specific neuromodulation.

A comparison of bradykinin and substance P responses in dissociated cells and in the brainstem slice revealed a similar distribution of bradykinin sensitivity when normalized to the substance P response of a given cell (Fig. 3D). About 28% of inspiratory neurons were relatively unaffected by bradykinin (with a <20% increase in firing rate; Fig. 3C); this lack of response could not be predicted by firing pattern (Fig. 3B). The proportion of inspiratory neurons unaffected by bradykinin was expected to be larger, given that ~50% of dissociated substance P-sensitive cells were unresponsive to bradykinin (Table S1). However, it may be that not all substance-P sensitive neurons in dissociated culture are preBötC neurons.

One way in which we will explore further the cell-specific constellations of VRC neurons is through the application of subtype-selective conotoxins. We have used this strategy to identify differences in the voltage-gated Na, Ca, and K channels expressed in two different subclasses of cold- and menthol-sensitive DRG neurons (Teichert et al., 2012a). The ever-expanding toolkit of selective pharmacological agents, including the conotoxins among many others, will make constellation pharmacology an increasingly powerful platform for single-cell profiling. With our approach we should be able to tease apart the differential physiological roles of divergent neuronal subclasses. By combining insights at the molecular and cellular level with insights at the network level, we hope to achieve a more integrated understanding of cardiorespiratory functions, including breathing-pattern generation and modulation, thus providing a test case that bridges molecular and systems neuroscience.

4.6 Materials and methods

Materials and methods either have been described in detail previously (Ramirez et al., 1996; Smith et al., 2013b; Teichert et al., 2014; Teichert et al., 2012a; Teichert et al., 2012b) or are described in Supplementary Materials and Methods. Transverse medullary brainstem slices were taken from male and female P7–10 mice with a C57BL/6 background as described previously (Ramirez et al., 1996). All procedures in this study were approved by the Institutional Animal Care and Use Committees of the University of Utah or Seattle Children’s Research Institute.

4.7 Supplemental materials and methods

4.7.1 Preparation of Solutions

The medium for culturing ventral respiratory column (VRC) neurons, Eagle's minimal essential medium (MEM) + supplements, was MEM (Invitrogen) supplemented with 10% (vol/vol) FBS (HyClone), penicillin (100 U/mL), streptomycin (100 μg/mL), 1× Glutamax (Invitrogen), 10 mM Hepes, and 0.4% (wt/vol) glucose. The medium was adjusted to pH 7.4 with NaOH and then was filtered through a 0.22-μm filter under sterile conditions. Before use, the medium was stored at 4 °C. It was warmed to 37 °C in a tissue-culture incubator just before use.

We used artificial cerebrospinal fluid (aCSF) for tissue preparations (brain slices and microdissection) and calcium-imaging experiments. It consisted of the following (in mM): 118 NaCl, 3 KCl, 1.5 CaCl2, 1 MgCl2, 25 NaHCO3, 1 NaH2PO4, and 30 D-glucose. For use in tissue preparations, we bubbled carbogen (95% O2 and 5% CO2) through the aCSF to oxygenate the solution and to adjust its pH to 7.4. For use in calcium-imaging experiments, aCSF was adjusted to pH 7.4 with HCl and then was stored at 4 °C until used in experiments at room temperature.

All stock solutions of pharmacological agents were stored at −20 °C in small-volume aliquots to avoid repetitive freezing and thawing. All working concentrations were obtained by diluting stock solutions into aCSF. The following stocks were kept in aqueous solutions, typically either physiological saline or water: 2 mM histamine dihydrochloride (Acros Organics), 1 mM ATP disodium salt trihydrate (Sigma-Aldrich), 1 M acetylcholine chloride (Sigma-Aldrich), 200 μM substance P (Peptides International), 1 mM bradykinin, 20 mM norepinephrine, 3 M glutamate, 1 M atropine. α-Conotoxin ArIB[V11L;V16D] was not stored in solution. PNU-120596 stocks were 100 mM in DMSO. Fura- 2-

acetoxymethyl ester (Fura-2-AM; Invitrogen) stocks were 1 mM in DMSO, distributed into single-use aliquots and stored at −20 °C.

4.7.2 Mouse cell preparations and culture

Preparation and culture of mouse dorsal-root ganglion (DRG) cells was reported previously in detail (1, 2). The following methods apply to preparation and culture of mouse VRC cells. All procedures in this study comply with the rules and regulations in the National Institutes of Health Guide for the Care and Use of Laboratory Animals (3) and were approved by the Institutional Animal Care and Use Committee (IACUC) of the University of Utah Health Sciences Center. WT C57BL/6 mice at postnatal day (P) 7-8 were anesthetized by rapid hypothermia on ice before rapid decapitation.

We prepared a homemade dissecting plate by pouring silicone elastamer (Sylgard) into a 100-mm-wide tissue-culture dish and allowed the silicone elastamer to harden. The head was pinned to the Sylgard plate, and the skin and the connective tissues were removed. The skull was cut along the sutures with fine scissors to separate the interparietal region of the skull and expose the superior colliculus, inferior colliculus, and cerebellum. Ice-cold aCSF was applied to keep the tissue moist and cold. A one-sided razor blade was used to make a deep cut along the interface between the inferior colliculus and cerebellum, and the cerebellum was removed to isolate the brainstem. The brainstem and upper cervical spinal cord were isolated in ice-cold aCSF bubbled with carbogen. The brainstem was glued to a slant agar block using cyanoacrylate with its rostral end up and its dorsal side attached to an agar block, which was mounted and secured on a specimen tray. The agar block was cut at a slant forming a 110° angle

between the agar block surface and the horizontal specimen tray (a 20° angle from vertical). The vibratome blade was set at a 20° angle below horizontal so that it sliced at a right angle to the surface of the agar block. Slicing at this angle enabled us to observe the projections from the pre-Bötzinger complex (preBötC) to the XII nucleus and from the XII nucleus to the rootlets.

We sectioned the brainstem serially in a rostral-to-caudal direction. The first slice was cut at a thickness of 200 μm from the top (rostral end). From this point onwards, slices were made to observe facial nerves, which were the first landmark. The slice width varied with preparations; usually a slice of 400–500 μm from the top had to be removed to observe facial nerves. These facial nerves were observed over a thickness of 250–300 μm. Thus, a slice of 300 μm was made from the point of observing facial nerve. The next landmark was the opening of ventricle at the interface of the brainstem and the agar block. A slice of ~300–400 μm was cut to reveal the opening of the ventricle. From this point, 200-μm slices were cut until the ventricle closed. The last three slices before the complete ventricle closure were taken and were designated “rostral,” “medial,” and “caudal,” respectively. To ensure that we were cutting at the level of the preBötC, we calculated the percentage of class B cells responsive to substance P (a marker for preBötC) within dissociated cell cultures obtained from each slice: As expected, the 200-μm-thick medial slice, on average, had the highest percentage of substance P-responsive cells (8.6%) when compared with the rostral (7.3%) and caudal (4.1%) slices (n = 7 preparations). This finding suggested that the medial slice, on average, was near the center of the preBötC. In these slices, a faint hypoglossal nerve was observed, and the nucleus ambiguus sometimes was observed in the rostral slice.

The medial slice was placed in ice-cold HBSS, where the segments that contained the VRC and preBötC were microdissected and then transferred with a large-diameter fire-polished Pasteur pipette to a 15-mL conical tube. The total volume was adjusted to 900 µL with HBSS. Then 100 µL of 2.5% (wt/vol) trypsin was added [for a working concentration of 0.25% (wt/vol) trypsin)], and the tube was incubated at 37 °C in a water bath for 3–4 min. After incubation, the intact tissue segments were washed three times with 4 mL MEM + supplements. Each wash was performed by adding 4 mL MEM + supplements, allowing microdissected segments to settle to the bottom of the tube, and removing as much medium as possible with a fire-polished Pasteur pipette while avoiding the accidental removal of any tissue. After the final wash, the tissue segments were re-suspended in 1.5 mL MEM + supplements. The VRC suspension was triturated 5–10 times (or until there was no resistance) through a series of fire-polished pipettes, where each successive pipette had a smaller tip diameter. The solution became cloudy as individual cells dissociated from the slice fragments.

The cell suspension was centrifuged at 50 × g for 10 min. After centrifugation of the cell suspension, the supernatant was removed by aspiration, leaving behind the volume of medium required to plate dissociated VRC neurons, typically into six wells (130 µL total). Neurons were re-suspended in the remaining medium by gentle trituration with a 100-µL disposable plastic pipette tip. In several of the inner wells of a 24-well plate, 20 µL of the cell suspension was placed in the center of a silicone ring (3 mm i.d.) that was attached to the floor of each well as described previously (2). The wells at the edge of the plate were half-filled with sterile water to humidify the culture. Each plate was placed in the 37 °C incubator for 45–60 min to allow cells to settle and adhere. Then 1 mL MEM +

supplements solution was added very gently at the edge of each well to avoid any loosely adherent cells within the silicone ring. The plates were placed in a 37 °C, 5% CO2 tissue-culture incubator, and the cultures were used for imaging after 18–36 h.

4.7.3 Calcium imaging

We have described the calcium-imaging methods in detail previously (Teichert et al., 2012a; Teichert et al., 2012b). Briefly, the cells were loaded with Fura-2-AM in their growth medium for 1 h at 37° C, followed by 30 min at room temperature; then the medium containing Fura- 2-AM was replaced with aCSF at room temperature for calcium imaging. Changes in cytosolic calcium concentration, [Ca2+]i, were monitored over time by standard ratiometric calcium imaging methods, i.e., the ratio of fluorescence intensities at 510 nm obtained from intermittent (typically once every 2 s) excitation by 340-nm and 380-nm light (labeled as “340/380 nm” in the y-axis of calcium-imaging figures and described as “340/380-nm ratio” in the text). Upward or downward deflection of a calcium imaging trace represents an increase or decrease in [Ca2+]i, respectively. In all figures, arrows indicate a 15-s application of the specified compound or other perturbation. Horizontal bars indicate when other compounds were present in the bath solution.

4.7.4 Slice Electrophysiology

Electrophysiological experiments were performed in accordance with the protocols approved by the IACUC of the Seattle Children’s Research Institute. Transverse medullary brainstem slices were taken from male and female P7– 10 mice with a C57BL/6 background as described previously (Ramirez et al., 1996). Briefly, animals were

anesthetized with 4% isoflurane and were decapitated rapidly, and the brainstem was isolated in ice-cold aCSF equilibrated with carbogen (95% O2 and 5% CO2), pH 7.4, 305–312 mOSM. The brainstem was glued to an agar block on the mounting plate of an Electron Microscopy Sciences vibratome. The rostral face of the experimental slice was ~530 μm caudal to the opening of the fourth ventricle. From this landmark, a 550- to 580-μm slice that contained the preBötC was cut. The slice was transferred to a recording chamber with circulating aCSF (flow rate 10–15 mL/min, total circulating volume 100 mL) and was allowed to equilibrate to experimental temperature (30– 33 °C). The population rhythm was stimulated by elevating the extracellular potassium concentration from 3 to 8 mM over the course of 30 min. Extracellular recordings were obtained with glass suction electrodes (tip resistance >1 MOhm) filled with aCSF placed on the slice surface over the ventral respiratory column containing the preBötC. The recorded signal was sampled at 1.67 kHz, amplified 10,000×, filtered (low pass, 1.5 kHz; high pass, 250 Hz), rectified, and integrated using an electronic filter. Blind whole-cell patchclamp recordings were obtained in current clamp configuration using a Molecular Devices Multiclamp 700B amplifier sampling at 20 kHz. Patch electrodes were pulled (P-97 Flaming/Brown micropipette puller; Sutter Instrument Co.) from borosilicate glass with a resistance of 6–12 MΩ. The electrodes were filled with a saline solution containing (in mM): 140 K-gluconic acid, 1 CaCl2, 10 EGTA, 2 MgCl2, 4 Na2ATP, 10 Hepes (pH = 7.4). Both extracellular and intracellular recordings were obtained with Clampex 10.0 data acquisition module (Molecular Devices). When an intracellular recording was established, the inspiratory neuron was isolated pharmacologically from fast synaptic transmission by applying the mixture of 10 μM 6-cyano-7-nitroquinoxaline-2,3-dione, 10 μM 4-(3-

phosphonopropyl)piperazine-2-carboxylic acid, 50 μM picrotoxin, and 1 μM strychnine to inhibit AMPA glutamate receptors, NMDA glutamate receptors, GABAA receptors, and glycinergic receptors, respectively. Once the inspiratory neuron was isolated, the agonists substance P (1 μM), bradykinin (10 μM), and histamine (10 μM) were applied sequentially to the circulating medium at 10-min intervals. Recordings were stored on a computer for post hoc analysis. All drugs were obtained from Sigma Aldrich or Tocris Bioscience.

4.7.5 Statistical data analysis

The values shown under the heading “Average response to 100 mM [K+]o ± SD” in Table 2 were calculated using all the individual responses to 100 mM [K+]o of class A, B, and C cells from five independent experimental trials, with the SD calculated from all the individual responses. The quantification of the response shown in Table 2 is the change in the magnitude of the 340/380-nm ratio elicited by 100 mM [K+]o, as described above and as depicted in the y-axis of traces from Fig. 1. Larger numbers indicate a greater response or greater relative change in [Ca2+]i elicited by 100 mM [K+]o. The P value reported in Results for the difference in the average response to 100 mM [K+]o between class A and B cells was derived as follows: For each independent experimental trial (each trial included more than 100 cells), a sample mean for the response to 100 mM [K+]o was calculated separately for class A and B cells. Then the sample means for class A and B cells from independent experimental trials were compared using Student t test (two tailed, paired samples).

For the cluster analysis summarized in Table S1, 1,586 cells were scored for their responses to each of eight stimuli. Responses were scored as 0 = no response or as 1 =

response. A response to 100 mM [K+]o was defined as a maximum peak height ≥ 0.1 on the y-axis scale of the calcium-imaging experiments (340/380-nm ratio, as described above). A response to all other stimuli was defined as a maximum peak height ≥0.05 on the y-axis scale of the calcium imaging experiments (340/380-nm ratio). The binary cell-response data were clustered using the pam function in the cluster library of R. The manhattan distance function was used to define dissimilarities between pairs of cells which correspond to the number of scored differences between any two cell profiles. Five hundred bootstraps were used to establish the robustness of the medoids (prototype response profiles, as shown in Table S1) selected by the pam function. For each bootstrap trial, a random set of 1,586 cell-response profiles was selected with replacement and used for input into the pam function. The amount of variation explained by clustering was calculated as 1 − (diss)/n, where diss is the total dissimilarity remaining in the clusters and n is the total number of cell scores.

4.8 Supplemental Figures

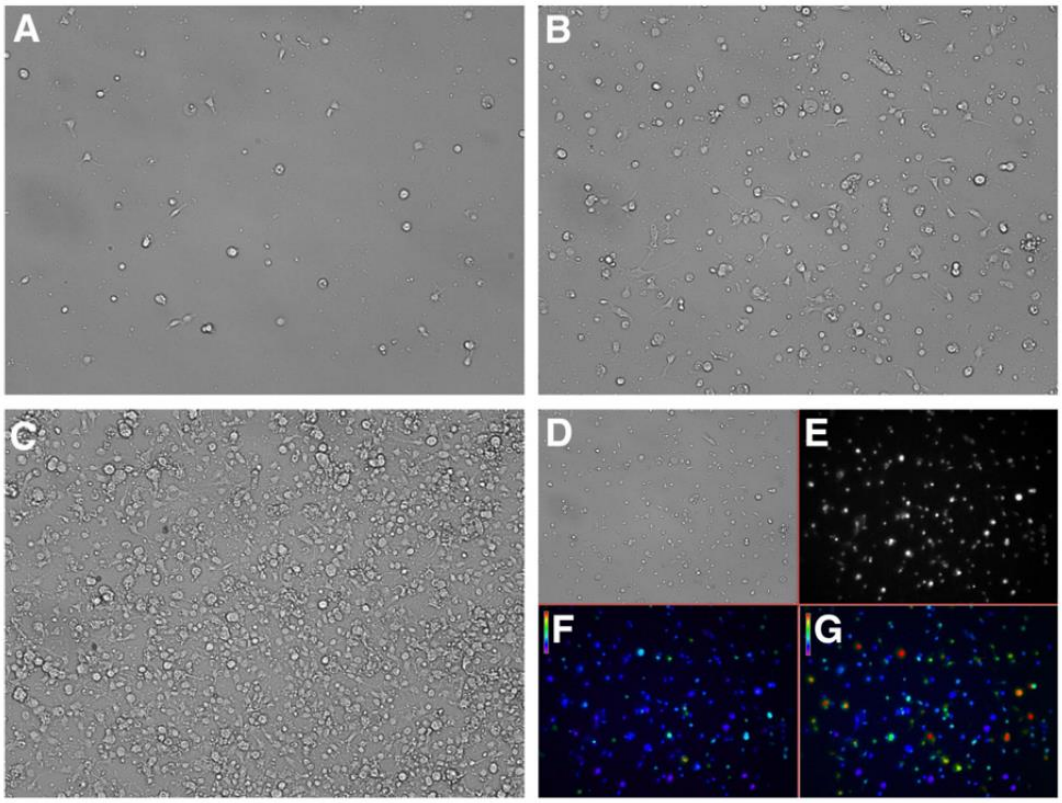

Supplementary Figure 1 (Fig. S1). Bright-field (A–D) and fluorescence (E–G) images of dissociated VRC cells in culture. Shown are cell cultures of inadequate, optimal, or excessive density for calcium-imaging experiments. (A) Inadequate density, 400 cells/mm^2. (B) Optimal density, 800 cells/mm^2. (C) Excessive density, 2,000 cells/mm^2. (D–G) All panels show the same field of view. (D) Bright-field image of dissociated VRC cells. (E) Fluorescence image of the cells loaded with Fura-2-AM dye (380-nm excitation and 510-nm emission). (F) Pseudocolored ratiometric image of cells at rest. The ratiometric image is a relative measure of [Ca2+]i and is obtained from the ratio of fluorescence intensities obtained at 510-nm emission by alternate exciting by 340-nm and 380-nm light. (G) Pseudocolored ratiometric image of cells immediately following a stimulus, demonstrating that only a subset of the cells responded to the stimulus with an increase in [Ca2+]i. Color scale (vertical bars) in F and G indicates relative [Ca2+]i, where purple/blue represent low levels of resting [Ca2+]i and yellow/red represent high levels of [Ca2+]i.

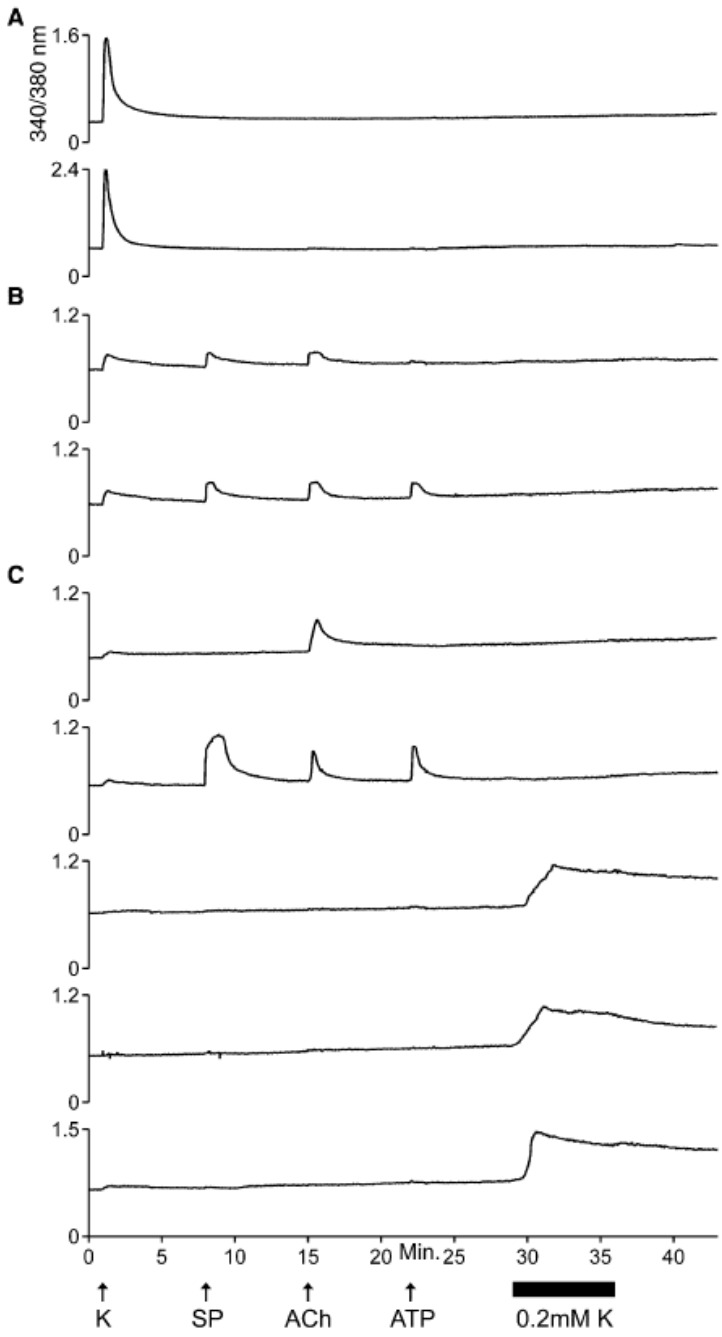

Supplementary Figure 2 (Fig. S2). Examples of calcium-imaging traces, presented as in Fig. 1, demonstrating responses to 0.2 mM [K+]o in VRC class C cells and the lack of responses to 0.2 mM [K+]o in class A and B cells. (A) Two examples are shown of class A cells that did not respond to 0.2 mM [K+]o with an increase in [Ca2+]i. (B) Two examples are shown of class B cells that did not respond to 0.2 mM [K+]o. (C) The upper two traces are examples of class C cells that did not respond to 0.2 mM [K+]o with an increase in [Ca2+]i. The lower three traces are examples of class C cells that did respond to 0.2 mM [K+]o with an increase in [Ca2+]i.

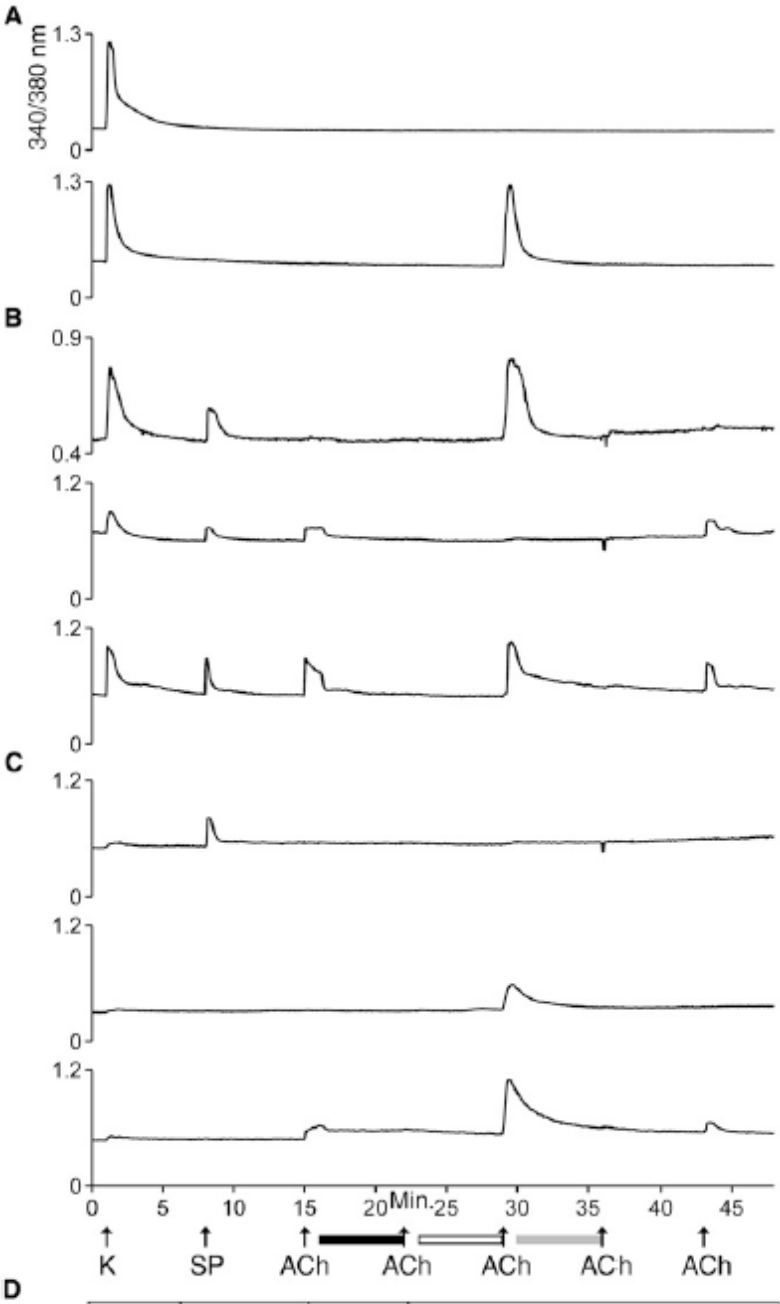

D

			% of ACh-responsive cells in each cell class		
Cell Class	Avg Resp. to 100 mM $[K^+]_o$	% of Total Cells	α7 nAChRs Only	mAChRs Only	Mix of α7 nAChRs and mAChRs
A	0.8	8%	66%	0%	0%
B	0.2	21%	19%	24%	49%
C	0.0	71%	4%	1%	3%

Supplementary Figure 3 (Fig. S3). Examples of calcium-imaging traces, presented as in Fig. 1, from experiments investigating acetylcholine (ACh) receptors (AChRs) in VRC cells. The black horizontal bar below the x-axis indicates the presence of 10 μM atropine in the bath, which blocked the response to the second application of 1 mM ACh. The open horizontal bar below the x-axis indicates the presence of both 10 μM atropine and 5 μM PNU-120596 (PNU) in the bath. Many cells responded to ACh only after application of PNU and in the continued presence of atropine. The gray horizontal bar below the x-axis indicates the presence in the bath of atropine, PNU, and 200 nM α-conotoxin ArIB[V11L;V16D], a highly selective blocker of α7 nicotinic acetylcholine receptors (nAChRs), which blocked the ACh responses elicited by PNU. After washout of these pharmacological agents, the final application of ACh at minute 43 demonstrated that muscarinic acetylcholine receptors (mAChRs) responded again (see ACh application at minute 15), but α7 nAChRs no longer responded in the absence of PNU. (A) Examples of traces from class A cells. (B) Examples of traces from class B cells. (C) Examples of traces from class C cells. (D) Compilation of data for class A, class B, and class C cells. This dataset was compiled for 2,267 cells from seven independent experimental trials, using cells prepared separately from three different mice.

Prototype response profile	Fraction of cells per cluster that responded to each stimulus								Cell count	No. of subclusters	Mean K+ response	K+ response SEM	Color code
	K	SP	ACh	ATP	NE	H	Br	Glu					
10000001	1.00	0.01	0.00	0.00	0.00	0.00	0.02	1.00	177	3	0.76	0.03	
10000000	1.00	0.02	0.00	0.00	0.00	0.00	0.00	0.00	47	2	0.58	0.05	
Total									224				
Mean											0.72		
10111101	1.00	0.00	0.99	1.00	1.00	1.00	0.00	1.00	104	2	0.35	0.02	1.00
10111111	1.00	0.00	0.93	1.00	1.00	1.00	1.00	1.00	58	2	0.34	0.02	0.90–0.99
10110101	1.00	0.08	0.92	1.00	0.00	1.00	0.00	1.00	38	3	0.28	0.03	0.80–0.89
10101101	1.00	0.06	0.94	0.00	1.00	1.00	0.00	1.00	36	3	0.29	0.03	0.50–0.79
10110001	0.85	0.09	0.91	1.00	0.00	0.00	0.00	1.00	33	4	0.21	0.03	0.21–0.49
10101111	1.00	0.00	0.97	0.00	1.00	0.97	1.00	1.00	30	3	0.27	0.03	0.11–0.20
10111100	0.96	0.00	1.00	1.00	1.00	1.00	0.15	0.00	26	3	0.34	0.04	0.01–0.10
10110000	1.00	0.09	0.82	1.00	0.00	0.00	0.00	0.00	22	3	0.24	0.04	0.00
10111001	1.00	0.00	1.00	0.80	1.00	0.00	0.05	0.85	20	4	0.37	0.04	
10100101	1.00	0.00	0.94	0.00	0.00	1.00	0.00	1.00	17	2	0.19	0.03	
10100001	1.00	0.06	1.00	0.00	0.00	0.00	0.00	1.00	17	2	0.38	0.08	
10101110	1.00	0.06	1.00	0.00	1.00	0.94	1.00	0.00	16	3	0.32	0.05	
10100111	0.93	0.00	0.86	0.00	0.00	0.71	1.00	1.00	14	4	0.35	0.08	
10100110	0.71	0.07	1.00	0.00	0.00	1.00	1.00	0.00	14	3	0.14	0.03	
11111101	1.00	1.00	1.00	1.00	1.00	1.00	0.00	1.00	13	1	0.40	0.05	
10100000	0.92	0.00	1.00	0.00	0.08	0.00	0.23	0.00	13	4	0.25	0.04	
10110100	1.00	0.00	1.00	1.00	0.00	1.00	0.00	0.00	12	1	0.25	0.04	
10110111	0.92	0.00	1.00	1.00	0.00	1.00	1.00	0.58	12	3	0.27	0.04	
11111111	0.91	1.00	0.91	0.82	1.00	1.00	1.00	0.82	11	4	0.27	0.04	
10011010	1.00	0.10	0.00	0.90	1.00	0.00	0.70	0.30	10	5	0.19	0.05	
10101100	1.00	0.10	1.00	0.00	1.00	1.00	0.00	0.00	10	2	0.30	0.06	
10100100	1.00	0.00	1.00	0.00	0.00	1.00	0.00	0.00	6	1	0.18	0.04	
10111010	1.00	0.20	1.00	1.00	1.00	0.00	1.00	0.00	5	2	0.16	0.06	
10010010	1.00	0.00	0.00	1.00	0.00	0.00	1.00	0.20	5	2	0.13	0.02	
Total									542				
Mean											0.30		
00000000	0.00	0.00	0.00	0.00	0.01	0.00	0.00	0.00	723	2	0.03	0.00	
00010000	0.00	0.14	0.00	1.00	0.00	0.00	0.00	0.00	21	2	0.03	0.00	
00000100	0.00	0.00	0.15	0.08	0.08	1.00	0.08	0.00	13	5	0.04	0.01	
00000010	0.06	0.00	0.00	0.13	0.13	0.00	1.00	0.13	16	5	0.05	0.01	
00110000	0.00	0.15	1.00	1.00	0.00	0.00	0.00	0.00	13	2	0.05	0.01	
00110010	0.22	0.00	1.00	1.00	0.11	0.11	1.00	0.00	9	4	0.07	0.02	
00101110	0.00	0.00	0.89	0.11	1.00	1.00	1.00	0.11	9	4	0.05	0.00	
00011001	0.17	0.00	0.00	1.00	0.83	0.00	0.33	1.00	6	4	0.05	0.01	
00000001	0.00	0.00	0.00	0.00	0.00	0.00	0.00	1.00	6	1	0.06	0.01	
00011110	0.00	0.00	0.00	1.00	1.00	0.75	0.75	0.00	4	3	0.04	0.01	
Total									820				
Mean											0.03		

Supplemental Table 1 (Table S1). Prototype response profile is the defining response pattern of each cluster to the eight stimuli (in order: K, SP, ACh, ATP, NE, H, Br, Glu), where 1 = response and 0 = no response. Under the heading of Fraction of cells per cluster that responded to each stimulus, each value different from 0 or 1 indicates that the response profiles of some cells in the cluster did not match the cluster perfectly. This cluster analysis, which produced 36 clusters, assumes an error rate in scoring of ~1%. Colors indicate the fraction of cells that responded to a particular stimulus; the color code is given in the far right column of the table. For this cluster analysis, we discarded 173 cells scored for the prior data analysis summarized in Table 2 (mostly from class C), because responses from those cells could not be scored accurately by automated methods. ACh, acetylcholine; Br, bradykinin; Glu, glutamate; H, histamine; K, [K+]o; NE, norepinephrine; SP, substance P.

Chapter 5

Discussion

*This chapter will be submitted with revision as a review article. This manuscript was co-authored by Jan-Marino Ramirez.

5.1 Abstract

Mammalian breathing consists of three phases: inspiration, postinspiration, and active expiration. Independent oscillatory networks that control inspiration and active expiration have been previously well-described; however, until recently, a localized population controlling postinspiration had not been identified. We recently published our discovery of a novel, excitatory, rhythm generating network, termed the postinspiratory complex (PiCo), which is both necessary and sufficient for generating postinspiratory motor output. Postinspiration is physiologically important for protecting the upper airway from aspiration and is gated by nuclei in the pons and midbrain. Respiratory generating circuits must also coordinate with non-ventilatory behaviors that occur during the postinspiratory phase such as vocalization, swallowing, and coughing. Dysfunction in the coordination of these behaviors can have serious health consequences. Traditionally, expiration is described as a passive process during resting conditions. However, in this review, we not only pose hypotheses regarding how the PiCo functionally integrates within the known context of the ponto-medullary respiratory network, but propose that "passive expiration" is actually an active phase that involves the recruitment of several muscles for breathing and associated postinspiratory behaviors. Our data serves as the basis for our current working model, the triple oscillator hypothesis, which postulates that three excitatory, rhythm generating networks in the medulla independently and actively control the three phases of mammalian respiration.

5.2 Introduction to the physiology of postinspiration

Whereas the central basis for inspiration has been theorized for hundreds of

years (St John, 2009), postinspiration was only identified as a distinct breathing phase less than 50 years ago (Bartlett et al., 1973; Richter, 1982; von Euler, 1983) and its function is still largely underappreciated (Dutschmann et al., 2014).

At rest, mammals oscillate between inspiration and postinspiration, or “passive expiration”. At the simplest level, inspiration is an active process generated by the contraction of external intercostal and diaphragm muscles, and expiration is passively produced by the relaxation of these muscles and the elastic recoil of the lungs. However, merged into this expiratory phase, muscle activation of the larynx and crural diaphragm actively occurs to produce the postinspiratory phase of breathing.

Compared to mammals, the postinspiratory phase is more apparent in reptiles wherein ventilation is transiently arrested after inspiration and before air is expired from the lungs (Takeda et al., 1986). In mammals, postinspiration serves as a mechanical brake to slow expiratory outflow without a complete arrest of lung ventilation (Dutschmann et al., 2014; Richter, 1982). The slowing of expiratory release is achieved by the adduction of laryngeal muscles which functions to increase upper airway resistance in animals (Gautier et al., 1973; Harding et al., 1980; Kuna and Vanoye, 1994; Tuck and Remmers, 1998) and humans (England et al., 1982) (Brancatisano et al., 1983). This results in the maintenance of functional residual capacity and maximizes the period for pulmonary oxygen/carbon dioxide gas exchange (Tuck et al., 2001). Laryngeal adduction additionally helps avoid lung collapse, or atelectasis (Dutschmann et al., 2014).

The crural diaphragm is also active during postinspiration, serving to maintain early expiratory muscle tension and stop the sudden relaxation of the diaphragm after the end of an inspiration (Easton et al., 1999; Subramanian and Holstege, 2011). Postinspiratory

medullary neurons have an inhibitory influence on the function of the crural diaphragm (Subramanian and Holstege, 2011).

Postinspiratory discharge is most often measured from motor output of the recurrent laryngeal nerve, which innervates the larynx (Dutschmann and Paton, 2002a; Lu et al., 2005; Paton et al., 1999) or the cervical vagal nerve (Abdala et al., 2009; Burke et al., 2010; Costa-Silva et al., 2010; Dutschmann et al., 2010) *in vivo*. Under control conditions, these recordings display an augmenting firing pattern during inspiration, followed by a decrementing after-discharge called postinspiratory activity (Gautier et al., 1973; Richter et al., 1986b).

5.3 Central control and modulation of postinspiration

Concerning the central origins of respiration, the control of postinspiration has by far received less investigation compared to the rhythmogenic control networks for inspiration and active expiration. The preBötC was discovered over a quarter century ago when it was demonstrated that the essential components of the neural circuitry that generate inspiration, including the rhythm, remain in a reduced, transverse medullary rodent slice (Smith et al., 1991). Active expiration, is putatively generated by an excitatory subpopulation within the retrotrapezoidal nucleus parafacial respiratory group (RTN/pFRG) the pF_L, or lateral parafacial region (Huckstepp et al., 2015). This is a conditional rhythm generator, however, that is only activated under high metabolic demand (Janczewski and Feldman, 2006). Thus, under physiological conditions, inspiration and expiration are largely dominated by alternating oscillations between inspiratory and postinspiratory neurons (Morschel and Dutschmann, 2009).

The BötC, located just rostral to the preBötC, is commonly given recognition for being the major source of premotor expiratory activity in the respiratory network (Ezure, 1990; Ezure et al., 2003; Jiang and Lipski, 1990). Indeed, the BötC primarily contains inhibitory neurons that fire during postinspiratory and late expiratory phases and also interacts with other compartments within the ventral medulla (Ezure, 1990; Ezure et al., 2003; Fedorko and Merrill, 1984; Jiang and Lipski, 1990; Long and Duffin, 1986; Shen et al., 2003; Tian et al., 1999). Neurons that are active in the postinspiratory phase can be found scattered across medullary compartments (Fisher et al., 2006; Smith et al., 2007). Until now, a strictly localized region for autonomously-generated postinspiratory activity had not been located. We recently published a manuscript that anatomically defines a novel population of excitatory neurons rostral to the BötC (Anderson et al., 2016) that we propose is responsible for the generation of the postinspiratory rhythm.

There are several different theories regarding the functional organization of brainstem respiratory circuits. Two of the most prevalent theories are: a three-phase model that relies on an inhibitory ring architecture to generate each of the three phases of breathing (Smith et al., 2007), and a dual-oscillator model in which inspiration and expiration alternate (Janczewski and Feldman, 2006). However, the functional and anatomical organization of brainstem respiratory centers has not been fully defined.

The inhibitory-ring hypothesis suggests that synaptic inhibitory interactions are the foundational basis for a hierarchy of three rhythm-generating mechanisms, spanning the pons and medulla, that generate the three phases of breathing (Richter and Smith, 2014; Smith et al., 2007; Smith et al., 2009). This model is based on a series of transection and pharmacological experiments. More specifically, serially transecting the brainstem rostral

to caudal in the working-heart brainstem preparation reduces a three-phase respiratory rhythm to a two-phase rhythm, eliminating fictive-postinspiration, when the pons is removed. Further transections reduce the two-phase rhythm to solely fictive-inspiratory bursts when networks rostral to the preBötC are removed. Moreover, blocking synaptic inhibition throughout the whole respiratory network resulted in an apnea and tonically active preBötC and BötC neurons (Smith et al., 2007). In support of this model, pharmacologically blocking inhibition in the preBötC or BötC *in vivo* reportedly perturbs, and sometimes eliminates respiratory activity, including postinspiration (Marchenko et al., 2016).

The dual-oscillator hypothesis is based on the idea that only two coupled rhythmogenic networks, the preBötC and RTN/pFRG, interact through excitatory mechanisms to control inspiratory and expiratory motor output, respectively (Janczewski and Feldman, 2006). In this model, postinspiration is not thought to be independently controlled, but is instead considered a motor subcomponent of the expiratory phase. The authors later demonstrate that inspiratory and postinspiratory motor output were unperturbed when synaptic inhibition was blocked locally in the preBötC and BötC in an *in vivo* adult rat preparation, and therefore postsynaptic inhibition was deemed not critical for respiratory rhythm generation (Janczewski et al., 2013).

In an attempt to reconcile some of the controversial aspects of these working models, we generated a novel *in vitro* preparation: a horizontal slice that retains the ventral portion of the neonatal mouse brainstem and keeps the networks within the ventral lateral medulla (also called the ventral respiratory column, or VRC) intact (Anderson et

al., 2016). This preparation allowed unprecedented accessibility for extracellular and intracellular manipulation to study mechanisms generating the phases of respiration.

Initial mapping experiments to characterize the activity across the dorsal face of the horizontal slice revealed fictive inspiratory bursting at the level of the preBötC that was temporally coincident to activity from the phrenic motor nerve at level C4 of the spinal cord, confirming that the rhythmic activity at the level of the preBötC was indeed respiratory (not published). Approximately 500 µm rostral to the preBötC, infrequent population bursts that occurred immediately after an inspiratory preBötC burst (i.e. in the postinspiratory phase) were recorded. We have termed this area the postinspiratory complex, or PiCo.

Anatomically, PiCo neurons co-expressing markers for Vglut2 and ChAT were located immediately caudal to the facial nucleus. This proximity could facilitate coordination between the facial motor nucleus and PiCo. The facial nucleus controls the muscles of the face, and damage of these motor neurons result in a condition called central facial palsy (Ahdab et al., 2013). Patients diagnosed with central facial palsy often suffer from difficulties in sucking, swallowing, and vocalization; oropharyngeal functions that occur during the postinspiratory phase (van Gelder and Borod, 1990).

Furthermore, the PiCo population was found to be dorsal to the documented location of the BötC (Alheid and McCrimmon, 2008; Merrill, 1981; Tan et al., 2010) and medial to the rostral portion of the nucleus ambiguus. The fact that both the preBötC and PiCo are situated adjacent to the length of the nucleus ambiguus likely helps to facilitate the coordination between breathing and other behaviors that require the modulation of the upper airway such as vocalization, swallowing, and coughing. Future experiments

that anatomically define ascending and descending projection patterns from the PiCo will be instructive in determining connectivity.

The frequency of spontaneous postinspiratory PiCo activity could be increased to match preBötC burst frequencies by applying low concentrations of norepinephrine to the horizontal slice preparation. We hypothesize that under more intact conditions, the Kölliker-fuse extends adrenergic projections into the medulla that synapse onto PiCo neurons. Perhaps since the horizontal slice lacks the sensory feedback from pulmonary stretch receptors in the pons, the activity of postinspiratory PiCo neurons may require excitatory drive from Kölliker-Fuse neurons (Dutschmann and Herbert, 2006) to burst at a frequency similar to the preBötC. This explanation could also elucidate why postinspiratory activity was eliminated in the absence of pontine input in the transection experiment described above (Smith et al., 2007). Indeed, the fact that spontaneous PiCo activity is infrequent without exogenous norepinephrine *in vitro* may help to explain why the PiCo was not discovered earlier.

To address the debate surrounding the role of inhibition in the generation of respiratory rhythms, we progressively blocked synaptic inhibition by bath applying strychnine, to block glycinergic receptors, and gabazine, to block $GABA_A$ receptors, while simultaneously recording from preBötC and PiCo in the horizontal slice (Anderson et al., 2016). The two rhythms were phasically unaffected by the addition of strychnine, but upon the application of gabazine (with or without strychnine), the two rhythms progressively synchronized. These data are consistent with previous *in vivo* experiments wherein hypoxia reduces network inhibition and triggers a shift of post-inspiratory neurons to discharge in the inspiratory phase (Richter and Smith, 2014). Previous studies

performed *in vivo* and *in situ*, however, have found that strychnine, in contrast to gabazine, resulted in the synchronization of inspiratory and postinspiratory motor output (Busselberg et al., 2001; Dutschmann and Paton, 2002a, b). The reason for this discrepancy is currently unknown, but the lack of descending pontine influence in the horizontal slice is likely a contributing factor.

Perhaps more importantly, the PiCo rhythm persisted in the absence of synaptic inhibition. It has been well-documented that preBötC rhythms persist after blocking chloride-mediated inhibition *in vitro* (Brockhaus and Ballanyi, 1998; Ren and Greer, 2006; Shao and Feldman, 1997), suggesting that rhythmogenesis does not require rebound from postsynaptic inhibition. The PiCo rhythm also continued after the blockade of NMDA receptors, and was only abolished after applying an AMPA receptor antagonist, CNQX. This suggests that inhibitory, specifically GABAergic, mechanisms help coordinate the timing between inspiratory and postinspiratory rhythms, but the PiCo rhythm is generated by excitatory, non-NMDA, glutamatergic mechanisms, similar to the preBötC. These *in vitro* observations indicate a non-obligatory role for inhibitory mechanisms in the generation of the PiCo rhythm, but further study will be required to confirm *in vivo*.

To dissect the functional interactions between the preBötC and PiCo, we utilized a strain of Dbx1-cre-ERT2 tamoxifen-inducible mice (Hirata et al., 2009). Rhythmogenic preBötC neurons are derived from progenitor cells that express the transcription factor protein Dbx1 (developing brain homeobox 1) (Bouvier et al., 2010; Gray, 2013; Gray et al., 2010). Dbx1-cre mice were bred with a cre-dependent reporter (Madisen et al., 2010), such that the resulting progeny, Dbx1 expressing cells born after embryonic day 10.5 (Picardo et al., 2013) also expressed light-gated ion channels, channelrhodopsin-2

(ChR2). Using a combined pharmacological and optogenetic approach in a series of horizontal slice experiments, our data suggest that *Dbx1*-derived inspiratory activity simultaneously excites and inhibits PiCo neurons through glutamatergic and GABAergic mechanisms, respectively. However, under normal physiological conditions, GABAergic inhibitory mechanisms dominate over the concurrent glutamatergic excitatory input from the preBötC. Whether rhythmogenic PiCo neurons are also derived from Dbx1 progenitor cells remains to be tested.

PiCo could also be functionally differentiated from networks generating inspiration and active expiration by the population response to neuromodulators including, but not limited to, DAMGO and somatostatin (SST). In the horizontal slice, DAMGO ([D-Ala^2, N-MePhe^4, Gly-ol]-enkephalin), a mu-opioid receptor agonist, eliminates the postinspiratory population rhythm at low concentrations. The injection of DAMGO into the PiCo *in vivo* significantly decreases the amplitude and duration of postinspiratory vagal motor output without significantly changing respiratory rate. The exquisite opiate sensitivity of PiCo neurons could underlie several clinical observations. For example, infants that were exposed to opiates in utero have decreased respiratory rhythm stability, less rhythmic swallowing, and a higher percentage of apneic swallows (defined as three or more swallows in the absence of a breathing movement) compared to controls (Gewolb et al., 2004). Acute heroin overdose patients can develop often-fatal aspiration pneumonia (Grigorakos et al., 2010), likely a result of a failure to coordinate breathing with swallowing. PiCo's sensitivity to low concentrations of opiates could also help explain the effectiveness of codeine in the alleviation of coughing (Eddy et al., 1969) and why serious side effects of codeine, and other opioids, include respiratory depression (Benyamin et

al., 2008). Finally, could PiCo's sensitivity to opioids help address why a bolus of fentanyl (an opiate) delivered at the beginning of anesthesia frequently triggers fentanyl-induced coughing (El Baissari et al., 2014)?

The PiCo was also specifically inhibited by the inhibitory neuropeptide, somatostatin, both in the horizontal slice and *in vivo*. Interestingly, in a study by Burke et al., the investigators aimed to inject somatostatin into the BötC *in vivo* (Burke et al., 2010). The injection specifically eliminated postinspiration as measured by an abolishment of cervical vagal motor activity. However, a few years later, the same author used immunohistological techniques to search for SST2a receptors and was unable to locate the receptors on BötC neurons (Le et al., 2016). Since PiCo sits just rostral to the anatomically defined BötC, it is within reason that the injection bolus could have either been large enough to at least partially encompass PiCo, or the injection tip may have been a little too rostral. The PiCo region would be a logical next candidate in the search of SST2a receptors.

Under higher concentrations of norepinephrine in the horizontal slice, the PiCo rhythm outpaced the preBötC rhythm in the horizontal slice. Indeed, at higher burst frequencies, PiCo bursts can occur in any phase relative to an inspiratory burst except for during a preBötC burst, further consistent with an inhibitory influence of the preBötC onto PiCo. To test whether PiCo could function as an independent rhythm generator, PiCo was isolated in a transverse slice immediately rostral to the conventional preBötC transverse slice. Using coordinates derived from horizontal slice recordings, robust, but infrequent spontaneous population PiCo bursts were recorded, and the rhythm could be stimulated by norepinephrine application.

Thus, similar to the preBötC, the PiCo meets the four criteria necessary to define it as a mammalian rhythmogenic circuit (Feldman and Kam, 2014). (1) Inhibiting PiCo neurons by injecting DAMGO into the PiCo *in vivo* severely attenuates postinspiratory vagal activity. (2) The PiCo projects to an appropriate motorneuron population that can be recorded as postinspiratory activity in the cervical vagal nerve. (3) Modulatory afferents such as DAMGO and SST can alter the frequency of PiCo activity *in vitro* and *in vivo*. (4) When isolated, the PiCo can still generate rhythmic activity when sufficiently driven by exogenous norepinephrine.

Based on these results taken together, we postulate a new encompassing theory, a triple-oscillator hypothesis, which attempts to integrate portions of previously proposed models for the spatial and functional architecture of respiratory rhythm generating networks. Similar to the inhibitory-ring model (Richter and Smith, 2014; Smith et al., 2007), we hypothesize that the three phases of respiration are generated by three oscillatory mechanisms, and consistent with the dual-oscillator model (Janczewski and Feldman, 2006), two of the oscillatory networks are likely the preBötC, for inspiration, and a subpopulation within the RTN/pFRG, for active expiration. In our proposed model, we add the hypothesis that the PiCo is a third oscillatory network that is independently controlling postinspiratory motor output. Thus, we postulate that three, anatomically-distinct, excitatory, rhythm generating networks: the preBötC, PiCo, and pF_L are individually responsible for the generation of each of the three phases of breathing. Our *in vitro* data from both horizontal and transverse slices indicate that inhibitory mechanisms are not necessary for inspiratory or postinspiratory rhythmogenesis, but play an important role in the patterning and coordination between the respiratory phases.

5.4 Postinspiratory behaviors

The postinspiratory phase is not only important for breathing, but several non-ventilatory behaviors as well. These behaviors include vocalization, swallowing, coughing, and vomiting and must all be precisely coordinated with breathing.

Postinspiratory activity is critical for airflow modulation during human speech (Dutschmann et al., 2008). Vocalization occurs through the adduction of laryngeal muscles that allows one to control the tension of their vocal cords (Ludlow, 2005). Professional human singers have learned through training to carefully regulate the patterning of a variety of neck muscles during expiration. In a study measuring electromyogram (EMG) activity in professional classical singers, the start of phonation occurred just after an inhalation, in the postinspiratory phase, and coincided with peak EMG activity in several neck muscles (Pettersen and Westgaard, 2005). Additionally, professional opera singers tend to show greater activity in a range of respiratory muscles compared to students (Watson et al., 2012).

From a neural perspective, very little is understood about how medullary networks become active during the production of vocalization (Schmidt et al., 2012). Much of the current literature regarding the relationship between circuits underlying breathing and vocal control has been derived from studies in songbirds. Songbirds produce diverse and complex vocal patterns which must coordinate temporally with respiratory patterns (Zollinger et al., 2008). The brain nuclei that control vocal production in songbirds, referred to as the “song system” (Castelino and Schmidt, 2010; Nottebohm et al., 1976), send projections in a top-down manner to respiratory nuclei in the ventrolateral medulla

that are thought to be homologous to respiratory nuclei in mammalian systems (Schmidt et al., 2012). Interestingly, evidence suggests that the respiratory control network also provides input to the song control centers in a “bottom-up” manner, serving to relay feedback about respiratory homeostasis and phase information. Whether this type of bi-directional projection pattern also exists in mammals remains to be tested.

Swallowing, also referred to as deglutition, is a complex, but stereotyped motor pattern that requires the coordination of over 25 pairs of muscles and can occur as an isolated or rhythmic behavior (Jean, 2001; Miller, 1982). Swallowing and breathing share a common anatomical pathway, both sharing the pharynx as a conduit, and must be coordinated to protect the airway (Bautista et al., 2014b; Ghannouchi et al., 2016). When a person swallows, the adduction of their laryngeal muscles close the vocal folds and seal the glottis and thus protect the lower airways from the inhalation of food or liquid into the lungs (Doty and Bosma, 1956; McCulloch et al., 1996; Shaker et al., 1990). Swallows are most often initiated during the postinspiratory/expiratory phase in healthy individuals (Boden et al., 2009) (Bautista et al., 2014b; Dick et al., 1993), and laryngeal adductor motor neurons in the nucleus ambiguus (Bieger and Hopkins, 1987) are active during postinspiration and swallowing (Gestreau et al., 2000) (Bautista and Dutschmann, 2014). However, interestingly, breathing ceases during the actual swallow and is referred to as a swallow apnea (Loch et al., 1982). This can be observed at the neuronal level as well, for example, neurons active during inspiratory and expiratory phases in the rostral medulla of guinea pigs are rendered silent during a fictive swallow (Sugiyama et al., 2014). Fictive swallows are also associated with a delay in the subsequent inspiration (Saito et al., 2003) (Bonis et al., 2013), resetting the respiratory rhythm.

The minimal circuitry thought to be necessary for the generation of the swallow in rodent models is located in and around the nucleus tractus solitarus (NTS) in the dorsal medulla and termed the dorsal swallow group (DSG) (Jean, 2001; Jean and Car, 1979; Kessler and Jean, 1985). It is further proposed that the neurons that make up the ventral swallow group (VSG) are located in the reticular formation, dorsomedial to the nucleus ambiguus, and are responsible for motor and premotor control of the upper airway (Kessler and Jean, 1985) (Jean, 2001). Unlike respiratory circuits that are constantly active, the initiation of a swallow is gated under resting conditions and requires either sensory or cortical input command to function (Bautista and Dutschmann, 2014). Laryngeal adductor muscle activation are a final motor output for both swallowing and breathing (Bianchi and Gestreau, 2009; Bolser et al., 2006; Davenport et al., 2011). The nucleus ambiguus and vagus nerves innervate both the larynx and the pharynx that are involved with swallowing and respiration (Broussard and Altschuler, 2000). The close proximity of medullary breathing centers to the nucleus ambiguus and the dorsal motor nucleus of the vagus likely facilitate the tight coordination between the two behaviors and the inhibition of breathing during a swallow apnea (Hadjikoutis et al., 2000). It has been proposed that central control networks for breathing reconfigure during a swallow to take part in swallow generation. In fact, several studies demonstrate respiratory-modulated neurons that alter their activity due to a swallow (Gestreau et al., 1996; Jean et al., 1975; Jiang and Lipski, 1992; Saito et al., 2003).

Coughing is a defense reflex that aims to prevent aspiration by producing high velocity expiratory airflow to eject matter away from the airway (Bolser et al., 2013; Fontana and Lavorini, 2006). A cough is made up of three phases: inspiration,

compression, and expulsion. The compressive phase is produced by projectile-like activity of expiratory laryngeal muscles during rising, intense motor activation of expiratory thoracic and abdominal muscles (Bolser et al., 2013). According to some recent models, it is hypothesized that a common network of neurons generates both coughing and breathing behaviors (Shannon et al., 2000; Shannon et al., 1998). Furthermore, the network can reconfigure to generate either behavior by altering excitability of key neuronal populations, presynaptic modulation, and/or recruiting previously silent neurons (Bolser et al., 2013).

Vomiting and retching are additional non-ventilatory behaviors that occur during the postinspiratory phase (Lang et al., 2002). At least two muscles, the geniohyoid and the thyrohyoid muscles, are innervated by superior laryngeal nerves and their respective motorneurons are active during both fictive swallowing and vomiting (Umezaki et al., 1998).

Clearly, the activation of a multitude of muscles must be intricately orchestrated to control these postinspiratory behaviors during the expiratory phase. This tight control of repetitive activity patterns additionally supports the idea that expiration under lower metabolic demand is not merely “passive”, but actually an active phase.

5.5 Gating and modulation of postinspiratory behaviors

The Kölliker-Fuse and parabrachial nuclei, located in the pons, are relay nuclei for reflex and higher-order central nervous system inputs that regulate the control of postinspiratory activity (Dick et al., 1994; Kobayashi et al., 2005; Smith et al., 2007). This reflex control can automatically stop breathing to protect the upper airway, for example

by closing the glottis in a dive response (Dutschmann and Paton, 2002c) or in response to a noxious substance, independent of medullary rhythm and pattern generating circuits (Dutschmann et al., 2004). It is speculated that the pons is involved in rapid inspiratory-to-expiratory phase transition during these types of “higher” behavioral adaptations that also include swallowing, sniffing, coughing, sneezing and vocalization (Dutschmann and Dick, 2012; Morschel and Dutschmann, 2009).

Pharmacological inhibition of Kölliker-Fuse circuitry evokes a loss of postinspiratory motor output, while microinjections of glutamate trigger tonic excitation of laryngeal motor output in an *in situ* perfused brainstem preparation (Dutschmann and Herbert, 2006). This strong modulation of postinspiratory upper airway activity support the hypothesis that the Kölliker-Fuse functions as a gate for postinspiratory behaviors and coordinates with respiratory generating circuits in the medulla to shape and adapt the breathing pattern (Bonis et al., 2013; Bonis et al., 2011; Dutschmann and Dick, 2012; Oku and Dick, 1992). For instance, projections from higher vocalization centers could synapse onto postinspiratory neurons in the Kölliker-Fuse (Smotherman et al., 2006; Zornik and Kelley, 2008) to modulate the expiratory duty-cycle via direct descending input onto medullary respiratory networks and thereby influencing motor drive for laryngeal adductor muscles that are active during vocalization (Morschel and Dutschmann, 2009).

Kölliker-fuse nuclei extend dense, descending projections into the caudal pons, medullary ventral respiratory column, nucleus tractus solitarus, and the nucleus ambiguus (Dobbins and Feldman, 1994; Ellenberger and Feldman, 1990; Herbert et al., 1990). Postinspiratory neural activity in the medulla and cervical vagal nerve activity have been shown to be enhanced by pontine input and decreased by either pharmacologically

reducing or removing the pons (Dutschmann and Herbert, 2006; Rybak et al., 2004). Interestingly, despite the rich descending projections, only a few monosynaptic connections between pontine and medullary neurons have been identified (Bianchi and St John, 1981, 1982; Segers et al., 2008; Segers et al., 1985).

The periaqueductal gray (PAG), located in the midbrain, is thought to play a central role in modulating breathing for behavioral and emotional expression (Subramanian, 2013; Subramanian et al., 2008). It is hypothesized that the PAG functions to ensure that breathing can be continuously adjusted, especially in the awake state, to make adjustments for changes in the surrounding environment (Subramanian and Holstege, 2010). Emotional reactions such as flight and aggression (Bandler and Carrive, 1988), anxiety (Lovick et al., 2000), fear (Zhang et al., 1990), and vocalization (Zhang et al., 1994) require a motor pattern change in respiration that is thought to be modulated by the PAG (Subramanian, 2013). Electrical or neurochemical stimulation of the PAG elicits vocalizations in cat (Bandler and Carrive, 1988; Carrive et al., 1987; Kanai and Wang, 1962; Zhang et al., 1994), while lesions result in mutism in cat (Adametz and O'Leary, 1959; Kelly et al., 1946) and in monkey (Jurgens and Pratt, 1979). In cat, limbic, prefrontal, and anterior cingulate cortex areas integrate visual, auditory, and somatosensory information and relays it to the PAG (Subramanian and Holstege, 2009). The PAG, in turn, projects to medullary respiratory circuits and is postulated to appropriately alter respiratory motor output based on the surrounding situation (Subramanian and Holstege, 2009). Specifically, the PAG can modulate the activity of postinspiratory medullary neurons, which contribute to the switch of eupnea to behavioral breathing (Subramanian, 2013).

5.6 Dysfunction of postinspiratory behaviors

The tight timing relationship between postinspiration and inspiration is vitally important and dysfunction between the two can result in serious health consequences. As noted in a previous section, swallow apneas most frequently occur during expiration in healthy individuals (Hiss et al., 2001; McFarland et al., 2016). However, in elderly persons, the odds of respiratory resumption of the swallow apnea occurring during the inspiratory phase increase (Martin-Harris et al., 2005; Shaker et al., 1992; Yagi et al., 2016). This discoordination can lead to pulmonary aspiration, wherein food or fluid is routed into the lungs instead of the stomach. A potentially-fatal lung infection, aspiration pneumonia, can subsequently develop. In fact, aspiration pneumonia is the leading cause of death in patients with neurodegenerative diseases including dementia (Alagiakrishnan et al., 2013; Easterling and Robbins, 2008), Parkinson's disease (Lin et al., 2012), and Alzheimer's disease (Kalia, 2003). Dysphagia, or the impairment of swallowing, is likely due to the disruption of voluntary and autonomic control of the quality and timing of oral and pharyngeal movements during a swallow in patients with neurodegenerative disease (Troche et al., 2011). Combined swallowing and respiratory impairment is witnessed in 28-85% of individuals diagnosed with Parkinson's Disease (Troche et al., 2011). Additionally, the dysfunction in neural coordination underlying breathing and swallowing behaviors is frequently evident in these neurological diseases (Aydogdu et al., 2011; Gross et al., 2008; Hadjikoutis et al., 2000; Shaker et al., 1992).

A similar discoordination between breathing and swallowing occurs in patients diagnosed with chronic obstructive pulmonary disease (COPD) (Gross et al., 2009),

amyotrophic lateral sclerosis (Aydogdu et al., 2011), oropharyngeal cancer (Brodsky et al., 2010), and ataxic telangiectasia (Lefton-Greif, MA 2016). Often swallowing dysfunction is ascribed to weakening of aging muscles in the upper airway and digestive tract; however, there is evidence for lack of coordination at the neuronal level in many of these diseases (Hadjikoutis et al., 2000; Shaker et al., 1992).

Rett syndrome is a neurodevelopmental disorder that is characterized by normal development for the first 6-18 months of life, followed by neurological decline and breathing abnormalities (Julu et al., 2001; Katz et al., 2009; Ramirez et al., 2013b). Data obtained from an *in situ* brainstem preparation in a mouse-model for Rett syndrome indicated that erratic breathing and apneas were linked to instabilities in postinspiratory, laryngeal adductor motor output during early expiration (Stettner et al., 2007). The impaired postinspiratory motor activity results in apneas with glottal closure and thus potentially provides an explanation for the loss of speech and disturbances in swallowing associated with Rett syndrome patients (Stettner et al., 2008). It is hypothesized that disturbances in vocalization and swallowing observed in Rett syndrome are related, at least in part, to brainstem dysfunction (Katz et al., 2009; Stettner et al., 2007; Stettner et al., 2008).

Swallow and cough are important for the prevention and correction of aspiration. Studying the spatiotemporal coordination between cough and swallow suggest that the response to aspiration is actually a meta-behavior (Pitts et al., 2012; Pitts et al., 2013). In other words, it is hypothesized that cough and swallow are controlled as a single functional unit to prevent and limit aspiration (Bolser et al., 2015). Depressed cough reflexes and reduced responses to stimuli in the pharynx are common among elderly

populations that develop aspiration pneumonia (De Leon, 2016; Sekizawa et al., 1990). When aspirated material does not trigger an appropriate cough response, it is termed “silent aspiration”, and is often a consequence of patients with both dystussia (disordered coughing) and dysphagia (Ebihara et al., 2016; Smith Hammond and Goldstein, 2006). Concurrent dystussia and dysphagia are frequently observed in patients with neurological conditions including Parkinson’s disease, Alzheimer’s disease, and stroke (Pitts et al., 2009; Pitts et al., 2012; Smith Hammond et al., 2009; Smith Hammond et al., 2001; Troche et al., 2014b) providing further evidence that these behaviors have common underlying control mechanisms (Bolser et al., 2015). An extended compression phase, reduced expiratory peak flow, and cough volume acceleration have all been identified as predictors of dysphagia in Parkinson’s Disease (Pitts et al., 2010; Smith Hammond et al., 2009).

5.7 Conclusion

Just as the preBötC serves as an excitatory, independent premotor control network for inspiratory motor output, we show that the PiCo is an excitatory, independent control network for postinspiratory vagal motor output. Postinspiration requires the active contraction of laryngeal and crural diaphragm muscles, and therefore is not merely a passive phase in itself. Moreover, the generation of other postinspiratory behaviors involves the activation of a host of additional head and neck muscles that must coordinate with breathing. The complex orchestration necessary for swallowing, coughing, or vocalizing while continuing to breathe is an active process indeed.

The PiCo's ability to function autonomously, and not be dependent on post-inhibitory rebound of the preBötC, is perhaps logical when one recognizes that multiple postinspiratory behaviors can occur between inspiratory breaths. For example, humans frequently cough several times in succession before taking the next inspiration (Vovk et al., 2007). Current models of respiratory control cannot explain this repeating sequence of coughing without intervening breaths (Bolser et al., 2015; O'Connor et al., 2012). The addition of PiCo into these models may help further our understanding of the dynamics between breathing and airway protective mechanisms at the neuronal level. The elucidation of PiCo's involvement in the control of postinspiratory behaviors (coughs, swallows, and vocalization) that must be coordinated with breathing still requires careful experimentation. However, preliminarily we have recorded multiple postinspiratory vagal burst waveforms *in vivo* that could possibly represent the premotor basis for various postinspiratory behaviors.

PiCo could be functioning as a mediator between the networks that generate swallows, in the nucleus tractus solitarus, and motorneurons that innervate respiratory muscles. We further hypothesize that descending pontine input from the Kölliker-Fuse gates and modulates postinspiratory behaviors such as swallowing and vocalization by projecting directly onto PiCo neurons, which in turn synapse onto nucleus ambiguus motorneurons that control muscles of the upper airway. The proximity of medullary breathing centers to the nucleus ambiguus likely facilitates not only coordination between breathing and behaviors like swallowing, vocalization, and coughing, but also the concurrent coordination with cardio-circuitry (see reviews on cardiorespiratory coupling: (Dick et al., 2014; Garcia et al., 2013; Zoccal et al., 2014)). It is likely that PiCo, as a

respiratory microcircuit, is connected to the brain regions that control these behaviors (Ramirez et al., 2016).

Additional studies will also be necessary to unravel PiCo's role, if any, in the dysfunctional coordination between breathing and postinspiratory behaviors in patients with neurodegenerative disease and in the elderly. It is possible that the PiCo could serve as a future therapeutic target for those prone to developing aspiration pneumonia.

Oscillators have been described for inspiration and active expiration and we believe that the PiCo is the missing oscillator responsible for postinspiration. Collectively, our working model, the triple oscillator hypothesis, suggests that the preBötC, PiCo, and pF_L independently generate the three phases of breathing via excitatory interactions. Moreover, our data suggests that inhibition mediates the coordination of phasing and patterning of the respiratory rhythm. We hope that our initial anatomical localization and functional characterization of PiCo will help spur future work to better define how PiCo integrates with other brainstem networks to produce and coordinate a multitude of behaviors. Insights gained from this accessible and tractable multiple oscillator system could also potentially guide models for other rhythmic motor behaviors such as locomotion.

Chapter 6

Conclusions and future directions

4.1 Summary of key findings

This dissertation opens with an overarching review on respiratory rhythm generation. I felt it was important to give the readers a broad background of the respiratory control field as well as outline the current hypotheses regarding how medullary oscillators give rise to the three phases of breathing. The review introduces individual theories of rhythmogenesis, the controversial role of synaptic inhibition, and the known interactions between oscillatory networks.

The second chapter is a manuscript, published in *Nature,* which includes the core of my graduate work. This paper introduces and characterizes a novel, independent, oscillatory network responsible for the generation of the postinspiratory phase of breathing. We termed this area the postinspiratory complex, or PiCo. The PiCo was discovered using a new *in vitro* horizontal slice preparation that kept the entire medullary ventral respiratory column intact. Immunohistochemistry and *in situ* hybridization were used to anatomically localize the PiCo population in relation to brainstem motornuclei and to show that these neurons co-express both glutamate and acetylcholine. The PiCo population was differentially sensitive to neuromodulators including norepinephrine, somatostatin, and DAMGO compared to other known respiratory rhythm generators. Using a combined optogenetic and pharmacological approach, we demonstrated that PiCo and the inspiratory-generating network, the preBötzinger complex (preBötC), are

dependent on glutamatergic mechanisms and have a mutual inhibitory influence on each other. *In vivo*, postinspiratory vagal motor output was evoked by optogenetically photo-stimulating cholinergic neurons in PiCo, and was dramatically reduced by injecting somatostatin or DAMGO bilaterally into PiCo. These data suggest that the PiCo population is both necessary and sufficient for the generation of postinspiration. When PiCo was isolated in a transverse slice, the network generated bursts autonomously, indicating that PiCo can function as an independent, rhythm generating network. This observation led to our current working hypothesis, the triple oscillator hypothesis, positing that three distinct rhythm generating networks independently generate the three phases of respiration.

The following chapter is a published review on the central and peripheral influences on obstructive sleep apnea (OSA). This disorder is characterized by the repetitive occlusion of the upper airway that leads to episodic bouts of apnea, and thus, hypoxia. The resulting morbidity/mortality of OSA is the result of not only peripheral obstruction, but also the dynamic interplay between neuromodulation, behavioral state, and differential activation of medullary respiratory networks and their associated motor outputs. This manuscript reviews the current literature before the discovery of PiCo. However, PiCo likely provides premotor control to pharyngeal and laryngeal muscles of the upper airway; and therefore, I believe that future studies will accredit a fundamental role to mechanisms involving PiCo in the clinical manifestation of OSA.

During my graduate school tenure, a collaboration between the Ramirez and Olivera labs was established. The fourth chapter is the published result of one of the collaborative projects. The Olivera lab in Utah pioneered a new approach called

constellation pharmacology in which subpopulations with unique patterns of receptors and ion channels are identified by dissociating cells and using fluorescent calcium imaging. By combining this technology with our lab's expertise in respiratory networks and electrophysiology, we embarked on a joint project. The Utah group dissected the preBötC population from *in vitro* transverse slices and dissociated the cell population. They pharmacologically perfused various modulators over the cells and measured the individual changes in fluorescence when cells were activated. They were able to identify three distinct subpopulations, or classes, of preBötC cells that had a unique constellation of responses to individual modulators such as bradykinin, substance P, and histamine. We helped to validate the technique by intracellularly recording from inspiratory neurons in the more intact *in vitro* preBötC transverse slices and found examples of each of the three neuronal classes using the same neuromodulators.

Finally, the fifth chapter is a review focused more specifically on postinspiration. It first discusses the physiological importance of the phase, postinspiratory behaviors such as vocalization and swallowing, the detrimental consequences of discoordination between breathing and these behaviors, and the gating influence of the Kölliker-fuse nucleus and the periaqueductal gray. Then the review breaks down the major findings of the discovery of PiCo (Chapter 2) and puts them into a larger context; more accessible and digestible to those outside of the small respiratory control field. Currently the major foci of the field are inspiration and active expiration, and I wanted to help shed light on the importance of the oft-overlooked phase, postinspiration. Further understanding of PiCo could yield future clinical implications as well as generalized applicability for other multiple-oscillator rhythm generating networks.

4.2. Future directions

My hope is that the discovery of this new respiratory oscillator, PiCo, will lead to years of fruitful research, just as the discovery of preBötC has over the last quarter century. Future potential avenues of study incorporate both basic science and translational questions.

One necessary next step is to more fully characterize the PiCo population. A complete study in which scores of PiCo neurons are intracellularly recorded, either individually or through multi-array techniques, would contribute data (burst data and estimates of connectivity between PiCo neurons) useful for models of respiratory rhythmogenesis. Elucidating ascending and descending projection patterns of PiCo neurons to/from other populations in the brainstem, midbrain, motor nuclei, and even higher cortical centers would also provide valuable detail for models of rhythm generation.

Immunohistochemical techniques could be utilized to identify expression profiles that are unique to PiCo neurons. Based on the results described herein, the logical receptor types to initially label include somatostatin 2a, mu-opioid, and alpha-1 noradrenergic receptors. The collaboration with Toto Olivera's group in Utah creates additional opportunity to phenotypically characterize the PiCo population. Their technique, constellation pharmacology, dissociates groups of cells and discovers "constellations", or unique combinations, of receptors and ion channels using fluorescent calcium imaging (Teichert et al., 2015). In the paper we co-published we focused on neurons in the preBötC region (Raghuraman et al., 2014). Future studies can reveal unique receptor and ion channel combinations specific to PiCo neurons, and determine

whether the PiCo population consists of phenotypically homogenous or heterogeneous collection of cells. Additionally, when an expression profile has successfully been identified, one could start searching for the PiCo population in human brainstem. A similar approach, positive immunostaining for NK1 and somatostatin and negative for markers of monoaminergic neurons, was used to identify the putative homolog to the preBötC in humans in 2011 (Schwarzacher et al., 2011).

The observation that human patients with neurodegenerative disease often exhibit a discoordination between breathing and swallowing (a postinspiratory behavior) means PiCo could have translational relevance. Horizontal slices could be obtained from the brainstems of mouse models for Parkinson's (Blesa et al., 2012) or Alzheimer's disease (Elder et al., 2010) and compared to controls for differences in immunohistochemical expression patterns. Electrophysiologically, abnormalities in the timing relationship between PiCo and preBötC bursts could be examined, as well as burst frequency, amplitude, and area compared to age-matched controls. One initial hurdle to achieving success in these physiology experiments, however, is to establish a reliable method with which to produce rhythms from adult horizontal slices. Progress to overcome this limitation is ongoing, and current methods involve the adjustment of slicing temperature and ACSF ingredients (Ankri et al., 2014; Huang and Uusisaari, 2013; Ting et al., 2014).

If the homolog for PiCo is identified in human, then healthy tissue could be histologically compared to post-mortem tissue derived from patients diagnosed with Parkinson's or Alzheimer's disease. Depending on the results, these observations could give valuable insight into the pathogenesis of these diseases and could also help in the targeted development of novel therapeutics.

Another potential translational application involves obstructive sleep apnea (OSA). OSA occurs when breathing ceases due to the repetitive, episodic collapse of the pharyngeal airway that is the result of an obstruction or increased airway resistance (Ramirez et al., 2013a). Chronic intermittent hypoxia (CIH) is the main component of OSA and can be recapitulated in a mouse model for the disorder (Garcia et al., 2016). To my knowledge, only one study has looked at postinspiration in conjunction with CIH and found that after exposure to intermittent bouts of hypoxia, laryngeal motorneurons decreased glottal adduction during postinspiration, suggesting that upper airway resistance is reduced (Moraes and Machado, 2015). The group also found that these changes were not associated with intrinsic electrophysiological properties and hypothesized that the changes were occurring, not at the motorneuron level, but in respiratory control networks (Moraes and Machado, 2015). At this juncture, I would venture the testable hypothesis that PiCo neurons are orchestrating changes in the upper airway after exposure to CIH.

An important opportunity for further study is to investigate the role of PiCo in various postinspiratory behaviors including vocalization and swallowing. FOXP2 is a gene that is associated with speech and language development in humans (Heckman et al., 2016) and mutations lead to the abnormal development and function of vocal production (Fujita et al., 2008; Lai et al., 2001; Shu et al., 2005). Genetic modifications of the mouse Foxp2 gene, the orthologue of human FOXP2, modulates ultrasonic vocalizations (Gaub et al., 2010; Groszer et al., 2008; Heckman et al., 2016). Potential low-hanging-fruit experimentation would utilize Cre recombinase-inducible Foxp2 knockout mice (French et al., 2007) by recording from PiCo in horizontal slice

preparations and analyzing any abnormalities in PiCo bursting. If a significant number of rhythmogenic PiCo neurons express Foxp2, a knockout of Foxp2 would presumably eliminate PiCo bursting or severely decrease burst amplitude. To begin to study the relationship between PiCo and swallowing, one could elicit a swallow *in vivo* with an oral water injection above the laryngeal apparatus (Bautista et al., 2014a) or into the pharynx (Lang, 2009) while electrophysiologically recording extracellular PiCo activity *in vivo*. Furthermore, one could specifically inhibit PiCo neurons by injecting somatostatin bilaterally into PiCo in an awake, behaving mouse and test whether the mouse has an impaired ability to vocalize or swallow.

The horizontal slice retains the RTN/pFRG, the network that is reportedly responsible for active expiration (Janczewski and Feldman, 2006). Theoretically, one could begin to study the interaction between all three respiratory oscillators in a single, *in vitro* preparation. One potential drawback, however, is that the RTN/pFRG is located along the ventral edge of the medulla. Thus, to easily access this population, the horizontal slice would have to be flipped upside down (ventral side facing up) from the orientation that is most accessible for preBötC and PiCo. There are two possible solutions. One is to carefully try to access the RTN/pFRG from the dorsal side of the slice by gently going through the tissue to reach the ventral side. Alternatively, when the slice is ventral side up, the PiCo could be accessed by going through the slice in a similar manner, and inspiratory activity could be recorded from phrenic activity at spinal level C4. Once all three rhythms are able to be recorded simultaneously, there are several experiments one could accomplish. The networks could be manipulated with hypercapnia, hypoxia, neuromodulators, toxins, or optogenetic light stimulation, and the

interaction between the individual networks could be examined. Results from these *in vitro* experiments could also help guide further, more invasive, *in vivo* experiments.

Results derived from the experiments outlined here should provide guided hypotheses for a multitude of questions to address *in vivo*, and perhaps, ultimately, for the eventual development of therapies for those that suffer from centrally-derived respiratory disorders. The possibilities for further study involving PiCo seem boundless. Of course, the uncovering of answers will, more often than not, lead to more questions. I invite other investigators to take this initial identification of the postinspiratory complex and apply their own unique perspective and techniques to help dissect the physiological functionalities of the PiCo network.

References

Abd-El-Malek, S., 1938. A contribution to the study of the movements of the tongue in animals, with special reference to the cat. Journal of anatomy 73, 15-30 11.

Abdala, A.P., Rybak, I.A., Smith, J.C., Paton, J.F., 2009. Abdominal expiratory activity in the rat brainstem-spinal cord in situ: patterns, origins and implications for respiratory rhythm generation. J Physiol 587, 3539-3559.

Adametz, J., O'Leary, J.L., 1959. Experimental mutism resulting from periaqueductal lesions in cats. Neurology 9, 636-642.

Ahdab, R., Saade, H.S., Kikano, R., Ferzli, J., Tarcha, W., Riachi, N., 2013. Pure ipsilateral central facial palsy and contralateral hemiparesis secondary to ventro-medial medullary stroke. J Neurol Sci 332, 154-155.

Akahoshi, T., White, D.P., Edwards, J.K., Beauregard, J., Shea, S.A., 2001. Phasic mechanoreceptor stimuli can induce phasic activation of upper airway muscles in humans. The Journal of physiology 531, 677-691.

Alagiakrishnan, K., Bhanji, R.A., Kurian, M., 2013. Evaluation and management of oropharyngeal dysphagia in different types of dementia: a systematic review. Arch Gerontol Geriatr 56, 1-9.

Alchanatis, M., Tourkohoriti, G., Kakouros, S., Kosmas, E., Podaras, S., Jordanoglou, J.B., 2001. Daytime pulmonary hypertension in patients with obstructive sleep apnea: the effect of continuous positive airway pressure on pulmonary hemodynamics. Respiration; international review of thoracic diseases 68, 566-572.

Aldes, L.D., Chapman, M.E., Chronister, R.B., Haycock, J.W., 1992. Sources of noradrenergic afferents to the hypoglossal nucleus in the rat. Brain research bulletin 29, 931-942.

Alheid, G.F., McCrimmon, D.R., 2008. The chemical neuroanatomy of breathing. Respir Physiol Neurobiol 164, 3-11.

Anderson, T.M., Garcia, A.J., 3rd, Baertsch, N.A., Pollak, J., Bloom, J.C., Wei, A.D., 2016. A novel excitatory network for the control of breathing. Nature 536, 76-80.

Ankri, L., Yarom, Y., Uusisaari, M.Y., 2014. Slice it hot: acute adult brain slicing in physiological temperature. J Vis Exp, e52068.

Aston-Jones, G., Bloom, F.E., 1981. Activity of norepinephrine-containing locus coeruleus neurons in behaving rats anticipates fluctuations in the sleep-waking cycle. The Journal of neuroscience : the official journal of the Society for Neuroscience 1, 876-886.

Aydogdu, I., Tanriverdi, Z., Ertekin, C., 2011. Dysfunction of bulbar central pattern generator in ALS patients with dysphagia during sequential deglutition. Clin Neurophysiol 122, 1219-1228.

Baghdadwala, M.I., Duchcherer, M., Paramonov, J., Wilson, R.J., 2015. Three brainstem areas involved in respiratory rhythm generation in bullfrogs. J Physiol 593, 2941-2954.

Baguet, J.P., Barone-Rochette, G., Tamisier, R., Levy, P., Pepin, J.L., 2012. Mechanisms of cardiac dysfunction in obstructive sleep apnea. Nature reviews. Cardiology 9, 679-688.

Bailey, E.F., Fregosi, R.F., 2004. Coordination of intrinsic and extrinsic tongue muscles during spontaneous breathing in the rat. Journal of applied physiology 96, 440-449.

Bandler, R., Carrive, P., 1988. Integrated defence reaction elicited by excitatory amino acid microinjection in the midbrain periaqueductal grey region of the unrestrained cat. Brain Res 439, 95-106.

Barnes, B.J., Tuong, C.M., Mellen, N.M., 2007. Functional imaging reveals respiratory network activity during hypoxic and opioid challenge in the neonate rat tilted sagittal slab preparation. J Neurophysiol 97, 2283-2292.
Bartlett, D., Jr., 1971. Origin and regulation of spontaneous deep breaths. Respiration physiology 12, 230-238.
Bartlett, D., Jr., Remmers, J.E., Gautier, H., 1973. Laryngeal regulation of respiratory airflow. Respiration physiology 18, 194-204.
Bautista, T.G., Dutschmann, M., 2014. Ponto-medullary nuclei involved in the generation of sequential pharyngeal swallowing and concomitant protective laryngeal adduction in situ. J Physiol 592, 2605-2623.
Bautista, T.G., Fong, A.Y., Dutschmann, M., 2014a. Spontaneous swallowing occurs during autoresuscitation in the in situ brainstem preparation of rat. Respir Physiol Neurobiol 202, 35-43.
Bautista, T.G., Sun, Q.J., Pilowsky, P.M., 2014b. The generation of pharyngeal phase of swallow and its coordination with breathing: interaction between the swallow and respiratory central pattern generators. Prog Brain Res 212, 253-275.
Bell, H.J., Ferguson, C., Kehoe, V., Haouzi, P., 2009. Hypocapnia increases the prevalence of hypoxia-induced augmented breaths. American journal of physiology. Regulatory, integrative and comparative physiology 296, R334-344.
Bell, H.J., Haouzi, P., 2010. The hypoxia-induced facilitation of augmented breaths is suppressed by the common effect of carbonic anhydrase inhibition. Respiratory physiology & neurobiology 171, 201-211.
Bellingham, M.C., Berger, A.J., 1996. Presynaptic depression of excitatory synaptic inputs to rat hypoglossal motoneurons by muscarinic M2 receptors. Journal of neurophysiology 76, 3758-3770.
Bellingham, M.C., Funk, G.D., 2000. Cholinergic modulation of respiratory brain-stem neurons and its function in sleep-wake state determination. Clinical and experimental pharmacology & physiology 27, 132-137.
Benyamin, R., Trescot, A.M., Datta, S., Buenaventura, R., Adlaka, R., Sehgal, N., Glaser, S.E., Vallejo, R., 2008. Opioid complications and side effects. Pain Physician 11, S105-120.
Bernard, A., Sorensen, S.A., Lein, E.S., 2009. Shifting the paradigm: new approaches for characterizing and classifying neurons. Curr Opin Neurobiol 19, 530-536.
Berry, R.B., Gleeson, K., 1997. Respiratory arousal from sleep: mechanisms and significance. Sleep 20, 654-675.
Bhattacharjee, R., Kheirandish-Gozal, L., Spruyt, K., Mitchell, R.B., Promchiarak, J., Simakajornboon, N., Kaditis, A.G., Splaingard, D., Splaingard, M., Brooks, L.J., Marcus, C.L., Sin, S., Arens, R., Verhulst, S.L., Gozal, D., 2010. Adenotonsillectomy outcomes in treatment of obstructive sleep apnea in children: a multicenter retrospective study. American journal of respiratory and critical care medicine 182, 676-683.
Bhattacharjee, R., Kim, J., Alotaibi, W.H., Kheirandish-Gozal, L., Capdevila, O.S., Gozal, D., 2012. Endothelial dysfunction in children without hypertension: potential contributions of obesity and obstructive sleep apnea. Chest 141, 682-691.
Bianchi, A.L., Gestreau, C., 2009. The brainstem respiratory network: an overview of a half century of research. Respir Physiol Neurobiol 168, 4-12.
Bianchi, A.L., St John, W.M., 1981. Pontile axonal projections of medullary respiratory neurons. Respir Physiol 45, 167-183.

Bianchi, A.L., St John, W.M., 1982. Medullary axonal projections of respiratory neurons of pontile pneumotaxic center. Respir Physiol 48, 357-373.
Bickelmann, A.G., Burwell, C.S., Robin, E.D., Whaley, R.D., 1956. Extreme obesity associated with alveolar hypoventilation; a Pickwickian syndrome. The American journal of medicine 21, 811-818.
Bieger, D., Hopkins, D.A., 1987. Viscerotopic representation of the upper alimentary tract in the medulla oblongata in the rat: the nucleus ambiguus. J Comp Neurol 262, 546-562.
Blesa, J., Phani, S., Jackson-Lewis, V., Przedborski, S., 2012. Classic and new animal models of Parkinson's disease. J Biomed Biotechnol 2012, 845618.
Boden, K., Cedborg, A.I., Eriksson, L.I., Hedstrom, H.W., Kuylenstierna, R., Sundman, E., Ekberg, O., 2009. Swallowing and respiratory pattern in young healthy individuals recorded with high temporal resolution. Neurogastroenterol Motil 21, 1163-e1101.
Bolser, D.C., Gestreau, C., Morris, K.F., Davenport, P.W., Pitts, T.E., 2013. Central neural circuits for coordination of swallowing, breathing, and coughing: predictions from computational modeling and simulation. Otolaryngol Clin North Am 46, 957-964.
Bolser, D.C., Pitts, T.E., Davenport, P.W., Morris, K.F., 2015. Role of the dorsal medulla in the neurogenesis of airway protection. Pulm Pharmacol Ther 35, 105-110.
Bolser, D.C., Poliacek, I., Jakus, J., Fuller, D.D., Davenport, P.W., 2006. Neurogenesis of cough, other airway defensive behaviors and breathing: A holarchical system? Respir Physiol Neurobiol 152, 255-265.
Bonis, J.M., Neumueller, S.E., Krause, K.L., Pan, L.G., Hodges, M.R., Forster, H.V., 2013. Contributions of the Kolliker-Fuse nucleus to coordination of breathing and swallowing. Respir Physiol Neurobiol 189, 10-21.
Bonis, J.M., Neumueller, S.E., Marshall, B.D., Krause, K.L., Qian, B., Pan, L.G., Hodges, M.R., Forster, H.V., 2011. The effects of lesions in the dorsolateral pons on the coordination of swallowing and breathing in awake goats. Respir Physiol Neurobiol 175, 272-282.
Bouvier, J., Thoby-Brisson, M., Renier, N., Dubreuil, V., Ericson, J., Champagnat, J., Pierani, A., Chedotal, A., Fortin, G., 2010. Hindbrain interneurons and axon guidance signaling critical for breathing. Nat Neurosci 13, 1066-1074.
Boyd, S.B., 2009. Management of obstructive sleep apnea by maxillomandibular advancement. Oral and maxillofacial surgery clinics of North America 21, 447-457.
Brancatisano, T., Collett, P.W., Engel, L.A., 1983. Respiratory movements of the vocal cords. J Appl Physiol Respir Environ Exerc Physiol 54, 1269-1276.
Bray, G.A., 1994. What's in a name? Mr. Dickens' "Pickwickian" fat boy syndrome. Obesity research 2, 380-383.
Brockhaus, J., Ballanyi, K., 1998. Synaptic inhibition in the isolated respiratory network of neonatal rats. Eur J Neurosci 10, 3823-3839.
Brodsky, M.B., McFarland, D.H., Dozier, T.S., Blair, J., Ayers, C., Michel, Y., Gillespie, M.B., Day, T.A., Martin-Harris, B., 2010. Respiratory-swallow phase patterns and their relationship to swallowing impairment in patients treated for oropharyngeal cancer. Head Neck 32, 481-489.
Brouillette, R.T., Thach, B.T., 1979. A neuromuscular mechanism maintaining extrathoracic airway patency. Journal of applied physiology 46, 772-779.
Broussard, D.L., Altschuler, S.M., 2000. Central integration of swallow and airway-protective reflexes. Am J Med 108 Suppl 4a, 62S-67S.

Bruce, E.N., Mitra, J., Cherniack, N.S., 1982. Central and peripheral chemoreceptor inputs to phrenic and hypoglossal motoneurons. Journal of applied physiology 53, 1504-1511.
Burke, P.G., Abbott, S.B., McMullan, S., Goodchild, A.K., Pilowsky, P.M., 2010. Somatostatin selectively ablates post-inspiratory activity after injection into the Botzinger complex. Neuroscience 167, 528-539.
Burns, B.D., 1963. The central control of respiratory movements. Br Med Bull 19, 7-9.
Busselberg, D., Bischoff, A.M., Paton, J.F., Richter, D.W., 2001. Reorganisation of respiratory network activity after loss of glycinergic inhibition. Pflugers Arch 441, 444-449.
Carrive, P., Dampney, R.A., Bandler, R., 1987. Excitation of neurones in a restricted portion of the midbrain periaqueductal grey elicits both behavioural and cardiovascular components of the defence reaction in the unanaesthetised decerebrate cat. Neurosci Lett 81, 273-278.
Carroll, M.S., Ramirez, J.M., 2013. Cycle-by-cycle assembly of respiratory network activity is dynamic and stochastic. J Neurophysiol 109, 296-305.
Carroll, M.S., Viemari, J.C., Ramirez, J.M., 2013. Patterns of inspiratory phase-dependent activity in the in vitro respiratory network. J Neurophysiol 109, 285-295.
Castelino, C.B., Schmidt, M.F., 2010. What birdsong can teach us about the central noradrenergic system. J Chem Neuroanat 39, 96-111.
Chamberlin, N.L., Eikermann, M., Fassbender, P., White, D.P., Malhotra, A., 2007. Genioglossus premotoneurons and the negative pressure reflex in rats. The Journal of physiology 579, 515-526.
Chan, E., Steenland, H.W., Liu, H., Horner, R.L., 2006. Endogenous excitatory drive modulating respiratory muscle activity across sleep-wake states. American journal of respiratory and critical care medicine 174, 1264-1273.
Chase, M.H., Soja, P.J., Morales, F.R., 1989. Evidence that glycine mediates the postsynaptic potentials that inhibit lumbar motoneurons during the atonia of active sleep. The Journal of neuroscience : the official journal of the Society for Neuroscience 9, 743-751.
Chen, X., Kombian, S.B., Zidichouski, J.A., Pittman, Q.J., 1999. Dopamine depresses glutamatergic synaptic transmission in the rat parabrachial nucleus in vitro. Neuroscience 90, 457-468.
Chen, Y., Li, G., Huang, L.Y., 2012. P2X7 receptors in satellite glial cells mediate high functional expression of P2X3 receptors in immature dorsal root ganglion neurons. Mol Pain 8, 9.
Cherniack, N.S., von Euler, C., Glogowska, M., Homma, I., 1981. Characteristics and rate of occurrence of spontaneous and provoked augmented breaths. Acta physiologica Scandinavica 111, 349-360.
Cheron, G., Marquez-Ruiz, J., Dan, B., 2016. Oscillations, Timing, Plasticity, and Learning in the Cerebellum. Cerebellum 15, 122-138.
Chitravanshi, V.C., Sapru, H.N., 1995. Chemoreceptor-sensitive neurons in commissural subnucleus of nucleus tractus solitarius of the rat. The American journal of physiology 268, R851-858.
Costa-Silva, J.H., Zoccal, D.B., Machado, B.H., 2010. Glutamatergic antagonism in the NTS decreases post-inspiratory drive and changes phrenic and sympathetic coupling during chemoreflex activation. J Neurophysiol 103, 2095-2106.
Costa-Silva, J.H., Zoccal, D.B., Machado, B.H., 2012. Chronic intermittent hypoxia alters glutamatergic control of sympathetic and respiratory activities in the commissural NTS of

rats. American journal of physiology. Regulatory, integrative and comparative physiology 302, R785-793.
Cui, Y., Kam, K., Sherman, D., Janczewski, W.A., Zheng, Y., Feldman, J.L., 2016. Defining preBotzinger Complex Rhythm- and Pattern-Generating Neural Microcircuits In Vivo. Neuron 91, 602-614.
Davenport, P.W., Bolser, D.C., Morris, K.F., 2011. Swallow remodeling of respiratory neural networks. Head Neck 33 Suppl 1, S8-13.
De Leon, A., 2016. The aging digestive tract. What should we anesthesiologists know about it? Minerva Anestesiol.
Del Negro, C.A., Koshiya, N., Butera, R.J., Jr., Smith, J.C., 2002. Persistent sodium current, membrane properties and bursting behavior of pre-botzinger complex inspiratory neurons in vitro. J Neurophysiol 88, 2242-2250.
Del Negro, C.A., Morgado-Valle, C., Hayes, J.A., Mackay, D.D., Pace, R.W., Crowder, E.A., Feldman, J.L., 2005. Sodium and calcium current-mediated pacemaker neurons and respiratory rhythm generation. J Neurosci 25, 446-453.
Dempsey, J.A., Veasey, S.C., Morgan, B.J., O'Donnell, C.P., 2010. Pathophysiology of sleep apnea. Physiological reviews 90, 47-112.
Dergacheva, O., Griffioen, K.J., Neff, R.A., Mendelowitz, D., 2010. Respiratory modulation of premotor cardiac vagal neurons in the brainstem. Respir Physiol Neurobiol 174, 102-110.
Destexhe, A., 2000. Modelling corticothalamic feedback and the gating of the thalamus by the cerebral cortex. J Physiol Paris 94, 391-410.
Dick, T.E., Bellingham, M.C., Richter, D.W., 1994. Pontine respiratory neurons in anesthetized cats. Brain Res 636, 259-269.
Dick, T.E., Dutschmann, M., Feldman, J.L., Fong, A.Y., Hulsmann, S., Morris, K.M., Ramirez, J.M., Smith, J.C., Respiratory Neurobiology, C., 2015. Facts and challenges in respiratory neurobiology. Respir Physiol Neurobiol.
Dick, T.E., Hsieh, Y.H., Dhingra, R.R., Baekey, D.M., Galan, R.F., Wehrwein, E., Morris, K.F., 2014. Cardiorespiratory coupling: common rhythms in cardiac, sympathetic, and respiratory activities. Prog Brain Res 209, 191-205.
Dick, T.E., Oku, Y., Romaniuk, J.R., Cherniack, N.S., 1993. Interaction between central pattern generators for breathing and swallowing in the cat. J Physiol 465, 715-730.
Dobbins, E.G., Feldman, J.L., 1994. Brainstem network controlling descending drive to phrenic motoneurons in rat. J Comp Neurol 347, 64-86.
Dobbins, E.G., Feldman, J.L., 1995. Differential innervation of protruder and retractor muscles of the tongue in rat. The Journal of comparative neurology 357, 376-394.
Doi, A., Ramirez, J.M., 2008. Neuromodulation and the orchestration of the respiratory rhythm. Respiratory physiology & neurobiology 164, 96-104.
Doi, A., Ramirez, J.M., 2010. State-dependent interactions between excitatory neuromodulators in the neuronal control of breathing. J Neurosci 30, 8251-8262.
Doty, R.W., Bosma, J.F., 1956. An electromyographic analysis of reflex deglutition. J Neurophysiol 19, 44-60.
Douglas, N.J., White, D.P., Weil, J.V., Pickett, C.K., Zwillich, C.W., 1982. Hypercapnic ventilatory response in sleeping adults. The American review of respiratory disease 126, 758-762.
Dutschmann, M., Dick, T.E., 2012. Pontine mechanisms of respiratory control. Compr Physiol 2, 2443-2469.

Dutschmann, M., Herbert, H., 2006. The Kolliker-Fuse nucleus gates the postinspiratory phase of the respiratory cycle to control inspiratory off-switch and upper airway resistance in rat. Eur J Neurosci 24, 1071-1084.
Dutschmann, M., Jones, S.E., Subramanian, H.H., Stanic, D., Bautista, T.G., 2014. The physiological significance of postinspiration in respiratory control. Prog Brain Res 212, 113-130.
Dutschmann, M., Menuet, C., Stettner, G.M., Gestreau, C., Borghgraef, P., Devijver, H., Gielis, L., Hilaire, G., Van Leuven, F., 2010. Upper airway dysfunction of Tau-P301L mice correlates with tauopathy in midbrain and ponto-medullary brainstem nuclei. J Neurosci 30, 1810-1821.
Dutschmann, M., Morschel, M., Kron, M., Herbert, H., 2004. Development of adaptive behaviour of the respiratory network: implications for the pontine Kolliker-Fuse nucleus. Respir Physiol Neurobiol 143, 155-165.
Dutschmann, M., Morschel, M., Reuter, J., Zhang, W., Gestreau, C., Stettner, G.M., Kron, M., 2008. Postnatal emergence of synaptic plasticity associated with dynamic adaptation of the respiratory motor pattern. Respir Physiol Neurobiol 164, 72-79.
Dutschmann, M., Paton, J.F., 2002a. Glycinergic inhibition is essential for co-ordinating cranial and spinal respiratory motor outputs in the neonatal rat. J Physiol 543, 643-653.
Dutschmann, M., Paton, J.F., 2002b. Inhibitory synaptic mechanisms regulating upper airway patency. Respir Physiol Neurobiol 131, 57-63.
Dutschmann, M., Paton, J.F., 2002c. Trigeminal reflex regulation of the glottis depends on central glycinergic inhibition in the rat. Am J Physiol Regul Integr Comp Physiol 282, R999-R1005.
Easterling, C.S., Robbins, E., 2008. Dementia and dysphagia. Geriatr Nurs 29, 275-285.
Easton, P.A., Katagiri, M., Kieser, T.M., Platt, R.S., 1999. Postinspiratory activity of costal and crural diaphragm. J Appl Physiol (1985) 87, 582-589.
Eastwood, P.R., Szollosi, I., Platt, P.R., Hillman, D.R., 2002. Comparison of upper airway collapse during general anaesthesia and sleep. Lancet 359, 1207-1209.
Ebihara, S., Sekiya, H., Miyagi, M., Ebihara, T., Okazaki, T., 2016. Dysphagia, dystussia, and aspiration pneumonia in elderly people. J Thorac Dis 8, 632-639.
Eckert, D.J., Jordan, A.S., Merchia, P., Malhotra, A., 2007a. Central sleep apnea: Pathophysiology and treatment. Chest 131, 595-607.
Eckert, D.J., Malhotra, A., Jordan, A.S., 2009a. Mechanisms of apnea. Progress in cardiovascular diseases 51, 313-323.
Eckert, D.J., Malhotra, A., Lo, Y.L., White, D.P., Jordan, A.S., 2009b. The influence of obstructive sleep apnea and gender on genioglossus activity during rapid eye movement sleep. Chest 135, 957-964.
Eckert, D.J., McEvoy, R.D., George, K.E., Thomson, K.J., Catcheside, P.G., 2007b. Genioglossus reflex inhibition to upper-airway negative-pressure stimuli during wakefulness and sleep in healthy males. The Journal of physiology 581, 1193-1205.
Eddy, N.B., Friebel, H., Hahn, K.J., Halbach, H., 1969. Codeine and its alternates for pain and cough relief. 5. Discussion and summary. Bull World Health Organ 40, 721-730.
El Baissari, M.C., Taha, S.K., Siddik-Sayyid, S.M., 2014. Fentanyl-induced cough--pathophysiology and prevention. Middle East J Anaesthesiol 22, 449-456.
Elder, G.A., Gama Sosa, M.A., De Gasperi, R., 2010. Transgenic mouse models of Alzheimer's disease. Mt Sinai J Med 77, 69-81.

Ellenberger, H.H., 1999. Distribution of bulbospinal gamma-aminobutyric acid-synthesizing neurons of the ventral respiratory group of the rat. J Comp Neurol 411, 130-144.
Ellenberger, H.H., Feldman, J.L., 1990. Brainstem connections of the rostral ventral respiratory group of the rat. Brain Res 513, 35-42.
England, S.J., Bartlett, D., Jr., Knuth, S.L., 1982. Comparison of human vocal cord movements during isocapnic hypoxia and hypercapnia. J Appl Physiol Respir Environ Exerc Physiol 53, 81-86.
Enoz, M., 2007. Effects of nasal pathologies on obstructive sleep apnea. Acta medica 50, 167-170.
Evans, J.A., Elliott, J.A., Gorman, M.R., 2010. Dynamic interactions between coupled oscillators within the hamster circadian pacemaker. Behavioral neuroscience 124, 87-96.
Ezure, K., 1990. Synaptic connections between medullary respiratory neurons and considerations on the genesis of respiratory rhythm. Prog Neurobiol 35, 429-450.
Ezure, K., Tanaka, I., Kondo, M., 2003. Glycine is used as a transmitter by decrementing expiratory neurons of the ventrolateral medulla in the rat. J Neurosci 23, 8941-8948.
Fedorko, L., Merrill, E.G., 1984. Axonal projections from the rostral expiratory neurones of the Botzinger complex to medulla and spinal cord in the cat. J Physiol 350, 487-496.
Feldman, J.L., Del Negro, C.A., 2006. Looking for inspiration: new perspectives on respiratory rhythm. Nat Rev Neurosci 7, 232-242.
Feldman, J.L., Del Negro, C.A., Gray, P.A., 2013. Understanding the rhythm of breathing: so near, yet so far. Annu Rev Physiol 75, 423-452.
Feldman, J.L., Kam, K., 2014. Facing the challenge of mammalian neural microcircuits: Taking a few breaths may help. J Physiol.
Fenik, V., Davies, R.O., Kubin, L., 2004. Combined antagonism of aminergic excitatory and amino acid inhibitory receptors in the XII nucleus abolishes REM sleep-like depression of hypoglossal motoneuronal activity. Archives italiennes de biologie 142, 237-249.
Fenik, V.B., Davies, R.O., Kubin, L., 2005a. Noradrenergic, serotonergic and GABAergic antagonists injected together into the XII nucleus abolish the REM sleep-like depression of hypoglossal motoneuronal activity. Journal of sleep research 14, 419-429.
Fenik, V.B., Davies, R.O., Kubin, L., 2005b. REM sleep-like atonia of hypoglossal (XII) motoneurons is caused by loss of noradrenergic and serotonergic inputs. American journal of respiratory and critical care medicine 172, 1322-1330.
Fenik, V.B., Ogawa, H., Davies, R.O., Kubin, L., 2005c. Carbachol injections into the ventral pontine reticular formation activate locus coeruleus cells in urethane-anesthetized rats. Sleep 28, 551-559.
Fenik, V.B., Rukhadze, I., Kubin, L., 2008. Inhibition of pontine noradrenergic A7 cells reduces hypoglossal nerve activity in rats. Neuroscience 157, 473-482.
Findley, L.J., Wilhoit, S.C., Suratt, P.M., 1985. Apnea duration and hypoxemia during REM sleep in patients with obstructive sleep apnea. Chest 87, 432-436.
Fisher, J.A., Marchenko, V.A., Yodh, A.G., Rogers, R.F., 2006. Spatiotemporal activity patterns during respiratory rhythmogenesis in the rat ventrolateral medulla. J Neurophysiol 95, 1982-1991.
Fogel, R.B., Malhotra, A., Pillar, G., Edwards, J.K., Beauregard, J., Shea, S.A., White, D.P., 2001. Genioglossal activation in patients with obstructive sleep apnea versus control subjects. Mechanisms of muscle control. American journal of respiratory and critical care medicine 164, 2025-2030.

Fontana, G.A., Lavorini, F., 2006. Cough motor mechanisms. Respir Physiol Neurobiol 152, 266-281.
Franco, P., Verheulpen, D., Valente, F., Kelmanson, I., de Broca, A., Scaillet, S., Groswasser, J., Kahn, A., 2003. Autonomic responses to sighs in healthy infants and in victims of sudden infant death. Sleep medicine 4, 569-577.
Franco, S.J., Muller, U., 2013. Shaping our minds: stem and progenitor cell diversity in the mammalian neocortex. Neuron 77, 19-34.
French, C.A., Groszer, M., Preece, C., Coupe, A.M., Rajewsky, K., Fisher, S.E., 2007. Generation of mice with a conditional Foxp2 null allele. Genesis 45, 440-446.
Fujita, E., Tanabe, Y., Shiota, A., Ueda, M., Suwa, K., Momoi, M.Y., Momoi, T., 2008. Ultrasonic vocalization impairment of Foxp2 (R552H) knockin mice related to speech-language disorder and abnormality of Purkinje cells. Proc Natl Acad Sci U S A 105, 3117-3122.
Fuller, D.D., Williams, J.S., Janssen, P.L., Fregosi, R.F., 1999. Effect of co-activation of tongue protrudor and retractor muscles on tongue movements and pharyngeal airflow mechanics in the rat. The Journal of physiology 519 Pt 2, 601-613.
Funk, G.D., Parkis, M.A., Selvaratnam, S.R., Walsh, C., 1997. Developmental modulation of glutamatergic inspiratory drive to hypoglossal motoneurons. Respiration physiology 110, 125-137.
Funk, G.D., Smith, J.C., Feldman, J.L., 1994. Development of thyrotropin-releasing hormone and norepinephrine potentiation of inspiratory-related hypoglossal motoneuron discharge in neonatal and juvenile mice in vitro. Journal of neurophysiology 72, 2538-2541.
Funk, G.D., Zwicker, J.D., Selvaratnam, R., Robinson, D.M., 2011. Noradrenergic modulation of hypoglossal motoneuron excitability: developmental and putative state-dependent mechanisms. Archives italiennes de biologie 149, 426-453.
Garcia, A.J., 3rd, Khan, S.A., Kumar, G.K., Prabhakar, N.R., Ramirez, J.M., 2011a. Hydrogen peroxide differentially affects activity in the pre-Botzinger complex and hippocampus. Journal of neurophysiology 106, 3045-3055.
Garcia, A.J., 3rd, Koschnitzky, J.E., Dashevskiy, T., Ramirez, J.M., 2013. Cardiorespiratory coupling in health and disease. Auton Neurosci 175, 26-37.
Garcia, A.J., 3rd, Zanella, S., Dashevskiy, T., Khan, S.A., Khuu, M.A., Prabhakar, N.R., Ramirez, J.M., 2016. Chronic Intermittent Hypoxia Alters Local Respiratory Circuit Function at the Level of the preBotzinger Complex. Front Neurosci 10, 4.
Garcia, A.J., 3rd, Zanella, S., Koch, H., Doi, A., Ramirez, J.M., 2011b. Chapter 3--networks within networks: the neuronal control of breathing. Prog Brain Res 188, 31-50.
Gaub, S., Groszer, M., Fisher, S.E., Ehret, G., 2010. The structure of innate vocalizations in Foxp2-deficient mouse pups. Genes Brain Behav 9, 390-401.
Gautier, H., Remmers, J.E., Bartlett, D., Jr., 1973. Control of the duration of expiration. Respir Physiol 18, 205-221.
Gestreau, C., Grelot, L., Bianchi, A.L., 2000. Activity of respiratory laryngeal motoneurons during fictive coughing and swallowing. Exp Brain Res 130, 27-34.
Gestreau, C., Milano, S., Bianchi, A.L., Grelot, L., 1996. Activity of dorsal respiratory group inspiratory neurons during laryngeal-induced fictive coughing and swallowing in decerebrate cats. Exp Brain Res 108, 247-256.
Gewolb, I.H., Fishman, D., Qureshi, M.A., Vice, F.L., 2004. Coordination of suck-swallow-respiration in infants born to mothers with drug-abuse problems. Dev Med Child Neurol 46, 700-705.

Ghannouchi, I., Speyer, R., Doma, K., Cordier, R., Verin, E., 2016. Swallowing function and chronic respiratory diseases: Systematic review. Respir Med 117, 54-64.
Gleeson, K., Zwillich, C.W., White, D.P., 1990. The influence of increasing ventilatory effort on arousal from sleep. The American review of respiratory disease 142, 295-300.
Glogowska, M., Richardson, P.S., Widdicombe, J.G., Winning, A.J., 1972. The role of the vagus nerves, peripheral chemoreceptors and other afferent pathways in the genesis of augmented breaths in cats and rabbits. Respiration physiology 16, 179-196.
Gourevitch, B., Mellen, N., 2014. The preBotzinger complex as a hub for network activity along the ventral respiratory column in the neonate rat. Neuroimage 98, 460-474.
Gozal, D., 2000. Obstructive sleep apnea in children. Minerva pediatrica 52, 629-639.
Gozal, D., Hakim, F., Kheirandish-Gozal, L., 2013. Chemoreceptors, baroreceptors, and autonomic deregulation in children with obstructive sleep apnea. Respiratory physiology & neurobiology 185, 177-185.
Gozal, D., Khalyfa, A., Capdevila, O.S., Kheirandish-Gozal, L., Khalyfa, A.A., Kim, J., 2012. Cognitive function in prepubertal children with obstructive sleep apnea: a modifying role for NADPH oxidase p22 subunit gene polymorphisms? Antioxidants & redox signaling 16, 171-177.
Gozal, D., Kheirandish-Gozal, L., 2009. Obesity and excessive daytime sleepiness in prepubertal children with obstructive sleep apnea. Pediatrics 123, 13-18.
Gozal, D., Kheirandish-Gozal, L., 2012. Childhood obesity and sleep: relatives, partners, or both?--a critical perspective on the evidence. Annals of the New York Academy of Sciences 1264, 135-141.
Gozal, E., Shah, Z.A., Pequignot, J.M., Pequignot, J., Sachleben, L.R., Czyzyk-Krzeska, M.F., Li, R.C., Guo, S.Z., Gozal, D., 2005. Tyrosine hydroxylase expression and activity in the rat brain: differential regulation after long-term intermittent or sustained hypoxia. Journal of applied physiology 99, 642-649.
Grace, K.P., Hughes, S.W., Horner, R.L., 2013. Identification of the Mechanism Mediating Genioglossus Muscle Suppression in REM Sleep. American journal of respiratory and critical care medicine 187, 311-319.
Gray, P.A., 2013. Transcription factors define the neuroanatomical organization of the medullary reticular formation. Front Neuroanat 7, 7.
Gray, P.A., Hayes, J.A., Ling, G.Y., Llona, I., Tupal, S., Picardo, M.C., Ross, S.E., Hirata, T., Corbin, J.G., Eugenin, J., Del Negro, C.A., 2010. Developmental origin of preBotzinger complex respiratory neurons. J Neurosci 30, 14883-14895.
Gray, P.A., Rekling, J.C., Bocchiaro, C.M., Feldman, J.L., 1999. Modulation of respiratory frequency by peptidergic input to rhythmogenic neurons in the preBotzinger complex. Science 286, 1566-1568.
Gray, R., Rajan, A.S., Radcliffe, K.A., Yakehiro, M., Dani, J.A., 1996. Hippocampal synaptic transmission enhanced by low concentrations of nicotine. Nature 383, 713-716.
Grigorakos, L., Sakagianni, K., Tsigou, E., Apostolakos, G., Nikolopoulos, G., Veldekis, D., 2010. Outcome of acute heroin overdose requiring intensive care unit admission. J Opioid Manag 6, 227-231.
Grillner, S., 2003. The motor infrastructure: from ion channels to neuronal networks. Nature reviews. Neuroscience 4, 573-586.
Grillner, S., El Manira, A., 2015. The intrinsic operation of the networks that make us locomote. Curr Opin Neurobiol 31, 244-249.

Gross, R.D., Atwood, C.W., Jr., Ross, S.B., Eichhorn, K.A., Olszewski, J.W., Doyle, P.J., 2008. The coordination of breathing and swallowing in Parkinson's disease. Dysphagia 23, 136-145.
Gross, R.D., Atwood, C.W., Jr., Ross, S.B., Olszewski, J.W., Eichhorn, K.A., 2009. The coordination of breathing and swallowing in chronic obstructive pulmonary disease. Am J Respir Crit Care Med 179, 559-565.
Groszer, M., Keays, D.A., Deacon, R.M., de Bono, J.P., Prasad-Mulcare, S., Gaub, S., Baum, M.G., French, C.A., Nicod, J., Coventry, J.A., Enard, W., Fray, M., Brown, S.D., Nolan, P.M., Paabo, S., Channon, K.M., Costa, R.M., Eilers, J., Ehret, G., Rawlins, J.N., Fisher, S.E., 2008. Impaired synaptic plasticity and motor learning in mice with a point mutation implicated in human speech deficits. Curr Biol 18, 354-362.
Guntheroth, W.G., 2011. Cheyne-Stokes respiration: hypoxia plus a deep breath that interrupts hypoxic drive, initiating cyclic breathing. Medical hypotheses 77, 714-716.
Guyenet, P.G., Sevigny, C.P., Weston, M.C., Stornetta, R.L., 2002. Neurokinin-1 receptor-expressing cells of the ventral respiratory group are functionally heterogeneous and predominantly glutamatergic. J Neurosci 22, 3806-3816.
Hadjikoutis, S., Pickersgill, T.P., Dawson, K., Wiles, C.M., 2000. Abnormal patterns of breathing during swallowing in neurological disorders. Brain 123 (Pt 9), 1863-1873.
Harding, R., Johnson, P., McClelland, M.E., 1980. Respiratory function of the larynx in developing sheep and the influence of sleep state. Respiration physiology 40, 165-179.
Hartel, K., Schnell, C., Hulsmann, S., 2009. Astrocytic calcium signals induced by neuromodulators via functional metabotropic receptors in the ventral respiratory group of neonatal mice. Glia 57, 815-827.
Hartel, K., Singaravelu, K., Kaiser, M., Neusch, C., Hulsmann, S., Deitmer, J.W., 2007. Calcium influx mediated by the inwardly rectifying K+ channel Kir4.1 (KCNJ10) at low external K+ concentration. Cell Calcium 42, 271-280.
Haupt, M.E., Goodman, D.M., Sheldon, S.H., 2012. Sleep related expiratory obstructive apnea in children. Journal of clinical sleep medicine : JCSM : official publication of the American Academy of Sleep Medicine 8, 673-679.
Haxhiu, M.A., Cherniack, N.S., Mitra, J., van Lunteren, E., Strohl, K.P., 1992. Nonvagal modulation of hypoglossal neural activity. Respiration; international review of thoracic diseases 59, 65-71.
Heckman, J., McGuinness, B., Celikel, T., Englitz, B., 2016. Determinants of the mouse ultrasonic vocal structure and repertoire. Neurosci Biobehav Rev 65, 313-325.
Hedner, J.A., Wilcox, I., Laks, L., Grunstein, R.R., Sullivan, C.E., 1992. A specific and potent pressor effect of hypoxia in patients with sleep apnea. The American review of respiratory disease 146, 1240-1245.
Herbert, H., Moga, M.M., Saper, C.B., 1990. Connections of the parabrachial nucleus with the nucleus of the solitary tract and the medullary reticular formation in the rat. J Comp Neurol 293, 540-580.
Hilaire, G., Viemari, J.C., Coulon, P., Simonneau, M., Bevengut, M., 2004. Modulation of the respiratory rhythm generator by the pontine noradrenergic A5 and A6 groups in rodents. Respir Physiol Neurobiol 143, 187-197.
Hill, A.A., Garcia, A.J., 3rd, Zanella, S., Upadhyaya, R., Ramirez, J.M., 2011. Graded reductions in oxygenation evoke graded reconfiguration of the isolated respiratory network. Journal of neurophysiology 105, 625-639.

Hirata, T., Li, P., Lanuza, G.M., Cocas, L.A., Huntsman, M.M., Corbin, J.G., 2009. Identification of distinct telencephalic progenitor pools for neuronal diversity in the amygdala. Nature neuroscience 12, 141-149.
Hiss, S.G., Treole, K., Stuart, A., 2001. Effects of age, gender, bolus volume, and trial on swallowing apnea duration and swallow/respiratory phase relationships of normal adults. Dysphagia 16, 128-135.
Hone, A.J., Meyer, E.L., McIntyre, M., McIntosh, J.M., 2012. Nicotinic acetylcholine receptors in dorsal root ganglion neurons include the alpha6beta4* subtype. FASEB J 26, 917-926.
Horner, R.L., 2000. Impact of brainstem sleep mechanisms on pharyngeal motor control. Respiration physiology 119, 113-121.
Horner, R.L., 2008. Neuromodulation of hypoglossal motoneurons during sleep. Respiratory physiology & neurobiology 164, 179-196.
Horner, R.L., 2009. Emerging principles and neural substrates underlying tonic sleep-state-dependent influences on respiratory motor activity. Philosophical transactions of the Royal Society of London. Series B, Biological sciences 364, 2553-2564.
Horner, R.L., Innes, J.A., Murphy, K., Guz, A., 1991. Evidence for reflex upper airway dilator muscle activation by sudden negative airway pressure in man. The Journal of physiology 436, 15-29.
Huang, S., Uusisaari, M.Y., 2013. Physiological temperature during brain slicing enhances the quality of acute slice preparations. Front Cell Neurosci 7, 48.
Huckstepp, R.T., Cardoza, K.P., Henderson, L.E., Feldman, J.L., 2015. Role of parafacial nuclei in control of breathing in adult rats. J Neurosci 35, 1052-1067.
Huckstepp, R.T., Henderson, L.E., Cardoza, K.P., Feldman, J.L., 2016. Interactions between respiratory oscillators in adult rats. Elife 5.
Hwang, J.C., St John, W.M., Bartlett, D., Jr., 1983. Respiratory-related hypoglossal nerve activity: influence of anesthetics. Journal of applied physiology 55, 785-792.
Jacobs, B.L., Fornal, C.A., 1991. Activity of brain serotonergic neurons in the behaving animal. Pharmacological reviews 43, 563-578.
Janczewski, W.A., Feldman, J.L., 2006. Distinct rhythm generators for inspiration and expiration in the juvenile rat. J Physiol 570, 407-420.
Janczewski, W.A., Tashima, A., Hsu, P., Cui, Y., Feldman, J.L., 2013. Role of inhibition in respiratory pattern generation. J Neurosci 33, 5454-5465.
Jean, A., 2001. Brain stem control of swallowing: neuronal network and cellular mechanisms. Physiol Rev 81, 929-969.
Jean, A., Car, A., 1979. Inputs to the swallowing medullary neurons from the peripheral afferent fibers and the swallowing cortical area. Brain Res 178, 567-572.
Jean, A., Car, A., Roman, C., 1975. Comparison of activity in pontine versus medullary neurones during swallowing. Exp Brain Res 22, 211-220.
Jiang, C., Lipski, J., 1990. Extensive monosynaptic inhibition of ventral respiratory group neurons by augmenting neurons in the Botzinger complex in the cat. Exp Brain Res 81, 639-648.
Jiang, C., Lipski, J., 1992. Synaptic inputs to medullary respiratory neurons from superior laryngeal afferents in the cat. Brain Res 584, 197-206.
Johnson, S.M., Koshiya, N., Smith, J.C., 2001. Isolation of the kernel for respiratory rhythm generation in a novel preparation: the pre-Botzinger complex "island". J Neurophysiol 85, 1772-1776.

Jordan, A.S., White, D.P., 2008. Pharyngeal motor control and the pathogenesis of obstructive sleep apnea. Respiratory physiology & neurobiology 160, 1-7.
Julu, P.O., Kerr, A.M., Apartopoulos, F., Al-Rawas, S., Engerstrom, I.W., Engerstrom, L., Jamal, G.A., Hansen, S., 2001. Characterisation of breathing and associated central autonomic dysfunction in the Rett disorder. Arch Dis Child 85, 29-37.
Jurgens, U., Pratt, R., 1979. Role of the periaqueductal grey in vocal expression of emotion. Brain Res 167, 367-378.
Kalia, M., 2003. Dysphagia and aspiration pneumonia in patients with Alzheimer's disease. Metabolism 52, 36-38.
Kam, K., Worrell, J.W., Janczewski, W.A., Cui, Y., Feldman, J.L., 2013. Distinct inspiratory rhythm and pattern generating mechanisms in the preBotzinger complex. J Neurosci 33, 9235-9245.
Kanai, T., Wang, S.C., 1962. Localization of the central vocalization mechanism in the brain stem of the cat. Exp Neurol 6, 426-434.
Kass, J.E., Akers, S.M., Bartter, T.C., Pratter, M.R., 1996. Rapid-eye-movement-specific sleep-disordered breathing: a possible cause of excessive daytime sleepiness. American journal of respiratory and critical care medicine 154, 167-169.
Katz, D.M., Dutschmann, M., Ramirez, J.M., Hilaire, G., 2009. Breathing disorders in Rett syndrome: progressive neurochemical dysfunction in the respiratory network after birth. Respir Physiol Neurobiol 168, 101-108.
Kelly, A.H., Beaton, L.E., Magoun, H.W., 1946. A midbrain mechanism for facio-vocal activity. J Neurophysiol 9, 181-189.
Kessler, J.P., Jean, A., 1985. Identification of the medullary swallowing regions in the rat. Exp Brain Res 57, 256-263.
Ketz, N.A., Jensen, O., O'Reilly, R.C., 2015. Thalamic pathways underlying prefrontal cortex-medial temporal lobe oscillatory interactions. Trends Neurosci 38, 3-12.
Kiehn, O., 2006. Locomotor circuits in the mammalian spinal cord. Annual review of neuroscience 29, 279-306.
Kiehn, O., 2016. Decoding the organization of spinal circuits that control locomotion. Nat Rev Neurosci 17, 224-238.
Kim, H.C., Young, T., Matthews, C.G., Weber, S.M., Woodward, A.R., Palta, M., 1997. Sleep-disordered breathing and neuropsychological deficits. A population-based study. American journal of respiratory and critical care medicine 156, 1813-1819.
Kimoff, R.J., Cheong, T.H., Olha, A.E., Charbonneau, M., Levy, R.D., Cosio, M.G., Gottfried, S.B., 1994. Mechanisms of apnea termination in obstructive sleep apnea. Role of chemoreceptor and mechanoreceptor stimuli. American journal of respiratory and critical care medicine 149, 707-714.
Kline, D.D., Takacs, K.N., Ficker, E., Kunze, D.L., 2002. Dopamine modulates synaptic transmission in the nucleus of the solitary tract. Journal of neurophysiology 88, 2736-2744.
Kobayashi, S., Onimaru, H., Inoue, M., Inoue, T., Sasa, R., 2005. Localization and properties of respiratory neurons in the rostral pons of the newborn rat. Neuroscience 134, 317-325.
Koch, H., Garcia, A.J., 3rd, Ramirez, J.M., 2011. Network reconfiguration and neuronal plasticity in rhythm-generating networks. Integr Comp Biol 51, 856-868.
Koch, H., Zanella, S., Elsen, G.E., Smith, L., Doi, A., Garcia, A.J., 3rd, Wei, A.D., Xun, R., Kirsch, S., Gomez, C.M., Hevner, R.F., Ramirez, J.M., 2013. Stable Respiratory Activity Requires Both

P/Q-Type and N-Type Voltage-Gated Calcium Channels. The Journal of neuroscience : the official journal of the Society for Neuroscience 33, 3633-3645.
Koizumi, H., Smith, J.C., 2008. Persistent Na+ and K+-dominated leak currents contribute to respiratory rhythm generation in the pre-Botzinger complex in vitro. J Neurosci 28, 1773-1785.
Krause, K.L., Forster, H.V., Kiner, T., Davis, S.E., Bonis, J.M., Qian, B., Pan, L.G., 2009. Normal breathing pattern and arterial blood gases in awake and sleeping goats after near total destruction of the presumed pre-Botzinger complex and the surrounding region. J Appl Physiol (1985) 106, 605-619.
Kubin, L., Davies, R.O., Pack, A.I., 1998. Control of Upper Airway Motoneurons During REM Sleep. News in physiological sciences : an international journal of physiology produced jointly by the International Union of Physiological Sciences and the American Physiological Society 13, 91-97.
Kuna, S.T., Vanoye, C.R., 1994. Laryngeal response during forced vital capacity maneuvers in normal adult humans. Am J Respir Crit Care Med 150, 729-734.
Ladewig, T., Lalley, P.M., Keller, B.U., 2004. Serotonergic modulation of intracellular calcium dynamics in neonatal hypoglossal motoneurons from mouse. Brain research 1001, 1-12.
Lai, C.S., Fisher, S.E., Hurst, J.A., Vargha-Khadem, F., Monaco, A.P., 2001. A forkhead-domain gene is mutated in a severe speech and language disorder. Nature 413, 519-523.
Lalley, P.M., Bischoff, A.M., Schwarzacher, S.W., Richter, D.W., 1995. 5-HT2 receptor-controlled modulation of medullary respiratory neurones in the cat. The Journal of physiology 487 (Pt 3), 653-661.
Lam, D.J., Jensen, C.C., Mueller, B.A., Starr, J.R., Cunningham, M.L., Weaver, E.M., 2010. Pediatric sleep apnea and craniofacial anomalies: a population-based case-control study. The Laryngoscope 120, 2098-2105.
Lang, I.M., 2009. Brain stem control of the phases of swallowing. Dysphagia 24, 333-348.
Lang, I.M., Dana, N., Medda, B.K., Shaker, R., 2002. Mechanisms of airway protection during retching, vomiting, and swallowing. Am J Physiol Gastrointest Liver Physiol 283, G529-536.
Lavie, P., 1984. Nothing new under the moon. Historical accounts of sleep apnea syndrome. Archives of internal medicine 144, 2025-2028.
Le, S., Turner, A.J., Parker, L.M., Burke, P.G., Kumar, N.N., Goodchild, A.K., McMullan, S., 2016. Somatostatin 2a receptors are not expressed on functionally identified respiratory neurons in the ventral respiratory column of the rat. J Comp Neurol 524, 1384-1398.
Leung, C.G., Mason, P., 1999. Physiological properties of raphe magnus neurons during sleep and waking. Journal of neurophysiology 81, 584-595.
Leung, R.S., Bradley, T.D., 2001. Sleep apnea and cardiovascular disease. American journal of respiratory and critical care medicine 164, 2147-2165.
Lieske, S.P., Ramirez, J.M., 2006a. Pattern-specific synaptic mechanisms in a multifunctional network. I. Effects of alterations in synapse strength. Journal of neurophysiology 95, 1323-1333.
Lieske, S.P., Ramirez, J.M., 2006b. Pattern-specific synaptic mechanisms in a multifunctional network. II. Intrinsic modulation by metabotropic glutamate receptors. Journal of neurophysiology 95, 1334-1344.
Lieske, S.P., Thoby-Brisson, M., Telgkamp, P., Ramirez, J.M., 2000. Reconfiguration of the neural network controlling multiple breathing patterns: eupnea, sighs and gasps [see comment]. Nat Neurosci 3, 600-607.

Lin, C.W., Chang, Y.C., Chen, W.S., Chang, K., Chang, H.Y., Wang, T.G., 2012. Prolonged swallowing time in dysphagic Parkinsonism patients with aspiration pneumonia. Arch Phys Med Rehabil 93, 2080-2084.
Liu, X., Sood, S., Liu, H., Horner, R.L., 2005. Opposing muscarinic and nicotinic modulation of hypoglossal motor output to genioglossus muscle in rats in vivo. The Journal of physiology 565, 965-980.
Llinas, R.R., 2013. The olivo-cerebellar system: a key to understanding the functional significance of intrinsic oscillatory brain properties. Front Neural Circuits 7, 96.
Loch, W.E., Loch, W.E., Reiriz, H.M., Loch, M.H., 1982. Swallow apnea--rhinomanometric manifestation and classification. Rhinology 20, 179-191.
Long, S., Duffin, J., 1986. The neuronal determinants of respiratory rhythm. Prog Neurobiol 27, 101-182.
Lovick, T.A., Parry, D.M., Stezhka, V.V., Lumb, B.M., 2000. Serotonergic transmission in the periaqueductal gray matter in relation to aversive behaviour: morphological evidence for direct modulatory effects on identified output neurons. Neuroscience 95, 763-772.
Lu, I.J., Lee, K.Z., Lin, J.T., Hwang, J.C., 2005. Capsaicin administration inhibits the abducent branch but excites the thyroarytenoid branch of the recurrent laryngeal nerves in the rat. J Appl Physiol (1985) 98, 1646-1652.
Ludlow, C.L., 2005. Central nervous system control of the laryngeal muscles in humans. Respir Physiol Neurobiol 147, 205-222.
Luo, P., Zhang, J., Yang, R., Pendlebury, W., 2006. Neuronal circuitry and synaptic organization of trigeminal proprioceptive afferents mediating tongue movement and jaw-tongue coordination via hypoglossal premotor neurons. The European journal of neuroscience 23, 3269-3283.
Madisen, L., Mao, T., Koch, H., Zhuo, J.M., Berenyi, A., Fujisawa, S., Hsu, Y.W., Garcia, A.J., 3rd, Gu, X., Zanella, S., Kidney, J., Gu, H., Mao, Y., Hooks, B.M., Boyden, E.S., Buzsaki, G., Ramirez, J.M., Jones, A.R., Svoboda, K., Han, X., Turner, E.E., Zeng, H., 2012. A toolbox of Cre-dependent optogenetic transgenic mice for light-induced activation and silencing. Nat Neurosci 15, 793-802.
Madisen, L., Zwingman, T.A., Sunkin, S.M., Oh, S.W., Zariwala, H.A., Gu, H., Ng, L.L., Palmiter, R.D., Hawrylycz, M.J., Jones, A.R., Lein, E.S., Zeng, H., 2010. A robust and high-throughput Cre reporting and characterization system for the whole mouse brain. Nature neuroscience 13, 133-140.
Malhotra, A., Fogel, R.B., Edwards, J.K., Shea, S.A., White, D.P., 2000. Local mechanisms drive genioglossus activation in obstructive sleep apnea. American journal of respiratory and critical care medicine 161, 1746-1749.
Malhotra, A., White, D.P., 2002. Obstructive sleep apnoea. Lancet 360, 237-245.
Mann, E.A., Burnett, T., Cornell, S., Ludlow, C.L., 2002. The effect of neuromuscular stimulation of the genioglossus on the hypopharyngeal airway. The Laryngoscope 112, 351-356.
Marchenko, V., Koizumi, H., Mosher, B., Koshiya, N., Tariq, M.F., Bezdudnaya, T.G., Zhang, R., Molkov, Y.I., Rybak, I.A., Smith, J.C., 2016. Perturbations of Respiratory Rhythm and Pattern by Disrupting Synaptic Inhibition within Pre-Botzinger and Botzinger Complexes. eNeuro 3.
Martin-Harris, B., Brodsky, M.B., Michel, Y., Ford, C.L., Walters, B., Heffner, J., 2005. Breathing and swallowing dynamics across the adult lifespan. Arch Otolaryngol Head Neck Surg 131, 762-770.

Matsumoto, S., Takeda, M., Saiki, C., Takahashi, T., Ojima, K., 1997. Effects of vagal and carotid chemoreceptor afferents on the frequency and pattern of spontaneous augmented breaths in rabbits. Lung 175, 175-186.
McCrea, D.A., Rybak, I.A., 2008. Organization of mammalian locomotor rhythm and pattern generation. Brain Res Rev 57, 134-146.
McCulloch, T.M., Perlman, A.L., Palmer, P.M., Van Daele, D.J., 1996. Laryngeal activity during swallow, phonation, and the Valsalva maneuver: an electromyographic analysis. Laryngoscope 106, 1351-1358.
McFarland, D.H., Martin-Harris, B., Fortin, A.J., Humphries, K., Hill, E., Armeson, K., 2016. Respiratory-swallowing coordination in normal subjects: Lung volume at swallowing initiation. Respir Physiol Neurobiol 234, 89-96.
McNamara, F., Wulbrand, H., Thach, B.T., 1998. Characteristics of the infant arousal response. Journal of applied physiology 85, 2314-2321.
Meier, M., Andreas, S., 2012. [Mechanisms of cardiovascular co-morbidity in patients with obstructive sleep apnoea syndrome]. Pneumologie 66, 650-657.
Mellen, N.M., Mishra, D., 2010. Functional anatomical evidence for respiratory rhythmogenic function of endogenous bursters in rat medulla. J Neurosci 30, 8383-8392.
Mellen, N.M., Thoby-Brisson, M., 2012. Respiratory circuits: development, function and models. Curr Opin Neurobiol 22, 676-685.
Merrill, E.G., 1981. Where are the real respiratory neurons? Fed Proc 40, 2389-2394.
Merrill, E.G., Fedorko, L., 1984. Monosynaptic inhibition of phrenic motoneurons: a long descending projection from Botzinger neurons. J Neurosci 4, 2350-2353.
Mezzanotte, W.S., Tangel, D.J., White, D.P., 1992. Waking genioglossal electromyogram in sleep apnea patients versus normal controls (a neuromuscular compensatory mechanism). The Journal of clinical investigation 89, 1571-1579.
Miller, A.J., 1982. Deglutition. Physiol Rev 62, 129-184.
Moraes, D.J., Machado, B.H., 2015. Electrophysiological properties of laryngeal motoneurones in rats submitted to chronic intermittent hypoxia. J Physiol 593, 619-634.
Morgado-Valle, C., Baca, S.M., Feldman, J.L., 2010. Glycinergic pacemaker neurons in preBotzinger complex of neonatal mouse. J Neurosci 30, 3634-3639.
Morrison, J.L., Sood, S., Liu, H., Park, E., Liu, X., Nolan, P., Horner, R.L., 2003a. Role of inhibitory amino acids in control of hypoglossal motor outflow to genioglossus muscle in naturally sleeping rats. The Journal of physiology 552, 975-991.
Morrison, J.L., Sood, S., Liu, H., Park, E., Nolan, P., Horner, R.L., 2003b. GABAA receptor antagonism at the hypoglossal motor nucleus increases genioglossus muscle activity in NREM but not REM sleep. The Journal of physiology 548, 569-583.
Morschel, M., Dutschmann, M., 2009. Pontine respiratory activity involved in inspiratory/expiratory phase transition. Philos Trans R Soc Lond B Biol Sci 364, 2517-2526.
Muere, C., Neumueller, S., Olesiak, S., Miller, J., Langer, T., Hodges, M.R., Pan, L., Forster, H.V., 2015. Combined unilateral blockade of cholinergic, peptidergic, and serotonergic receptors in the ventral respiratory column does not affect breathing in awake or sleeping goats. J Appl Physiol (1985) 119, 308-320.
Narkiewicz, K., van de Borne, P.J., Montano, N., Dyken, M.E., Phillips, B.G., Somers, V.K., 1998. Contribution of tonic chemoreflex activation to sympathetic activity and blood pressure in patients with obstructive sleep apnea. Circulation 97, 943-945.

Nelson, S.B., Sugino, K., Hempel, C.M., 2006. The problem of neuronal cell types: a physiological genomics approach. Trends Neurosci 29, 339-345.
Nieto-Posadas, A., Flores-Martinez, E., Lorea-Hernandez, J.J., Rivera-Angulo, A.J., Perez-Ortega, J.E., Bargas, J., Pena-Ortega, F., 2014. Change in network connectivity during fictive-gasping generation in hypoxia: prevention by a metabolic intermediate. Front Physiol 5, 265.
Nottebohm, F., Stokes, T.M., Leonard, C.M., 1976. Central control of song in the canary, Serinus canarius. J Comp Neurol 165, 457-486.
O'Connor, R., Segers, L.S., Morris, K.F., Nuding, S.C., Pitts, T., Bolser, D.C., Davenport, P.W., Lindsey, B.G., 2012. A joint computational respiratory neural network-biomechanical model for breathing and airway defensive behaviors. Front Physiol 3, 264.
O'Driscoll, D.M., Foster, A.M., Ng, M.L., Yang, J.S., Bashir, F., Wong, S., Nixon, G.M., Davey, M.J., Anderson, V., Walker, A.M., Trinder, J., Horne, R.S., 2009. Central apnoeas have significant effects on blood pressure and heart rate in children. Journal of sleep research 18, 415-421.
Oku, Y., Dick, T.E., 1992. Phase resetting of the respiratory cycle before and after unilateral pontine lesion in cat. J Appl Physiol (1985) 72, 721-730.
Oliven, A., Carmi, N., Coleman, R., Odeh, M., Silbermann, M., 2001. Age-related changes in upper airway muscles morphological and oxidative properties. Experimental gerontology 36, 1673-1686.
Onimaru, H., Arata, A., Homma, I., 1989. Firing properties of respiratory rhythm generating neurons in the absence of synaptic transmission in rat medulla in vitro. Exp Brain Res 76, 530-536.
Onimaru, H., Homma, I., 2008. Two modes of respiratory rhythm generation in the newborn rat brainstem-spinal cord preparation. Adv Exp Med Biol 605, 104-108.
Onimaru, H., Ikeda, K., Kawakami, K., 2007. Defective interaction between dual oscillators for respiratory rhythm generation in Na+,K+-ATPase {alpha}2 subunit-deficient mice. J Physiol 584, 271-284.
Onimaru, H., Ikeda, K., Kawakami, K., 2008. CO2-sensitive preinspiratory neurons of the parafacial respiratory group express Phox2b in the neonatal rat. J Neurosci 28, 12845-12850.
Orem, J., Trotter, R.H., 1993. Medullary respiratory neuronal activity during augmented breaths in intact unanesthetized cats. Journal of applied physiology 74, 761-769.
Otsuka, R., Ono, T., Ishiwata, Y., Kuroda, T., 2000. Respiratory-related genioglossus electromyographic activity in response to head rotation and changes in body position. The Angle orthodontist 70, 63-69.
Pagliardini, S., Janczewski, W.A., Tan, W., Dickson, C.T., Deisseroth, K., Feldman, J.L., 2011. Active expiration induced by excitation of ventral medulla in adult anesthetized rats. J Neurosci 31, 2895-2905.
Pagliardini, S., Ren, J., Greer, J.J., 2003. Ontogeny of the pre-Botzinger complex in perinatal rats. J Neurosci 23, 9575-9584.
Parkis, M.A., Bayliss, D.A., Berger, A.J., 1995. Actions of norepinephrine on rat hypoglossal motoneurons. Journal of neurophysiology 74, 1911-1919.
Paton, J.F., 1996. A working heart-brainstem preparation of the mouse. J Neurosci Methods 65, 63-68.

Paton, J.F., Li, Y.W., Kasparov, S., 1999. Reflex response and convergence of pharyngoesophageal and peripheral chemoreceptors in the nucleus of the solitary tract. Neuroscience 93, 143-154.
Paton, J.F., Ramirez, J.M., Richter, D.W., 1994. Functionally intact in vitro preparation generating respiratory activity in neonatal and mature mammals. Pflugers Arch 428, 250-260.
Pawar, A., Peng, Y.J., Jacono, F.J., Prabhakar, N.R., 2008. Comparative analysis of neonatal and adult rat carotid body responses to chronic intermittent hypoxia. Journal of applied physiology 104, 1287-1294.
Peever, J.H., Shen, L., Duffin, J., 2002. Respiratory pre-motor control of hypoglossal motoneurons in the rat. Neuroscience 110, 711-722.
Pena, F., 2008. Contribution of pacemaker neurons to respiratory rhythms generation in vitro. Adv Exp Med Biol 605, 114-118.
Pena, F., Aguileta, M.A., 2007. Effects of riluzole and flufenamic acid on eupnea and gasping of neonatal mice in vivo. Neurosci Lett 415, 288-293.
Pena, F., Meza-Andrade, R., Paez-Zayas, V., Gonzalez-Marin, M.C., 2008. Gasping generation in developing Swiss-Webster mice in vitro and in vivo. Neurochemical research 33, 1492-1500.
Pena, F., Parkis, M.A., Tryba, A.K., Ramirez, J.M., 2004. Differential contribution of pacemaker properties to the generation of respiratory rhythms during normoxia and hypoxia. Neuron 43, 105-117.
Pena, F., Ramirez, J.M., 2002. Endogenous activation of serotonin-2A receptors is required for respiratory rhythm generation in vitro. The Journal of neuroscience : the official journal of the Society for Neuroscience 22, 11055-11064.
Pena, F., Ramirez, J.M., 2004. Substance P-mediated modulation of pacemaker properties in the mammalian respiratory network. J Neurosci 24, 7549-7556.
Peng, Y.J., Nanduri, J., Yuan, G., Wang, N., Deneris, E., Pendyala, S., Natarajan, V., Kumar, G.K., Prabhakar, N.R., 2009. NADPH oxidase is required for the sensory plasticity of the carotid body by chronic intermittent hypoxia. The Journal of neuroscience : the official journal of the Society for Neuroscience 29, 4903-4910.
Peng, Y.J., Overholt, J.L., Kline, D., Kumar, G.K., Prabhakar, N.R., 2003. Induction of sensory long-term facilitation in the carotid body by intermittent hypoxia: implications for recurrent apneas. Proceedings of the National Academy of Sciences of the United States of America 100, 10073-10078.
Peng, Y.J., Prabhakar, N.R., 2004. Effect of two paradigms of chronic intermittent hypoxia on carotid body sensory activity. Journal of applied physiology 96, 1236-1242; discussion 1196.
Peng, Y.J., Yuan, G., Ramakrishnan, D., Sharma, S.D., Bosch-Marce, M., Kumar, G.K., Semenza, G.L., Prabhakar, N.R., 2006. Heterozygous HIF-1alpha deficiency impairs carotid body-mediated systemic responses and reactive oxygen species generation in mice exposed to intermittent hypoxia. The Journal of physiology 577, 705-716.
Peppard, P.E., Young, T., Palta, M., Dempsey, J., Skatrud, J., 2000a. Longitudinal study of moderate weight change and sleep-disordered breathing. JAMA : the journal of the American Medical Association 284, 3015-3021.

Peppard, P.E., Young, T., Palta, M., Skatrud, J., 2000b. Prospective study of the association between sleep-disordered breathing and hypertension. The New England journal of medicine 342, 1378-1384.
Perez-Padilla, R., West, P., Kryger, M.H., 1983. Sighs during sleep in adult humans. Sleep 6, 234-243.
Pettersen, V., Westgaard, R.H., 2005. The activity patterns of neck muscles in professional classical singing. J Voice 19, 238-251.
Phillips, B., 2005. Sleep-disordered breathing and cardiovascular disease. Sleep medicine reviews 9, 131-140.
Picardo, M.C., Weragalaarachchi, K.T., Akins, V.T., Del Negro, C.A., 2013. Physiological and morphological properties of Dbx1-derived respiratory neurons in the pre-Botzinger complex of neonatal mice. J Physiol 591, 2687-2703.
Pitts, T., Bolser, D., Rosenbek, J., Troche, M., Okun, M.S., Sapienza, C., 2009. Impact of expiratory muscle strength training on voluntary cough and swallow function in Parkinson disease. Chest 135, 1301-1308.
Pitts, T., Morris, K., Lindsey, B., Davenport, P., Poliacek, I., Bolser, D., 2012. Co-ordination of cough and swallow in vivo and in silico. Exp Physiol 97, 469-473.
Pitts, T., Rose, M.J., Mortensen, A.N., Poliacek, I., Sapienza, C.M., Lindsey, B.G., Morris, K.F., Davenport, P.W., Bolser, D.C., 2013. Coordination of cough and swallow: a meta-behavioral response to aspiration. Respir Physiol Neurobiol 189, 543-551.
Pitts, T., Troche, M., Mann, G., Rosenbek, J., Okun, M.S., Sapienza, C., 2010. Using voluntary cough to detect penetration and aspiration during oropharyngeal swallowing in patients with Parkinson disease. Chest 138, 1426-1431.
Porges, W.L., Hennessy, E.J., Quail, A.W., Cottee, D.B., Moore, P.G., McIlveen, S.A., Parsons, G.H., White, S.W., 2000. Heart-lung interactions: the sigh and autonomic control in the bronchial and coronary circulations. Clinical and experimental pharmacology & physiology 27, 1022-1027.
Prabhakar, N.R., 2001. Oxygen sensing during intermittent hypoxia: cellular and molecular mechanisms. Journal of applied physiology 90, 1986-1994.
Prabhat, K.C., Goyal, L., Bey, A., Maheshwari, S., 2012. Recent advances in the management of obstructive sleep apnea: The dental perspective. Journal of natural science, biology, and medicine 3, 113-117.
Praud, J.P., D'Allest, A.M., Delaperche, M.F., Bobin, S., Gaultier, C., 1988. Diaphragmatic and genioglossus electromyographic activity at the onset and at the end of obstructive apnea in children with obstructive sleep apnea syndrome. Pediatric research 23, 1-4.
Ptak, K., Yamanishi, T., Aungst, J., Milescu, L.S., Zhang, R., Richerson, G.B., Smith, J.C., 2009. Raphe neurons stimulate respiratory circuit activity by multiple mechanisms via endogenously released serotonin and substance P. The Journal of neuroscience : the official journal of the Society for Neuroscience 29, 3720-3737.
Purvis, L.K., Butera, R.J., 2005. Ionic current model of a hypoglossal motoneuron. J Neurophysiol 93, 723-733.
Purvis, L.K., Smith, J.C., Koizumi, H., Butera, R.J., 2007. Intrinsic bursters increase the robustness of rhythm generation in an excitatory network. J Neurophysiol 97, 1515-1526.
Qian, Z.B., Qi, Y., Wu, Z.H., 2010. [Histamine H1 receptors modulate the discharge activities of inspiratory neurons in the medial region of neonatal rat nucleus retrofacialis ex vivo]. Nan Fang Yi Ke Da Xue Xue Bao 30, 54-56.

Quintana, A., Zanella, S., Koch, H., Kruse, S.E., Lee, D., Ramirez, J.M., Palmiter, R.D., 2012. Fatal breathing dysfunction in a mouse model of Leigh syndrome. The Journal of clinical investigation 122, 2359-2368.
Radulovacki, M., Pavlovic, S., Rakic, A., Janelidze, M., Shermulis, L., Carley, D.W., 2001. Riluzole suppresses post-sigh, but not spontaneous apnoeas during sleep in rats. The Journal of pharmacy and pharmacology 53, 1555-1559.
Raghuraman, S., Garcia, A.J., Anderson, T.M., Twede, V.D., Curtice, K.J., Chase, K., Ramirez, J.M., Olivera, B.M., Teichert, R.W., 2014. Defining modulatory inputs into CNS neuronal subclasses by functional pharmacological profiling. Proc Natl Acad Sci U S A 111, 6449-6454.
Ramirez, J.M., Dashevskiy, T., Marlin, I.A., Baertsch, N., 2016. Microcircuits in respiratory rhythm generation: commonalities with other rhythm generating networks and evolutionary perspectives. Curr Opin Neurobiol 41, 53-61.
Ramirez, J.M., Doi, A., Garcia, A.J., 3rd, Elsen, F.P., Koch, H., Wei, A.D., 2012. The cellular building blocks of breathing. Compr Physiol 2, 2683-2731.
Ramirez, J.M., Garcia, A., 3rd, 2007. Point: Medullary pacemaker neurons are essential for both eupnea and gasping in mammals. J Appl Physiol (1985) 103, 717-718; discussion 722.
Ramirez, J.M., Garcia, A.J., 3rd, Anderson, T.M., Koschnitzky, J.E., Peng, Y.J., Kumar, G.K., Prabhakar, N.R., 2013a. Central and peripheral factors contributing to obstructive sleep apneas. Respir Physiol Neurobiol 189, 344-353.
Ramirez, J.M., Koch, H., Garcia, A.J., 3rd, Doi, A., Zanella, S., 2011. The role of spiking and bursting pacemakers in the neuronal control of breathing. J Biol Phys 37, 241-261.
Ramirez, J.M., Quellmalz, U.J., Richter, D.W., 1996. Postnatal changes in the mammalian respiratory network as revealed by the transverse brainstem slice of mice. J Physiol 491 (Pt 3), 799-812.
Ramirez, J.M., Quellmalz, U.J., Wilken, B., Richter, D.W., 1998a. The hypoxic response of neurones within the in vitro mammalian respiratory network. J Physiol 507 (Pt 2), 571-582.
Ramirez, J.M., Richter, D.W., 1996. The neuronal mechanisms of respiratory rhythm generation. Curr Opin Neurobiol 6, 817-825.
Ramirez, J.M., Schwarzacher, S.W., Pierrefiche, O., Olivera, B.M., Richter, D.W., 1998b. Selective lesioning of the cat pre-Botzinger complex in vivo eliminates breathing but not gasping. The Journal of physiology 507 (Pt 3), 895-907.
Ramirez, J.M., Tryba, A.K., Pena, F., 2004. Pacemaker neurons and neuronal networks: an integrative view. Curr Opin Neurobiol 14, 665-674.
Ramirez, J.M., Viemari, J.C., 2005. Determinants of inspiratory activity. Respiratory physiology & neurobiology 147, 145-157.
Ramirez, J.M., Ward, C.S., Neul, J.L., 2013b. Breathing challenges in Rett syndrome: lessons learned from humans and animal models. Respir Physiol Neurobiol 189, 280-287.
Randerath, W.J., 2007. [Automatic positive airway pressure in titration and treatment of the obstructive sleep apnea syndrome]. Pneumologie 61, 228-232.
Rees, K., Spence, D.P., Earis, J.E., Calverley, P.M., 1995. Arousal responses from apneic events during non-rapid-eye-movement sleep. American journal of respiratory and critical care medicine 152, 1016-1021.

Rekling, J.C., Shao, X.M., Feldman, J.L., 2000. Electrical coupling and excitatory synaptic transmission between rhythmogenic respiratory neurons in the preBotzinger complex. J Neurosci 20, RC113.
Remmers, J.E., deGroot, W.J., Sauerland, E.K., Anch, A.M., 1978. Pathogenesis of upper airway occlusion during sleep. Journal of applied physiology 44, 931-938.
Ren, J., Greer, J.J., 2006. Modulation of respiratory rhythmogenesis by chloride-mediated conductances during the perinatal period. J Neurosci 26, 3721-3730.
Rey, S., Del Rio, R., Alcayaga, J., Iturriaga, R., 2004. Chronic intermittent hypoxia enhances cat chemosensory and ventilatory responses to hypoxia. The Journal of physiology 560, 577-586.
Reynolds, L.B., Jr., 1962. Characteristics of an inspiration-augmenting reflex in anesthetized cats. Journal of applied physiology 17, 683-688.
Richter, A., Heyne, K., Sagebiel, J., Weber, M., 1986a. [Respiratory emergency in the newborn infant: extreme laryngotracheo-esophageal cleft (esophagotrachea)]. Monatsschr Kinderheilkd 134, 874-877.
Richter, D.W., 1982. Generation and maintenance of the respiratory rhythm. J Exp Biol 100, 93-107.
Richter, D.W., Ballanyi, K., Schwarzacher, S., 1992. Mechanisms of respiratory rhythm generation. Curr Opin Neurobiol 2, 788-793.
Richter, D.W., Jordan, D., Ballantyne, D., Meesmann, M., Spyer, K.M., 1986b. Presynaptic depolarization in myelinated vagal afferent fibres terminating in the nucleus of the tractus solitarius in the cat. Pflugers Arch 406, 12-19.
Richter, D.W., Smith, J.C., 2014. Respiratory rhythm generation in vivo. Physiology (Bethesda) 29, 58-71.
Robinson, D.M., Peebles, K.C., Kwok, H., Adams, B.M., Clarke, L.L., Woollard, G.A., Funk, G.D., 2002. Prenatal nicotine exposure increases apnoea and reduces nicotinic potentiation of hypoglossal inspiratory output in mice. The Journal of physiology 538, 957-973.
Robinson, I., Reddy, A.B., 2014. Molecular mechanisms of the circadian clockwork in mammals. FEBS Lett 588, 2477-2483.
Rosenwasser, A.M., Turek, F.W., 2015. Neurobiology of Circadian Rhythm Regulation. Sleep Med Clin 10, 403-412.
Ruangkittisakul, A., Kottick, A., Picardo, M.C., Ballanyi, K., Del Negro, C.A., 2014. Identification of the pre-Botzinger complex inspiratory center in calibrated "sandwich" slices from newborn mice with fluorescent Dbx1 interneurons. Physiol Rep 2.
Ruangkittisakul, A., Panaitescu, B., Ballanyi, K., 2011. K(+) and Ca(2)(+) dependence of inspiratory-related rhythm in novel "calibrated" mouse brainstem slices. Respir Physiol Neurobiol 175, 37-48.
Ruangkittisakul, A., Schwarzacher, S.W., Secchia, L., Poon, B.Y., Ma, Y., Funk, G.D., Ballanyi, K., 2006. High sensitivity to neuromodulator-activated signaling pathways at physiological [K+] of confocally imaged respiratory center neurons in on-line-calibrated newborn rat brainstem slices. J Neurosci 26, 11870-11880.
Rubin, J.E., Hayes, J.A., Mendenhall, J.L., Del Negro, C.A., 2009. Calcium-activated nonspecific cation current and synaptic depression promote network-dependent burst oscillations. Proc Natl Acad Sci U S A 106, 2939-2944.

Rukhadze, I., Fenik, V.B., Benincasa, K.E., Price, A., Kubin, L., 2010. Chronic intermittent hypoxia alters density of aminergic terminals and receptors in the hypoglossal motor nucleus. American journal of respiratory and critical care medicine 182, 1321-1329.
Rybak, I.A., Ptak, K., Shevtsova, N.A., McCrimmon, D.R., 2003. Sodium currents in neurons from the rostroventrolateral medulla of the rat. J Neurophysiol 90, 1635-1642.
Rybak, I.A., She{Rybak, v., N. A., Paton, J.F., Dick, T.E., St-John, W.M., Morschel, M., Dutschmann, M., 2004. Modeling the ponto-medullary respiratory network. Respir Physiol Neurobiol 143, 307-319.
Saboisky, J.P., Butler, J.E., McKenzie, D.K., Gorman, R.B., Trinder, J.A., White, D.P., Gandevia, S.C., 2007. Neural drive to human genioglossus in obstructive sleep apnoea. The Journal of physiology 585, 135-146.
Saboisky, J.P., Jordan, A.S., Eckert, D.J., White, D.P., Trinder, J.A., Nicholas, C.L., Gautam, S., Malhotra, A., 2010. Recruitment and rate-coding strategies of the human genioglossus muscle. Journal of applied physiology 109, 1939-1949.
Saboisky, J.P., Stashuk, D.W., Hamilton-Wright, A., Carusona, A.L., Campana, L.M., Trinder, J., Eckert, D.J., Jordan, A.S., McSharry, D.G., White, D.P., Nandedkar, S., David, W.S., Malhotra, A., 2012. Neurogenic changes in the upper airway of patients with obstructive sleep apnea. American journal of respiratory and critical care medicine 185, 322-329.
Saito, Y., 2009. Reflections on the brainstem dysfunction in neurologically disabled children. Brain & development 31, 529-536.
Saito, Y., Ezure, K., Tanaka, I., Osawa, M., 2003. Activity of neurons in ventrolateral respiratory groups during swallowing in decerebrate rats. Brain Dev 25, 338-345.
Sangkatumvong, S., Khoo, M.C., Kato, R., Detterich, J.A., Bush, A., Keens, T.G., Meiselman, H.J., Wood, J.C., Coates, T.D., 2011. Peripheral vasoconstriction and abnormal parasympathetic response to sighs and transient hypoxia in sickle cell disease. American journal of respiratory and critical care medicine 184, 474-481.
Saponjic, J., Radulovacki, M., Carley, D.W., 2007. Monoaminergic system lesions increase post-sigh respiratory pattern disturbance during sleep in rats. Physiology & behavior 90, 1-10.
Sauerland, E.K., Harper, R.M., 1976. The human tongue during sleep: electromyographic activity of the genioglossus muscle. Experimental neurology 51, 160-170.
Schmidt, M.F., McLean, J., Goller, F., 2012. Breathing and vocal control: the respiratory system as both a driver and a target of telencephalic vocal motor circuits in songbirds. Exp Physiol 97, 455-461.
Schwarzacher, S.W., Rub, U., Deller, T., 2011. Neuroanatomical characteristics of the human pre-Botzinger complex and its involvement in neurodegenerative brainstem diseases. Brain 134, 24-35.
Schwenke, D.O., Cragg, P.A., 2000. Carotid bodies and the sigh reflex in the conscious and anaesthetised guinea-pig. Advances in experimental medicine and biology 475, 801-813.
Sebe, J.Y., Berger, A.J., 2008. Inspiratory-phase short time scale synchrony in the brainstem slice is generated downstream of the pre-Botzinger complex. Neuroscience 153, 1390-1401.
Segers, L.S., Nuding, S.C., Dick, T.E., Shannon, R., Baekey, D.M., Solomon, I.C., Morris, K.F., Lindsey, B.G., 2008. Functional connectivity in the pontomedullary respiratory network. J Neurophysiol 100, 1749-1769.

Segers, L.S., Shannon, R., Lindsey, B.G., 1985. Interactions between rostral pontine and ventral medullary respiratory neurons. J Neurophysiol 54, 318-334.
Sekizawa, K., Ujiie, Y., Itabashi, S., Sasaki, H., Takishima, T., 1990. Lack of cough reflex in aspiration pneumonia. Lancet 335, 1228-1229.
Selvaratnam, S.R., Parkis, M.A., Funk, G.D., 1998. Developmental modulation of mouse hypoglossal nerve inspiratory output in vitro by noradrenergic receptor agonists. Brain research 805, 104-115.
Shaker, R., Dodds, W.J., Dantas, R.O., Hogan, W.J., Arndorfer, R.C., 1990. Coordination of deglutitive glottic closure with oropharyngeal swallowing. Gastroenterology 98, 1478-1484.
Shaker, R., Li, Q., Ren, J., Townsend, W.F., Dodds, W.J., Martin, B.J., Kern, M.K., Rynders, A., 1992. Coordination of deglutition and phases of respiration: effect of aging, tachypnea, bolus volume, and chronic obstructive pulmonary disease. Am J Physiol 263, G750-755.
Shannon, R., Baekey, D.M., Morris, K.F., Li, Z., Lindsey, B.G., 2000. Functional connectivity among ventrolateral medullary respiratory neurones and responses during fictive cough in the cat. J Physiol 525 Pt 1, 207-224.
Shannon, R., Baekey, D.M., Morris, K.F., Lindsey, B.G., 1998. Ventrolateral medullary respiratory network and a model of cough motor pattern generation. J Appl Physiol (1985) 84, 2020-2035.
Shao, X.M., Feldman, J.L., 1997. Respiratory rhythm generation and synaptic inhibition of expiratory neurons in pre-Botzinger complex: differential roles of glycinergic and GABAergic neural transmission. J Neurophysiol 77, 1853-1860.
Shao, X.M., Feldman, J.L., 2009. Central cholinergic regulation of respiration: nicotinic receptors. Acta pharmacologica Sinica 30, 761-770.
Shea, S.A., Horner, R.L., Banner, N.R., McKenzie, E., Heaton, R., Yacoub, M.H., Guz, A., 1988. The effect of human heart-lung transplantation upon breathing at rest and during sleep. Respiration physiology 72, 131-149.
Shen, L., Li, Y.M., Duffin, J., 2003. Inhibitory connections among rostral medullary expiratory neurones detected with cross-correlation in the decerebrate rat. Pflugers Arch 446, 365-372.
Sher, A.E., Schechtman, K.B., Piccirillo, J.F., 1996. The efficacy of surgical modifications of the upper airway in adults with obstructive sleep apnea syndrome. Sleep 19, 156-177.
Shott, S.R., Cunningham, M.J., 1992. Apnea and the elongated uvula. International journal of pediatric otorhinolaryngology 24, 183-189.
Shu, W., Cho, J.Y., Jiang, Y., Zhang, M., Weisz, D., Elder, G.A., Schmeidler, J., De Gasperi, R., Sosa, M.A., Rabidou, D., Santucci, A.C., Perl, D., Morrisey, E., Buxbaum, J.D., 2005. Altered ultrasonic vocalization in mice with a disruption in the Foxp2 gene. Proc Natl Acad Sci U S A 102, 9643-9648.
Silva, J.N., Tanabe, F.M., Moreira, T.S., Takakura, A.C., 2016. Neuroanatomical and physiological evidence that the retrotrapezoid nucleus/parafacial region regulates expiration in adult rats. Respir Physiol Neurobiol 227, 9-22.
Smith Hammond, C.A., Goldstein, L.B., 2006. Cough and aspiration of food and liquids due to oral-pharyngeal dysphagia: ACCP evidence-based clinical practice guidelines. Chest 129, 154S-168S.

Smith Hammond, C.A., Goldstein, L.B., Horner, R.D., Ying, J., Gray, L., Gonzalez-Rothi, L., Bolser, D.C., 2009. Predicting aspiration in patients with ischemic stroke: comparison of clinical signs and aerodynamic measures of voluntary cough. Chest 135, 769-777.
Smith Hammond, C.A., Goldstein, L.B., Zajac, D.J., Gray, L., Davenport, P.W., Bolser, D.C., 2001. Assessment of aspiration risk in stroke patients with quantification of voluntary cough. Neurology 56, 502-506.
Smith, J.C., Abdala, A.P., Borgmann, A., Rybak, I.A., Paton, J.F., 2013a. Brainstem respiratory networks: building blocks and microcircuits. Trends Neurosci 36, 152-162.
Smith, J.C., Abdala, A.P., Koizumi, H., Rybak, I.A., Paton, J.F., 2007. Spatial and functional architecture of the mammalian brain stem respiratory network: a hierarchy of three oscillatory mechanisms. J Neurophysiol 98, 3370-3387.
Smith, J.C., Abdala, A.P., Rybak, I.A., Paton, J.F., 2009. Structural and functional architecture of respiratory networks in the mammalian brainstem. Philos Trans R Soc Lond B Biol Sci 364, 2577-2587.
Smith, J.C., Ellenberger, H.H., Ballanyi, K., Richter, D.W., Feldman, J.L., 1991. Pre-Botzinger complex: a brainstem region that may generate respiratory rhythm in mammals. Science 254, 726-729.
Smith, J.C., Feldman, J.L., 1987. In vitro brainstem-spinal cord preparations for study of motor systems for mammalian respiration and locomotion. J Neurosci Methods 21, 321-333.
Smith, M.L., Niedermaier, O.N., Hardy, S.M., Decker, M.J., Strohl, K.P., 1996. Role of hypoxemia in sleep apnea-induced sympathoexcitation. Journal of the autonomic nervous system 56, 184-190.
Smith, N.J., Hone, A.J., Memon, T., Bossi, S., Smith, T.E., McIntosh, J.M., Olivera, B.M., Teichert, R.W., 2013b. Comparative functional expression of nAChR subtypes in rodent DRG neurons. Front Cell Neurosci 7, 225.
Smotherman, M., Kobayasi, K., Ma, J., Zhang, S., Metzner, W., 2006. A mechanism for vocal-respiratory coupling in the mammalian parabrachial nucleus. J Neurosci 26, 4860-4869.
Soja, P.J., Lopez-Rodriguez, F., Morales, F.R., Chase, M.H., 1991. The postsynaptic inhibitory control of lumbar motoneurons during the atonia of active sleep: effect of strychnine on motoneuron properties. The Journal of neuroscience : the official journal of the Society for Neuroscience 11, 2804-2811.
Soja, P.J., Morales, F.R., Baranyi, A., Chase, M.H., 1987. Effect of inhibitory amino acid antagonists on IPSPs induced in lumbar motoneurons upon stimulation of the nucleus reticularis gigantocellularis during active sleep. Brain research 423, 353-358.
Sokoloff, A.J., 2000. Localization and contractile properties of intrinsic longitudinal motor units of the rat tongue. Journal of neurophysiology 84, 827-835.
Sood, S., Liu, X., Liu, H., Horner, R.L., 2007. Genioglossus muscle activity and serotonergic modulation of hypoglossal motor output in obese Zucker rats. Journal of applied physiology 102, 2240-2250.
Sood, S., Morrison, J.L., Liu, H., Horner, R.L., 2005. Role of endogenous serotonin in modulating genioglossus muscle activity in awake and sleeping rats. American journal of respiratory and critical care medicine 172, 1338-1347.
St John, W.M., 2009. Noeud vital for breathing in the brainstem: gasping--yes, eupnoea--doubtful. Philos Trans R Soc Lond B Biol Sci 364, 2625-2633.

Stein, P.S., 2005. Neuronal control of turtle hindlimb motor rhythms. Journal of comparative physiology. A, Neuroethology, sensory, neural, and behavioral physiology 191, 213-229.
Stettner, G.M., Huppke, P., Brendel, C., Richter, D.W., Gartner, J., Dutschmann, M., 2007. Breathing dysfunctions associated with impaired control of postinspiratory activity in Mecp2-/y knockout mice. J Physiol 579, 863-876.
Stettner, G.M., Huppke, P., Gartner, J., Richter, D.W., Dutschmann, M., 2008. Disturbances of breathing in Rett syndrome: results from patients and animal models. Adv Exp Med Biol 605, 503-507.
Subramanian, H.H., 2013. Descending control of the respiratory neuronal network by the midbrain periaqueductal grey in the rat in vivo. J Physiol 591, 109-122.
Subramanian, H.H., Balnave, R.J., Holstege, G., 2008. The midbrain periaqueductal gray control of respiration. J Neurosci 28, 12274-12283.
Subramanian, H.H., Holstege, G., 2009. The nucleus retroambiguus control of respiration. J Neurosci 29, 3824-3832.
Subramanian, H.H., Holstege, G., 2010. Periaqueductal gray control of breathing. Adv Exp Med Biol 669, 353-358.
Subramanian, H.H., Holstege, G., 2011. Midbrain and medullary control of postinspiratory activity of the crural and costal diaphragm in vivo. Journal of neurophysiology 105, 2852-2862.
Sugino, K., Hempel, C.M., Miller, M.N., Hattox, A.M., Shapiro, P., Wu, C., Huang, Z.J., Nelson, S.B., 2006. Molecular taxonomy of major neuronal classes in the adult mouse forebrain. Nat Neurosci 9, 99-107.
Sugiyama, Y., Shiba, K., Mukudai, S., Umezaki, T., Hisa, Y., 2014. Activity of respiratory neurons in the rostral medulla during vocalization, swallowing, and coughing in guinea pigs. Neurosci Res 80, 17-31.
Susarla, S.M., Thomas, R.J., Abramson, Z.R., Kaban, L.B., 2010. Biomechanics of the upper airway: Changing concepts in the pathogenesis of obstructive sleep apnea. International journal of oral and maxillofacial surgery 39, 1149-1159.
Takeda, R., Remmers, J.E., Baker, J.P., Madden, K.P., Farber, J.P., 1986. Postsynaptic potentials of bulbar respiratory neurons of the turtle. Respiration physiology 64, 149-160.
Takeda, S., Eriksson, L.I., Yamamoto, Y., Joensen, H., Onimaru, H., Lindahl, S.G., 2001. Opioid action on respiratory neuron activity of the isolated respiratory network in newborn rats. Anesthesiology 95, 740-749.
Takemoto, H., 2001. Morphological analyses of the human tongue musculature for three-dimensional modeling. Journal of speech, language, and hearing research : JSLHR 44, 95-107.
Tan, W., Janczewski, W.A., Yang, P., Shao, X.M., Callaway, E.M., Feldman, J.L., 2008. Silencing preBotzinger complex somatostatin-expressing neurons induces persistent apnea in awake rat. Nat Neurosci 11, 538-540.
Tan, W., Pagliardini, S., Yang, P., Janczewski, W.A., Feldman, J.L., 2010. Projections of preBotzinger complex neurons in adult rats. J Comp Neurol 518, 1862-1878.
Tanaka, I., Ezure, K., Kondo, M., 2003. Distribution of glycine transporter 2 mRNA-containing neurons in relation to glutamic acid decarboxylase mRNA-containing neurons in rat medulla. Neurosci Res 47, 139-151.

Teichert, R.W., Memon, T., Aman, J.W., Olivera, B.M., 2014. Using constellation pharmacology to define comprehensively a somatosensory neuronal subclass. Proc Natl Acad Sci U S A 111, 2319-2324.
Teichert, R.W., Raghuraman, S., Memon, T., Cox, J.L., Foulkes, T., Rivier, J.E., Olivera, B.M., 2012a. Characterization of two neuronal subclasses through constellation pharmacology. Proc Natl Acad Sci U S A 109, 12758-12763.
Teichert, R.W., Schmidt, E.W., Olivera, B.M., 2015. Constellation pharmacology: a new paradigm for drug discovery. Annu Rev Pharmacol Toxicol 55, 573-589.
Teichert, R.W., Smith, N.J., Raghuraman, S., Yoshikami, D., Light, A.R., Olivera, B.M., 2012b. Functional profiling of neurons through cellular neuropharmacology. Proc Natl Acad Sci U S A 109, 1388-1395.
Telgkamp, P., Cao, Y.Q., Basbaum, A.I., Ramirez, J.M., 2002. Long-term deprivation of substance P in PPT-A mutant mice alters the anoxic response of the isolated respiratory network. Journal of neurophysiology 88, 206-213.
Thoby-Brisson, M., Karlen, M., Wu, N., Charnay, P., Champagnat, J., Fortin, G., 2009. Genetic identification of an embryonic parafacial oscillator coupling to the preBotzinger complex. Nat Neurosci 12, 1028-1035.
Thoby-Brisson, M., Ramirez, J.M., 2001. Identification of two types of inspiratory pacemaker neurons in the isolated respiratory neural network of mice. J Neurophysiol 86, 104-112.
Thomas, R.J., Terzano, M.G., Parrino, L., Weiss, J.W., 2004. Obstructive sleep-disordered breathing with a dominant cyclic alternating pattern--a recognizable polysomnographic variant with practical clinical implications. Sleep 27, 229-234.
Tian, G.F., Peever, J.H., Duffin, J., 1999. Botzinger-complex, bulbospinal expiratory neurones monosynaptically inhibit ventral-group respiratory neurones in the decerebrate rat. Exp Brain Res 124, 173-180.
Ting, J.T., Daigle, T.L., Chen, Q., Feng, G., 2014. Acute brain slice methods for adult and aging animals: application of targeted patch clamp analysis and optogenetics. Methods Mol Biol 1183, 221-242.
Troche, M.S., Brandimore, A.E., Godoy, J., Hegland, K.W., 2014a. A framework for understanding shared substrates of airway protection. J Appl Oral Sci 22, 251-260.
Troche, M.S., Brandimore, A.E., Okun, M.S., Davenport, P.W., Hegland, K.W., 2014b. Decreased cough sensitivity and aspiration in Parkinson disease. Chest 146, 1294-1299.
Troche, M.S., Huebner, I., Rosenbek, J.C., Okun, M.S., Sapienza, C.M., 2011. Respiratory-swallowing coordination and swallowing safety in patients with Parkinson's disease. Dysphagia 26, 218-224.
Tryba, A.K., Pena, F., Lieske, S.P., Viemari, J.C., Thoby-Brisson, M., Ramirez, J.M., 2008. Differential modulation of neural network and pacemaker activity underlying eupnea and sigh-breathing activities. Journal of neurophysiology 99, 2114-2125.
Tryba, A.K., Pena, F., Ramirez, J.M., 2003. Stabilization of bursting in respiratory pacemaker neurons. J Neurosci 23, 3538-3546.
Tryba, A.K., Pena, F., Ramirez, J.M., 2006. Gasping activity in vitro: a rhythm dependent on 5-HT2A receptors. The Journal of neuroscience : the official journal of the Society for Neuroscience 26, 2623-2634.
Tryba, A.K., Ramirez, J.M., 2004. Background sodium current stabilizes bursting in respiratory pacemaker neurons. J Neurobiol 60, 481-489.

Tuck, S.A., Dort, J.C., Remmers, J.E., 2001. Braking of expiratory airflow in obese pigs during wakefulness and sleep. Respir Physiol 128, 241-245.
Tuck, S.A., Remmers, J.E., 1998. Methods of assessing respiratory impedance during flow limited and non-flow limited inspirations. Adv Exp Med Biol 450, 119-126.
Tuomilehto, H., Seppa, J., Uusitupa, M., 2012. Obesity and obstructive sleep apnea - Clinical significance of weight loss. Sleep medicine reviews.
Umezaki, T., Nakazawa, K., Miller, A.D., 1998. Behaviors of hypoglossal hyoid motoneurons in laryngeal and vestibular reflexes and in deglutition and emesis. Am J Physiol 274, R950-955.
van Gelder, R.S., Borod, J.C., 1990. Neurobiological and cultural aspects of facial asymmetry. J Commun Disord 23, 273-286.
van Lunteren, E., 1993. Muscles of the pharynx: structural and contractile properties. Ear, nose, & throat journal 72, 27-29, 33.
Vanderveken, O.M., Boudewyns, A., Ni, Q., Kashyap, B., Verbraecken, J., De Backer, W., Van de Heyning, P., 2011. Cardiovascular implications in the treatment of obstructive sleep apnea. Journal of cardiovascular translational research 4, 53-60.
Verbraecken, J.A., De Backer, W.A., 2009. Upper airway mechanics. Respiration; international review of thoracic diseases 78, 121-133.
Viemari, J.C., Garcia, A.J., 3rd, Doi, A., Ramirez, J.M., 2011. Activation of alpha-2 noradrenergic receptors is critical for the generation of fictive eupnea and fictive gasping inspiratory activities in mammals in vitro. Eur J Neurosci 33, 2228-2237.
Viemari, J.C., Ramirez, J.M., 2006. Norepinephrine differentially modulates different types of respiratory pacemaker and nonpacemaker neurons. J Neurophysiol 95, 2070-2082.
Vlemincx, E., Van Diest, I., Lehrer, P.M., Aubert, A.E., Van den Bergh, O., 2010. Respiratory variability preceding and following sighs: a resetter hypothesis. Biological psychology 84, 82-87.
Voituron, N., Zanella, S., Menuet, C., Lajard, A.M., Dutschmann, M., Hilaire, G., 2010. Early abnormalities of post-sigh breathing in a mouse model of Rett syndrome. Respiratory physiology & neurobiology 170, 173-182.
Volgin, D.V., Mackiewicz, M., Kubin, L., 2001. Alpha(1B) receptors are the main postsynaptic mediators of adrenergic excitation in brainstem motoneurons, a single-cell RT-PCR study. Journal of chemical neuroanatomy 22, 157-166.
Volgin, D.V., Rukhadze, I., Kubin, L., 2008. Hypoglossal premotor neurons of the intermediate medullary reticular region express cholinergic markers. Journal of applied physiology 105, 1576-1584.
von Euler, C., 1983. On the central pattern generator for the basic breathing rhythmicity. J Appl Physiol Respir Environ Exerc Physiol 55, 1647-1659.
Vovk, A., Bolser, D.C., Hey, J.A., Danzig, M., Vickroy, T., Berry, R., Martin, A.D., Davenport, P.W., 2007. Capsaicin exposure elicits complex airway defensive motor patterns in normal humans in a concentration-dependent manner. Pulm Pharmacol Ther 20, 423-432.
Watson, A.H., Williams, C., James, B.V., 2012. Activity patterns in latissimus dorsi and sternocleidomastoid in classical singers. J Voice 26, e95-e105.
Watson, B.O., Buzsaki, G., 2015. Sleep, Memory & Brain Rhythms. Daedalus 144, 67-82.
Weese-Mayer, D.E., Kenny, A.S., Bennett, H.L., Ramirez, J.M., Leurgans, S.E., 2008. Familial dysautonomia: frequent, prolonged and severe hypoxemia during wakefulness and sleep. Pediatric pulmonology 43, 251-260.

Wheatley, J.R., Mezzanotte, W.S., Tangel, D.J., White, D.P., 1993. Influence of sleep on genioglossus muscle activation by negative pressure in normal men. The American review of respiratory disease 148, 597-605.
White, D.P., 2005. Pathogenesis of obstructive and central sleep apnea. American journal of respiratory and critical care medicine 172, 1363-1370.
Whiteaker, P., Christensen, S., Yoshikami, D., Dowell, C., Watkins, M., Gulyas, J., Rivier, J., Olivera, B.M., McIntosh, J.M., 2007. Discovery, synthesis, and structure activity of a highly selective alpha7 nicotinic acetylcholine receptor antagonist. Biochemistry 46, 6628-6638.
Wiggin, T.D., Anderson, T.M., Eian, J., Peck, J.H., Masino, M.A., 2012. Episodic swimming in the larval zebrafish is generated by a spatially distributed spinal network with modular functional organization. Journal of neurophysiology 108, 925-934.
Wilkinson, V., Malhotra, A., Nicholas, C.L., Worsnop, C., Jordan, A.S., Butler, J.E., Saboisky, J.P., Gandevia, S.C., White, D.P., Trinder, J., 2010. Discharge patterns of human genioglossus motor units during arousal from sleep. Sleep 33, 379-387.
Winter, S.M., Fresemann, J., Schnell, C., Oku, Y., Hirrlinger, J., Hulsmann, S., 2009. Glycinergic interneurons are functionally integrated into the inspiratory network of mouse medullary slices. Pflugers Arch 458, 459-469.
Won, C.H., Li, K.K., Guilleminault, C., 2008. Surgical treatment of obstructive sleep apnea: upper airway and maxillomandibular surgery. Proceedings of the American Thoracic Society 5, 193-199.
Wulbrand, H., McNamara, F., Thach, B.T., 1998. Suppression of sigma spindle electroencephalographic activity as a measure of transient arousal after spontaneous and occlusion-evoked sighs and startles. Pediatric research 44, 767-773.
Wulbrand, H., McNamara, F., Thach, B.T., 2008. The role of arousal related brainstem reflexes in causing recovery from upper airway occlusion in infants. Sleep 31, 833-840.
Yagi, N., Nagami, S., Lin, M.K., Yabe, T., Itoda, M., Imai, T., Oku, Y., 2016. A noninvasive swallowing measurement system using a combination of respiratory flow, swallowing sound, and laryngeal motion. Med Biol Eng Comput.
Yamuy, J., Fung, S.J., Xi, M., Morales, F.R., Chase, M.H., 1999. Hypoglossal motoneurons are postsynaptically inhibited during carbachol-induced rapid eye movement sleep. Neuroscience 94, 11-15.
Yasaki, E., Saito, Y., Nakano, K., Katsumori, H., Hayashi, K., Nishikawa, T., Osawa, M., 2001. Characteristics of breathing abnormality in Leigh and its overlap syndromes. Neuropediatrics 32, 299-306.
Younes, M., 2004. Role of arousals in the pathogenesis of obstructive sleep apnea. American journal of respiratory and critical care medicine 169, 623-633.
Younes, M., Loewen, A.H., Ostrowski, M., Laprairie, J., Maturino, F., Hanly, P.J., 2012. Genioglossus activity available via non-arousal mechanisms vs. that required for opening the airway in obstructive apnea patients. Journal of applied physiology 112, 249-258.
Young, T., Evans, L., Finn, L., Palta, M., 1997. Estimation of the clinically diagnosed proportion of sleep apnea syndrome in middle-aged men and women. Sleep 20, 705-706.
Young, T., Peppard, P.E., Gottlieb, D.J., 2002. Epidemiology of obstructive sleep apnea: a population health perspective. American journal of respiratory and critical care medicine 165, 1217-1239.
Zanella, S., Roux, J.C., Viemari, J.C., Hilaire, G., 2006. Possible modulation of the mouse respiratory rhythm generator by A1/C1 neurones. Respir Physiol Neurobiol 153, 126-138.

Zhang, S.P., Bandler, R., Carrive, P., 1990. Flight and immobility evoked by excitatory amino acid microinjection within distinct parts of the subtentorial midbrain periaqueductal gray of the cat. Brain Res 520, 73-82.
Zhang, S.P., Davis, P.J., Bandler, R., Carrive, P., 1994. Brain stem integration of vocalization: role of the midbrain periaqueductal gray. J Neurophysiol 72, 1337-1356.
Zhang, W., Mifflin, S.W., 1993. Excitatory amino acid receptors within NTS mediate arterial chemoreceptor reflexes in rats. The American journal of physiology 265, H770-773.
Zoccal, D.B., Furuya, W.I., Bassi, M., Colombari, D.S., Colombari, E., 2014. The nucleus of the solitary tract and the coordination of respiratory and sympathetic activities. Front Physiol 5, 238.
Zollinger, S.A., Riede, T., Suthers, R.A., 2008. Two-voice complexity from a single side of the syrinx in northern mockingbird Mimus polyglottos vocalizations. J Exp Biol 211, 1978-1991.
Zornik, E., Kelley, D.B., 2008. Regulation of respiratory and vocal motor pools in the isolated brain of Xenopus laevis. J Neurosci 28, 612-621.
Zucconi, M., Weber, G., Castronovo, V., Ferini-Strambi, L., Russo, F., Chiumello, G., Smirne, S., 1996. Sleep and upper airway obstruction in children with achondroplasia. The Journal of pediatrics 129, 743-749.

Tatiana M. Anderson

Ph.D. Candidate
tatianaa@uw.edu
Graduate Program in Neuroscience
University of Washington
Seattle Children's Research Institute

Positions

Graduate Researcher, 09/2011 to current
Seattle Children's Research Institute, Seattle, WA

- Personally awarded the Ruth L. Kirschstein National Research Service Award Grant. Funded 3 years; >$100,000.
- Project lead on research that culminated in a first-authored manuscript in *Nature* as well as 5 additional peer-reviewed publications. Disseminated research through oral and poster presentation at national and international conferences.
- Regularly quantitatively analyze complex data sets.
- Collaborate with members of Seattle Children's Institute and other national institutions.

Technology Licensing Fellow, 11/2015 to current
CoMotion tech transfer office, University of Washington, Seattle, WA

- Prepare technology profiles weekly that include competitive analyses, market analyses, and IP landscape of science and technology innovations as a deliverable for Technology Managers and Investigators.
- Author non-confidential summaries of marketing opportunities.

Lab Manager, 08/2007 to 07/2011
University of Minnesota Twin Cities, Minneapolis, MN

- Managed laboratory equipment purchasing, trained graduate students and postdocs
- Experience in study design, data analysis, electrophysiology, and writing that let to multiple publications.
- Performed as a teaching assistant for summer courses at Woods Hole Marine Biological Institute, MA.

Analytical Chemistry Technical Aide, 08/2006 to 06/2009
3M, Saint Paul, MN

- Laboratory technician for organic and materials scientists; performed experimental tests and submitted reports.
- Tested competitive products for proprietary patent infringement violations.

Education

Ph.D. Candidate in Neuroscience, (9/2011 to 1/2017)
University of Washington, Seattle, WA

Bachelor of Science in Neuroscience, Physiology; minor in Psychology, (9/2004 to 5/2009)
University of Minnesota, Minneapolis, MN

- Graduated summa cum laude with honors

Awards and Honors

Ruth L. Kirschstein National Research Service NIH Award (>$100,000; 2014-2017)
International Society for the Advancement of Respiratory Psychophysiology presentation award (2016)
NIH travel awards (2010; 2013)
Dean's List (2005, 2006, 2007, 2008)

Peer-Reviewed Publications

Anderson TM, Ramirez JM (February 14th, 2017). Respiratory rhythm generation: triple oscillator hypothesis. *F1000 Faculty Reviews.* 6:139 (doi: 10.12688/f1000research.10193.1).

Anderson TM, Garcia AJ, Baertsch NA, Pollak J, Bloom JC, Wei AD, Rai KG, Ramirez JM (July 27, 2016). A novel excitatory network for the control of breathing. *Nature,* doi:10.1038/nature18944.

Easton CR, Dickey CW, Moen SP, Neuzil KE, Barger Z, **Anderson TM**, Moody JW, Hevner RF (2016). Distinct calcium signals in developing cortical interneurons persist despite disorganization of cortex by Tbr1 KO. *Developmental Neurobiology,76*(7), 705-720.

Ramirez, JM, **Anderson, TM**, Garcia AJ (June 17, 2014). The ins and outs of breathing. *eLife*, 3:e03375

Raghuraman, S, Garcia, AJ, **Anderson, TM**, Twede, VD, Curtice, KJ, Chase, K, Ramirez, J-M, Teichert, RW (January 01, 2014). Defining modulatory inputs into CNS neuronal subclasses by functional pharmacological profiling. *Proceedings of the National Academy of Sciences of the United States of America, 111,* 17, 6449-54.

Ramirez, J-M, Garcia, AJ, **Anderson, TM**, Koschnitzky, J. E., Peng, Y.-J., Kumar, G. K., & Prabhakar, N. R. (November 01, 2013). Central and peripheral factors contributing to obstructive sleep apneas. *Respiratory Physiology & Neurobiology, 189,* 2, 344-353.

Wiggin TD, **Anderson TM**, Eian J, Peck JH, & Masino MA (August 01, 2012). Episodic swimming in the larval zebrafish is generated by a spatially distributed spinal network with modular functional organization. *Journal of Neurophysiology, 108,* 3, 925-934.

Anderson TM, Abbinanti MD, Peck JH, Gilmour M, Brownstone RM, Masino MA (2012). Low-threshold calcium currents contribute to locomotor-like activity in neonatal mouse, *Journal of Neurophysiology, 107,1,103-113.*

Seminars and Presentations

University of Tokyo and UW Joint Symposium (November 7th, 2016). PiCo: the discovery of a third oscillator in the control of breathing. Seattle, US.

International Society for the Advancement of Respiratory Psychophysiology (October 8th, 2016). The neurobiology of postinspiratory behaviors. Seattle, US.

Neuroscience Graduate Program Spring Symposium (May 25th, 2016). PiCo: A novel excitatory network for the control of breathing. Seattle, US.

Motor Systems SFN pre-meeting (October 16th, 2015). The triple oscillator hypothesis for the generation of breathing. Chicago, US.

Center for Integrative Brain Research Retreat (December 2nd, 2014). Mechanisms underlying the generation of inspiratory and postinspiratory activity. Seattle, US.

Neuroscience Graduate Program Retreat (Sept. 9, 2014). Mechanisms underlying the generation of inspiratory and post-inspiratory activity. Seattle, US.

Center for Integrative Brain Research Retreat (Nov. 30, 2012). Studying the neuronal basis of respiration across multiple networks. Seattle, US.

Poster Presentations and Abstracts

Ramirez SC, **Anderson TM**, Baertsch NA, Koschnitzky JE, Smith CV, Ramirez JM. The central nervous system in breathing disturbances of prematurity. American Thoracic Society International Conference. May 17, 2016.

Anderson TM, Garcia AJ 3rd, Bloom JC, Baertsch NA, Pollak J, Ramirez JM. Postinspiration: generated by an excitatory rhythmogenic network? Society for Neuroscience, Chicago, Illinois, October 2015.

Anderson TM, Garcia AJ 3rd, Bloom JC, Baertsch NA, Pollak J, Ramirez JM. Coupled oscillators underlying inspiration and postinspiration. Experimental Biology, Boston, Massachusetts, March 2015.

Garcia AJ 3rd, **Anderson TM,** Ramirez JM. Hypercapnic acidosis augments opioid suppression of rhythmogenesis from the preBötzinger complex. Sydney, Australia, October 2014

Anderson TM, Garcia AJ 3rd, Ramirez JM**.** Respiratory rhythm generation emerges from an excitatory column encompassing the preBötzinger and Bötzinger Complex. Society for Neuroscience, Washington DC, November 2014.

Garcia AJ 3rd, **Anderson TM,** Ramirez JM. Society for Neuroscience, Washington DC, November 2014.

Anderson TM, Garcia AJ 3rd, Ramirez JM**.** Coupled oscillators underlying inspiration and post-inspiration. Oxford Breathing Meeting, Sydney, Australia, October 2014.

Anderson TM, Garcia AJ 3rd, Ramirez JM**.** Examining the role of inhibition in establishing the three respiratory phases in a horizontal slice. Experimental Biology, April 2014.

Anderson TM, Garcia AJ 3rd, Ramirez JM**.** Examining the organization of the respiratory network in a novel slice preparation containing the entire ventral respiratory column. Society for Neuroscience, November 2013.

Garcia AJ 3rd, **Anderson TM,** Ramirez JM. Hypercapnia augments the suppressive action of [D-Ala2, N-MePhe4, Gly-ol]-enkephalin (DAMGO) on in vitro rhythmogenesis from the preBötzinger complex (preBötC). Society for Neuroscience, November 2013.

Anderson TM, Garcia AJ, Ramirez JM. The horizontal brainstem slice: a novel preparation to study cellular interactions of respiratory rhythmogenesis. Experimental Biology, April 2013.

Anderson TM, Peck JH, Masino MA. The swim central pattern generator in larval zebrafish is distributed along the rostro-caudal axis of the spinal cord with a rostral bias for coordination. Society for Neuroscience and Motor Systems Symposium, Washington DC, November 2011.

Lambert AM, **Anderson TM**, Masino MA. Dopaminergic modulation of spinal locomotor circuits in larval zebrafish. Society for Neuroscience, November 2010.

Anderson TM, Masino MA. Morphological characterization of spinal interneurons in larval zebrafish. University of Minnesota Undergraduate Research Symposium, April 2008.

Professional Society Memberships

Society for Neuroscience (2007-present)
American Physiological Society (2014-present)
International Society for the Advancement of Respiratory Psychophysiology (2016-present)

Outreach

Science Adventure Lab Study Assistant (2014-present)
Officer of University of Washington Outreach (2011-present)
Brain Awareness Week (2012-2016)
Pacific Science Center Life Sciences Research Weekend (2012-2015)